C-N BOND FORMATION EMPLOYING PALLADIUM AND NICKEL PRECATALYSTS
CONTAINING ANIONIC PHOSPHINOBENZIMIDAZOLE LIGANDS

By

Joseph P. Tassone

Submitted to

The Department of Chemistry, Lakehead University,

in Partial Fulfilment of the Requirements for the Degree of Master of Science

Supervisor: Dr. G. J. Spivak

Department of Chemistry, Lakehead University

Thunder Bay, Ontario, Canada, P7B 5E1

April 2016

To Mom, Papa, and Matthew,

with love.

Abstract

In this investigation, the catalytic utility of anionic, phosphinobenzimidzoles [Li(THF)$_2$][**1a**] and [Li(THF)$_4$][**1b**] in effecting the Buchwald-Hartwig amination reaction was examined. Specifically, the coordination chemistry of ligands [Li(THF)$_2$][**1a**] and [Li(THF)$_4$][**1b**] with palladium was studied in an attempt to synthesize a distinct precatalyst containing either **1a** or **1b** that could be screened for catalytic activity in the reaction of interest. Additionally, the screening of a Pd/[Li(THF)$_4$][**1b**] catalyst system for activity in the Buchwald-Hartwig amination reaction was conducted concurrently. Complex **6,** containing **1a**, and complexes **7-12**, containing **1b**, were successfully synthesized, and characterized using multi-nuclear NMR spectroscopy. An optimized [Pd(cinnamyl)Cl]$_2$/[Li(THF)$_4$][**1b**] catalyst system was also developed, and performed the coupling of activated and deactivated aryl bromides with a selection of amines in moderate to excellent yields (36-97%). A preference for primary vs. secondary amine coupling partners, as well as a high selectivity for the monoarylated product, was observed during the course of these studies. To highlight the remarkable potential of anionic ligands in catalysis, the catalytic efficiency of the [Pd(cinnamyl)Cl]$_2$/[Li(THF)$_4$][**1b**] catalyst system was compared with a corresponding system utilizing the related, neutral phosphinobenzimidazole **2**, with the anionic system displaying superior catalytic activity in the Buchwald-Hartwig amination reaction in almost all cases. This phenomenon was attributed to the more electron-rich catalytic intermediates present in the anionic system, enabling more rapid oxidative addition, and thus more efficient catalysis. Further screening of the anionic precatalyst [PPh$_4$][PdCl$_2$(κ^2-**1b**)] (**10**) and neutral precatalyst [PdCl$_2$(κ^2-**2**)] (**13**) corroborated these results. Finally, preliminary studies examining the potential of **1b** as an ancillary ligand in Ni-catalyzed C-N bond formation was undertaken. The coordination chemistry of **1b** with nickel was explored, resulting in the formation of complex **14**, whose tentative structure was assigned on the basis of NMR spectroscopic evidence. Furthermore, initial screening of a NiCl$_2$(DME)/[Li(THF)$_4$][**1b**] catalyst system in the cross-coupling of chlorobenzene and aniline did not result in observable product formation under various reaction conditions.

<u>Acknowledgements</u>

Firstly, I would like to express my sincere gratitude to my supervisor, Dr. Greg Spivak. I have spent the past six years working for Greg, and have thoroughly enjoyed my time in his lab. His guidance and encouragement were very much appreciated throughout the pursuit of my undergraduate and graduate degrees. Greg was always willing to assist with any problems I may have had, and was always eager to make sure that I was on track and poised for success. I was very fortunate to have Greg as a mentor, and will carry the lessons I've learned and the experiences I've gained working in his lab with me for many years to come. Thank you, Greg.

Secondly, but no less importantly, I must thank my lab-mate and friend, Jesse Walker. We've laughed together, complained together, eaten together, and TA-ed together, and I couldn't have asked for a better person with whom to share my lab experience. I truly appreciated his genuine willingness to help me with any of my problems (chemical or otherwise), and his relaxing demeanour always managed to calm me down when I was feeling particularly stressed. Thank you for your encouragement and friendship. You are the baddest of them all, Jes.

Lastly, I would like to thank my friends and family. I don't say it nearly enough, but I am very grateful for all of your love and support.

Table of Contents

List of Figures

List of Schemes

List of Tables

List of Abbreviations

OAc	acetate
acac	acetylacetonate
MeCN	acetonitrile
1-Ad	1-adamantyl
Ar^F	3,5-bis(trifluoromethyl)phenyl
BHA	Buchwald-Hartwig amination
δ	chemical shift
Cy	cyclohexyl
COD	1,5-cyclooctadiene
Cp	cyclopentadienyl
dba	*trans,trans*-dibenzylideneacetone
Et$_2$O	diethyl ether
DCM	dichloromethane
DME	dimethoxyethane
DMSO	dimethyl sulfoxide
d	doublet
EDG	electron-donating group
EWG	electron-withdrawing group
Et	ethyl
xs	excess
i-Pr	isopropyl
LDA	lithium diisopropylamide

MeOH	methanol
Me	methyl
m	multiplet
n-Bu	normal butyl
Ph	phenyl
cinnamyl	η^3-(3-phenyl-1-propenyl)
Pin	pinacol
allyl	η^3-(1-propenyl)
^{1}H	proton
^{11}B{^{1}H}	proton-decoupled boron
^{13}C{^{1}H}	proton-decoupled carbon
^{7}Li{^{1}H}	proton-decoupled lithium
^{31}P{^{1}H}	proton-decoupled phosphorus
sec-Bu	*sec*-butyl
s	singlet
t-Bu	*tert*-butyl
THF	tetrahydrofuran
TMEDA	*N,N,N′,N′*-tetramethylethylenediamine
OTf	triflate (trifluoromethanesulfonate)
t	triplet

1. <u>Introduction</u>

1.1 Ancillary Ligands in Catalysis: The Link Between Design and Activity

The majority of homogeneous catalytic transformations are mediated by ligands. Though typically not involved in catalysis directly, the ligand is an essential component of the reaction, establishing the steric and electronic environment around the metal required to enact the desired chemical change. Common ancillary ligands that are employed in such reactions include phosphines, which have a well-established role in catalytic applications.[1] Though structurally-simple phosphines, such as PPh3, are adequate for the promotion of straightforward transformations using common substrates, problems arise when more challenging substrates, which may be inherently less active, or prone to undesirable reactivity patterns, are utilized, or when chemoselectivity or stereoselectivity is important.[2] Thus, some condition of the reaction must be altered in order to resolve these issues. The most efficient method of changing the outcome of a catalytic reaction is to adjust the properties of the ancillary ligand. Since the steric and electronic environment at the metal center is dictated by its coordinated ligands, tailoring the ancillary ligand appropriately or selecting an ancillary ligand with suitable properties can vastly improve the effectiveness of the desired transformation.

For example, P(t-Bu)3 is an ancillary ligand that has demonstrated excellent activity in a variety of cross-coupling reactions.[2] However, its utility is restricted by the difficulties associated with its derivatization, including the inability to functionalize the tertiary carbon atoms, or to introduce molecular 'tags' for catalyst separation and recycling.[2] As an alternative to P(t-Bu)3, Beller *et al.*[3] developed cataCXium® A (**Figure 1.1**). This ligand mimics the bulky and electron-donating nature of P(t-Bu)3 by incorporating adamantyl groups, but can be prepared simply (and thus modified easily) from diadamantylphosphine.[2,3] To showcase the utility of cataCXium® A in

catalysis, various monodentate phosphines, including P(t-Bu)$_3$, were screened for activity in the Suzuki cross-coupling reaction (which generates a C-C bond).[2] Though exhibiting similar steric and electronic properties to P(t-Bu)$_3$, it was found that only cataCXium® A could promote the desired transformation at very low catalyst loadings (**Scheme 1.1**).[2] Clearly, the judicious choice of phosphine substituents in cataCXium® A provided a superior reactivity profile compared to P(t- Bu)$_3$, highlighting the benefits of ligand design.
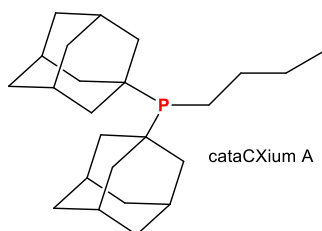
Figure 1.1. Chemical structure of cataCXium® A.
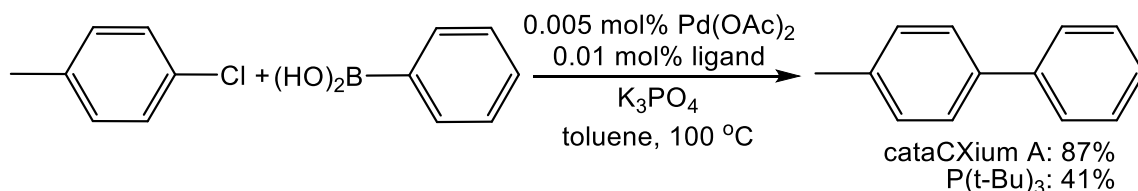
Scheme 1.1. Comparing the activities of cataCXium® A and P(t-Bu)$_3$ in the Suzuki reaction.

In addition to developing entirely new ancillary ligands, selecting a pre-existing ligand with more suitable steric and/or electronic properties can serve to address challenges in certain catalytic reactions. For example, Kumada *et al*.[4] highlighted the pronounced effect the bite angle of a bidentate phosphine can have on the outcome of a catalytic reaction. The researchers investigated two precatalysts in the coupling of bromobenzene with *sec*-BuMgCl (**Scheme 1.2**) – one containing diphenylphosphinoferrocene (dppf) and the other containing 1,1′-bis(diphenylphosphino)propane (dppp). The larger bite angle of dppf allowed for more efficient reductive elimination, affording the desired product in high yields. However, a mixture of both the

desired product and that arising from unwanted β-hydrogen elimination was found using the dppp precatalyst. Thus, it is evident that the judicious choice of ancillary ligand, in addition to ligand design, can successfully mitigate problems arising in catalytic reactions.

[PdCl$_2$(dppf)]: 95% (1 h)
[PdCl$_2$(dppp)]: 43% (24 h)
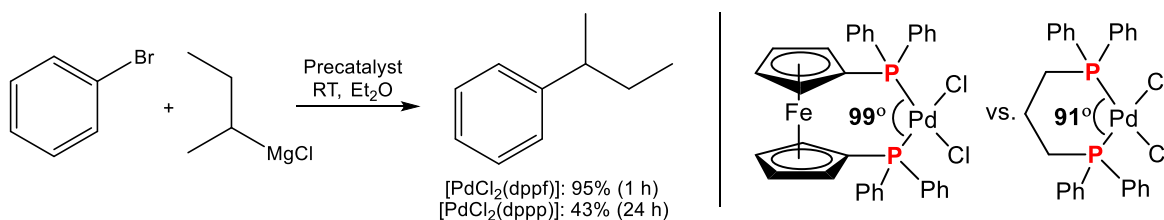
Scheme 1.2. Ancillary ligand bite angle effects in the coupling of bromobenzene with *sec*-BuMgCl.

1.2 Hybrid Ligands and Hemilability

Unlike phosphines, hybrid ligands are multidentate ligands containing two or more different heteroatoms that can coordinate to a metal centre.[5] The utility of bidentate hybrid ligands, particularly in catalysis,[5,6] largely stems from their mixed donor characteristics. The 'soft' donor atom (*e.g.* phosphorus) will bind strongly to late metals, whereas the tethered 'hard' donor atom (*e.g.* nitrogen or oxygen) will form a weaker coordinate bond due to metal-heteroatom dπ-pπ interactions.[6c] For early metals, the situation is reversed, with the harder donor atom binding irreversibly to the metal centre.[6c] In either case, this unique bonding situation can facilitate hemilability.[7] A hemilabile ligand is able to reversibly coordinate to a metal centre through various binding modes due to the more transient nature of one of its coordinate bonds (**Scheme 1.3**).[7] Though the electronic interactions between the mismatched donor atom and metal induces hemilability, the size of the chelate can also contribute to this phenomenon, with strained chelates favouring hemilabile behavior.[7]
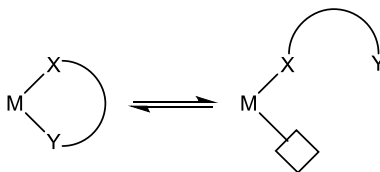
Scheme 1.3. Mechanism of hemilability.

Ligand hemilability is especially useful in catalysis, allowing the ligand to meet the dynamic electronic needs of the metal throughout the catalytic cycle by stabilizing low-coordinate intermediates, or by facilitating substrate coordination and product elimination.[7] Indeed, due to their advantageous catalytic properties, a variety of hemilabile, hybrid ligands have been successfully employed to promote important chemical transformations.[5-8] As an example, a catalyst system comprising of $Pd_2(dba)_3$ and [P,N]-hybrid ligand **L1** (**Figure 1.2**) developed by Hor *et al.*[9] successfully promoted the cross-coupling of challenging aryl chlorides with boronic acids at low catalyst loadings. The success of this catalyst system was attributed, in part, to the hemilabile nature of **L1**, which allowed the stabilization of low-coordination Pd(0) intermediates necessary for high catalytic efficiency. The hemilability of **L1** was demonstrated through stoichiometric experiments in which the ligand was reacted with equimolar amounts of $Pd_2(dba)_3$, giving rise to two distinct complexes with κ^2-*P,N* chelate and monodentate κ^1-*P* ligand coordination modes respectively. Crystallographic analysis of the chelate complex showed a very large P–Pd–N bond angle (~111°), which, in combination with the weakly basic imine donating group, certainly contributes to the observed hemilability, and thus utility, of the ligand.
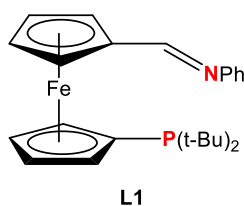
Figure 1.2. Chemical structure of a hemilabile [P,N]-hybrid ligand.

1.2.1 Anionic, Hybrid Ligands

An interesting class of hybrid ligands consists of those that have been rendered negatively charged (for examples, see **Figure 1.3**).[10-12] This seemingly simple modification provides anionic, hybrid ligands with additional catalytic properties when compared to analogous neutral ligands.

Firstly, anionic ligands are generally considered more powerful electron donors than their neutral counterparts.[13] The corresponding increase in electron density at the metal could then help facilitate key steps in the catalytic cycle (*e.g.* oxidative addition).[14] Secondly, anionic ligands can combine with metal precursors to form zwitterionic precatalyst complexes, which possess many beneficial properties.[15] Zwitterionic complexes exhibit greater solubility in low polarity media due to the formally neutral charge of the complex.[15] Additionally, charge separation prevents the deactivation of a zwitterionic precatalyst by molecules with polar functional groups (*e.g.* solvent molecules).[15] Furthermore, the lack of a coordinating counterion in zwitterionic complexes (compared to cationic complexes) mitigates unwanted reactivity patterns that would otherwise impede catalysis.[15]
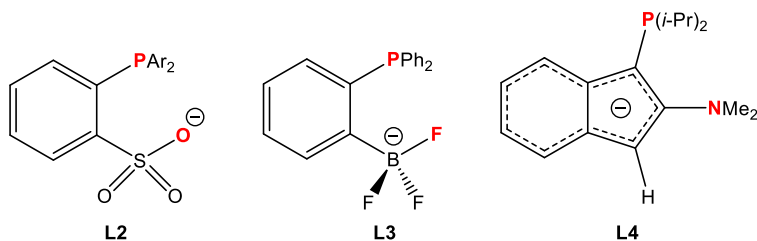
Figure 1.3. Examples of anionic, hybrid ligands.

The utility of anionic, hybrid ligands in promoting interesting or challenging chemical transformations has been demonstrated in recent years. Anionic [P,O]- and [P,F]-hybrid ligands[10,11] (**L2** and **L3**, **Figure 1.3**) have been developed to effect the coordination-insertion copolymerization of polar vinyl monomers with ethylene. It was speculated that the increase in electron density at the metal imparted by the anionic ligand would promote the desired π-coordination of the polar vinyl monomer, effectively preventing formation of the catalytically inactive, σ-bound complex.[11a] Indeed, a variety of palladium complexes containing anionic [P,O]-ligands have successfully polymerized ethylene with several polar vinyl monomers, including methyl acrylate and acrylonitrile, to yield highly linear copolymers.[10]

The potentially increased reactivity of zwitterionic precatalysts, which are preferentially formed when employing anionic ligands, vs. corresponding cationic precatalysts has been showcased in the transfer hydrogenation of ketones using a zwitterionic ruthenium complex bearing an anionic, indenide-based, [P,N]-hybrid ligand (**L4**, **Figure 1.3**) by Stradiotto *et al*.[16] Notably, 99% conversion of acetophenone to 1-phenylethanol was observed after five minutes in refluxing isopropanol for the zwitterionic precatalyst (**C1**, **Figure 1.4**), while only 4-23% conversion was observed after fifteen minutes under similar conditions using cationic ruthenium complexes of the form **C2** (**Figure 1.4**), which contained an analogous neutral ligand.

C1   vs.   **C2** (X = Cl, BF$_4$, SO$_3$CF$_3$, B(C$_6$F$_4$)$_4$)

Figure 1.4. Zwitterionic and cationic precatalysts for the transfer hydrogenation of ketones.

1.3 Pd-Catalyzed C-N Bond Formation: The Buchwald-Hartwig Amination Reaction

Hybrid ligands have been used extensively in the promotion of palladium-catalyzed cross-coupling reactions.[5] Among these transformations, the Buchwald-Hartwig amination (BHA) reaction (**Scheme 1.4**) for the formation of aryl C–N bonds has garnered significant research interest,[17] particularly in the synthesis of fine chemicals (*e.g.* pharmaceuticals, natural products, and agrochemicals).[18] Since a ligated Pd(0) species is the putative active catalyst in BHA, modifying the properties of the coordinated ancillary ligand(s) permits control over the efficacy of the reaction, with strongly electron-donating ligands promoting oxidative addition and sterically-encumbered ligands facilitating reductive elimination.[17] Accordingly, a variety of catalyst systems

featuring bulky, electron-rich ligands have been developed to promote BHA (for examples, see **Figure 1.5**). Buchwald *et al.*[17a,19] have developed monodentate biarylphosphines, such as BrettPhos and RuPhos (**Figure 1.5**), that demonstrate remarkable activity in this reaction. The main advantages of using these ancillary ligands is their straightforward, one-pot synthesis, permitting fine-tuning of the ligand scaffold for excellent catalytic versatility. Accordingly, precatalysts containing either BrettPhos or RuPhos can promote the amination of various primary and secondary amines, respectively, with functionalized (hetero)aryl halides at low catalyst loadings.
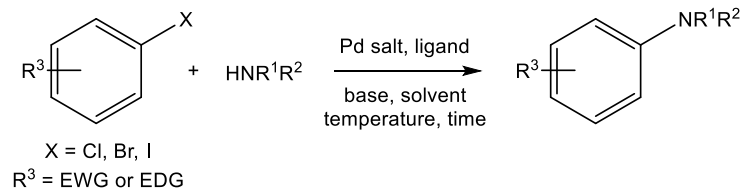
Scheme 1.4. The Buchwald-Hartwig amination reaction.
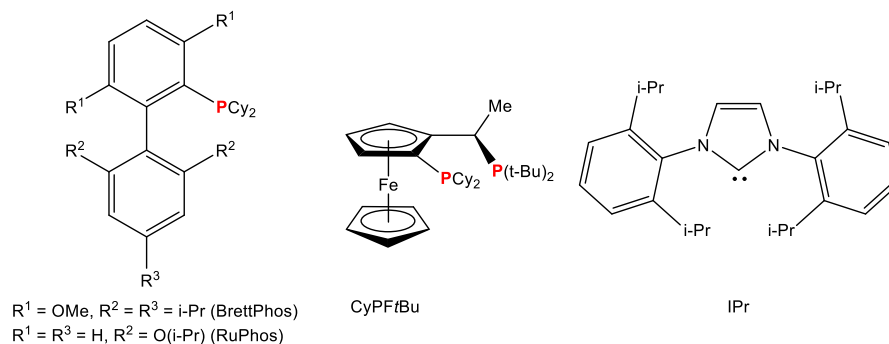
Figure 1.5. Examples of bulky, electron-donating ligands used in BHA.

Using the commercially-available ligand CyPF*t*Bu (**Figure 1.5**), Hartwig *et al.*[17b] were also able to achieve excellent activity for BHA. In addition to promoting the coupling of primary and secondary amines with activated and deactivated (hetero)aryl halides using low catalyst loadings under mild conditions, a Pd/CyPF*t*Bu catalyst system was the first to successfully accomplish the monoarylation of ammonia.

Though both monodentate and bidentate phosphines are clearly capable of promoting BHA, the groups of Nolan[17c,20] and Organ[17d] have demonstrated the successful employment of precatalysts containing bulky, electron-rich NHCs to accomplish this reaction. Notably, the use of precatalysts containing IPr (**Figure 1.5**) led to outstanding activity in the coupling of sterically-encumbered aryl halides with amines,[20] as well as deactivated (hetero)aryl halides with deactivated anilines and amines.[17d]

1.3.1 Hybrid Ligands as Ancillary Ligands in the Buchwald-Hartwig Amination Reaction

Given their advantageous catalytic properties, hybrid ligands have been successfully employed as ancillary ligands to facilitate BHA. Those ligands that have demonstrated remarkable activity effecting this transformation are typically based on [P,N]- or [P,O]-ligand scaffolds.[5,6c]

Among the [P,N]-hybrid ligands that have been utilized as ancillary ligands for BHA, Me-DalPhos (**Figure 1.6**), developed by Stradiotto *et al.*,[21] is arguably the most notable. Indeed, it was found that Me-DalPhos (or its t-Bu variant), in combination with either [Pd(allyl)Cl]$_2$ or [Pd(cinnamyl)Cl]$_2$, could facilitate the cross-coupling of deactivated or neutral aryl chlorides with primary and secondary alkylamines, primary and secondary anilines, ammonia, imines, and benzophenone hydrazone with moderate to excellent conversions (65-99%). *N*-heteroaryl chlorides were also shown to be highly active substrates. Additionally, aryl chlorides containing base-sensitive functional groups (*e.g.* ketones, esters, amides, *etc.*) could be tolerated using catalytic amounts of strong base (*i.e.* NaO(t-Bu)) for precatalyst activation, in combination with stoichiometric amounts of a weaker base (*i.e.* Cs$_2$CO$_3$ or LiN(SiMe$_3$)$_2$) to promote the reaction proper. All in all, the facile coupling of inexpensive aryl chlorides, as well as the remarkably broad substrates scope, with respect to both the aryl chloride and amine coupling partners, showcased

Me-DalPhos as a powerful hybrid, ancillary ligand for the promotion of BHA, spurring its commercial availability in subsequent years.[22]
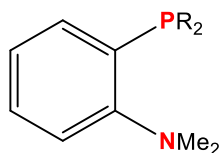
R = 1-Ad (Me-DalPhos), t-Bu

Figure 1.6. Chemical structure of the Me-DalPhos ligand used in BHA chemistry.

Similar to [P,N]-hybrid ligands, [P,O]-hybrid ligands have also shown to be effective ancillary ligands in the promotion of the BHA reaction. The metal chelate formed by a bidentate [P,O]-hybrid ligand can be considered weaker than that formed by other hybrid ligands, causing increased hemilabile behavior, and correspondingly, greater potential catalytic activity.[7a] With this in mind, Kwong *et al*.[23] developed Bphos (benzamide-derived phosphine) ligands (**Figure 1.7**) for use in BHA chemistry. Based on previous reports,[24] the researchers speculated that the weakly-coordinating amide moiety could act as a hemilabile donating group, facilitating substrate coordination and stabilization of the palladium centre as needed. In addition to its potential hemilability, the attractiveness of the Bphos ligand class stems from their straightforward synthesis from inexpensive starting materials, as well as the facile tuning of the backbone, amide, and phosphine moieties, permitting the tailoring of these ligands for maximum catalytic versatility. To showcase the activity of this ligand class, a Pd(OAc)$_2$/**L5** catalyst system was used to couple a variety of substituted aryl chlorides, containing either electron-donating or electron-withdrawing substituents, with primary and secondary alkylamines, and primary and secondary anilines, in excellent yields (88-96%). Additionally, *N*-heteroaryl chlorides and aryl chlorides containing base-sensitive groups (specifically cyano-, methoxy- and ester functionalities) were successfully employed as substrates with no appreciable loss of activity.
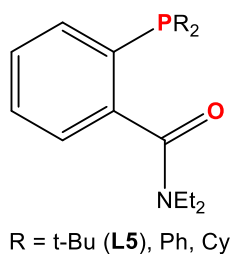
Figure 1.7. Bphos ligands for use in BHA chemistry.

1.3.2 Anionic Ligands as Ancillary Ligands in the Buchwald-Hartwig Amination Reaction

Despite the apparent advantages of utilizing anionic ligands in catalysis, their use as ancillary ligands for promoting BHA remains virtually unexplored. Indeed, only one such example exists in the literature. In this investigation by Liu and coworkers,[25] the phosphonium salt **L6** (**Figure 1.8**), in conjunction with Pd(dba)$_2$, was used as a catalyst system to facilitate the coupling of substituted (hetero)aryl chlorides and bromides with morpholine, octylamine, aniline, and 2-methylaniline, which generally proceeded with moderate to excellent yields (55-99%). The authors speculated that the activity of this catalyst system stemmed from the *in situ* generation of the anionic phosphine indenide (**Scheme 1.5**), which would impart greater electron density at the metal centre and subsequently increase the rate of reaction. The presence of this species during catalysis was deemed feasible through stoichiometric experiments in which **L6** was treated with excess base and monitored using ^{31}P NMR spectroscopy, cleanly forming the anionic phosphine.
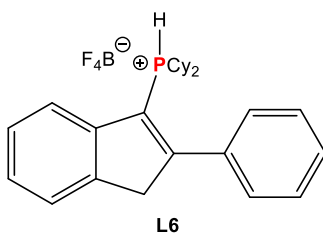
Figure 1.8. Phosphonium salt used in the promotion of BHA.
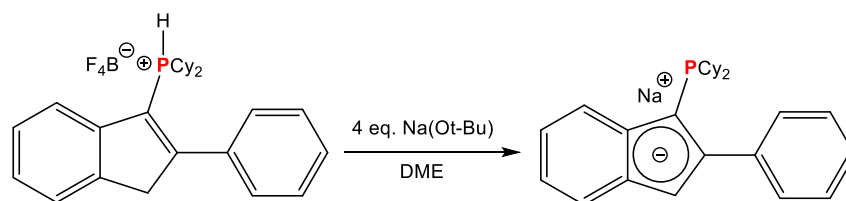
Scheme 1.5. *In situ* generation of an anionic phosphine indenide.

1.4 Nickel-Catalyzed C-N Bond Formation

In an effort to establish 'greener' methods for catalysis, researchers are increasingly looking toward nickel as a suitable alternative for palladium. The numerous benefits to such a substitution have been recently reviewed.[26] Firstly, nickel is earth-abundant and inexpensive, while palladium is not readily available, and thus, costlier. Additionally, nickel reacts efficiently with inexpensive aryl chlorides, further boosting its attractiveness. However, effective promotion of nickel-catalyzed reactions typically requires the use of Ni(0) precursors, which are difficult to prepare and store due to their sensitivity to air and moisture. Furthermore, large catalyst loadings (5-20 mol%) of nickel precursor are typically required to promote the desired catalytic transformation, essentially negating the cost-effectiveness of utilizing nickel.

Despite these drawbacks, several examples of nickel-catalyzed C-N bond formation have been reported.[27] Notably, in recent years, the use of preformed nickel precatalysts (**Figure 1.9**) has permitted this reaction to proceed with more acceptable catalyst loadings and reaction conditions.[27a,b] These precatalysts also highlight the use of bisphosphines as prominent ancillary ligands for nickel-catalyzed C-N bond formation.[28]
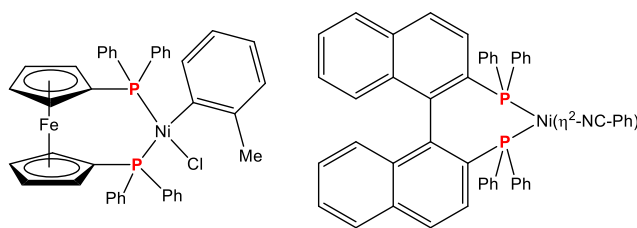
Figure 1.9. Examples of nickel precatalysts used in Ni-catalyzed C-N bond formation.

1.5 Phosphino(benz)imidazoles: Versatile Ancillary Ligands for Cross-Coupling Chemistry

Though there exist countless ancillary ligands suitable for the promotion of a particular reaction, phosphino(benz)imidazoles represent a class of hybrid ligands which boast excellent activity in a variety of catalytic applications, including several cross-coupling reactions. For example, phosphinobenzimidazole **L7** (**Figure 1.10**) is an effective ancillary ligand for the promotion of both the Suzuki cross-coupling reaction, as well as BHA,[29] while phosphinoimidazole **L8** (**Figure 1.10**) has demonstrated its capabilities as an ancillary ligand for Pd-catalyzed ammonia monoarylation.[30] Furthermore, phosphinoimidazole **L9** (**Figure 1.10**) is capable of promoting the Pd-catalyzed hydroxylation of aryl halides,[31] and a palladium precatalyst incorporating **L9** can promote this reaction at ambient temperatures.[32]
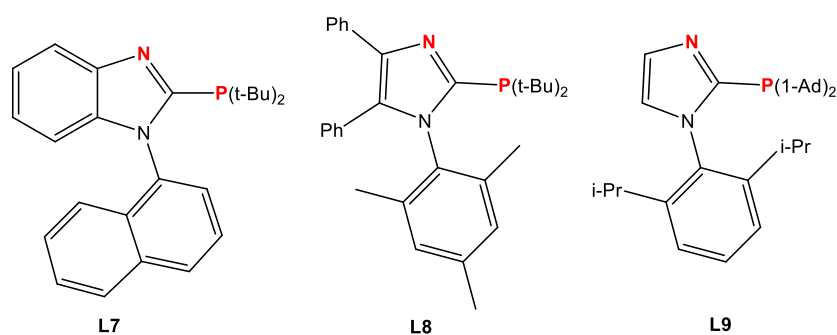
Figure 1.10. Select phosphino(benz)imidazole ligands used in cross-coupling chemistry.

The phosphino(benz)imidazole class of hybrid ligands exhibit many attractive qualities that make them desirable for use in catalysis. The core (benz)imidazole scaffold can be prepared easily, permitting straightforward tailoring of the molecule through the modification of the backbone, the introduction of functional groups at the N1-position, and the installation of phosphines with different substituents at the C2-position.[33-35] This then allows greater versatility when designing these ligands to promote a particular catalytic reaction with potentially challenging substrates. Additionally, the inherent hybrid nature of the phosphino(benz)imidazole ligand class lends itself

well to catalytic applications. Thus, it is evident that phosphino(benz)imidazoles are versatile and effective ancillary ligands, displaying high activities for catalytic cross-coupling reactions.

1.6 Anionic, Hemilabile Phopshinobenzimidazoles

Given the advantages and established activity of employing phosphino(benz)imidazoles as ancillary ligands in catalysis, as well as the additional catalytic benefits imparted by rendering ligands negatively charged, the synthesis of anionic phosphino(benz)imidazoles could enable the development of a new class of ancillary ligands with impressive catalytic potential. To this end, we recently reported[36] the synthesis of the anionic phosphinobenzimidaozle ligand [Li(THF)$_2$][**1a**] (**Figure 1.11**), where the negative charge is introduced through a tethered tetraphenylborate group at the N1-position. Upon examining the coordination chemistry of [Li(THF)$_2$][**1a**] with ruthenium, it was found that both κ^2-*P,N* bidentate chelate and κ^1-*P* monodentate binding modes were reversibly accessible in solution, indicating hemilabile behaviour. The hemilability of the ligand is linked to the strained four-membered chelate that forms upon chelation to the metal. Additionally, [Li(THF)$_2$][**1a**] readily forms zwitterionic ruthenium complexes, such as the piano-stool complex [CpRu(**1a**)(PPh$_3$)] (**Figure 1.12**). Furthermore, preliminary catalytic investigations suggest that zwitterionic complexes such as [CpRu(**1a**)(PPh$_3$)] exhibit more pronounced activity in transfer hydrogenation and isomerization reactions compared to analogous cationic complexes, showcasing the impressive potential of anionic phosphinobenzimidazoles as ancillary ligands in catalysis.

[Li(THF)$_2$][**1a**]
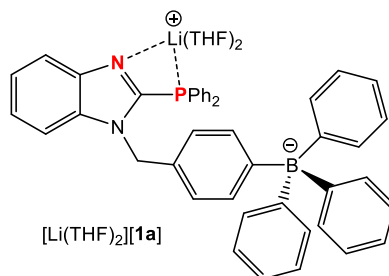
Figure 1.11. A novel, anionic, phosphinobenzimidazole ligand.
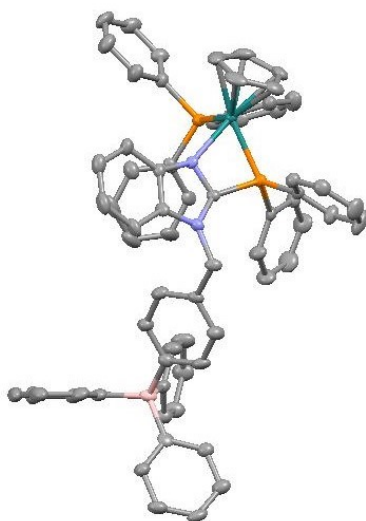
Figure 1.12. Solid-state structure of [CpRu(**1a**)(PPh$_3$)].

2. <u>Research Intentions</u>

The continuing demand for more efficient catalytic processes requires the parallel development of highly active ancillary ligands to facilitate these transformations. Correspondingly, the Buchwald-Hartwig amination reaction continues to play a dominant role in the production of fine chemicals, such as pharmaceuticals and natural products, precipitating the design and implementation of countless ancillary ligands to effect this reaction using challenging substrates, or under mild conditions. However, there remains a class of ligands whose capability in this reaction has yet to be fully realized – anionic ligands. The simplicity with which some ligand scaffolds can be rendered negatively charged, coupled with the large potential gain in catalytic activity, necessitates a more careful study of this ligand class for use in BHA. Thus, the focus of this work will involve assessing the catalytic utility of anionic phosphinobenzimidazole ligands [Li(THF)$_2$][**1a**] and [Li(THF)$_4$][**1b**] (**Figure 2.1**) as ancillary ligands in the Buchwald-Hartwig amination reaction. The phosphinobenzimidazole ligand scaffold is ideal for this study as it is easily modifiable, allowing the straightforward introduction of a pendant anionic functional group, and possesses all of the inherent catalytic benefits of hybrid ligands.
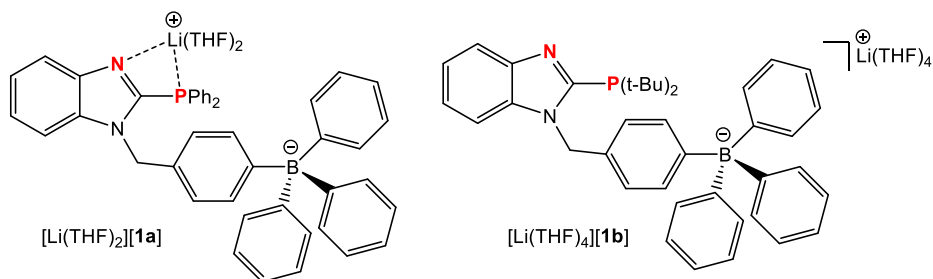
Figure 2.1. Anionic, phosphinobenzimidazoles used in this study.

In undertaking this investigation, two major research avenues will be explored. Firstly, the coordination chemistry of the aforementioned ligands with palladium will be examined in an attempt to generate precatalyst complexes that can then be screened for activity in BHA.

Meanwhile, a more 'traditional' screening process will be undertaken so as to identify the optimal conditions under which this reaction can occur with a Pd/[Li(THF)$_2$][**1a**] or Pd/[Li(THF)$_4$][**1b**] catalyst system. Once an active catalyst system or precatalyst containing [Li(THF)$_2$][**1a**] or [Li(THF)$_4$][**1b**] has been found, comparing the ability of analogous neutral ligands to effect BHA under optimized conditions will highlight what impact, if any, utilizing anionic ancillary ligands has on this reaction.

As an additional area of interest, related studies will attempt to assess the activity of [Li(THF)$_2$][**1a**] and [Li(THF)$_4$][**1b**] in Ni-catalyzed C-N bond formation. The cost and sustainability benefits of utilizing nickel in C-N bond formation is compelling researchers to increasingly pursue development in this area, which could ultimately result in the more environmentally-friendly and economical synthesis of fine chemicals. Thus, it is important to investigate new ancillary ligands for the promotion of this reaction. As with the aforementioned catalytic studies with palladium, [Li(THF)$_2$][**1a**] and [Li(THF)$_4$][**1b**] will be combined with nickel precursors in an effort to generate a distinct nickel precatalyst that can then be assessed for catalytic activity. Likewise, screening [Li(THF)$_2$][**1a**] and [Li(THF)$_4$][**1b**], in combination with nickel precursors, for activity in nickel-catalyzed C-N bond formation will also be undertaken.

3. <u>Experimental</u>

3.1 General Considerations

All manipulations were carried out under an inert N_2 atmosphere using standard Schlenk line techniques, unless otherwise indicated. Hexanes, CH_2Cl_2, and benzene were pre-dried over 4Å molecular sieves, passed through a column of alumina, purged with N_2, and stored over activated 4Å molecular sieves in bulbs with Teflon taps prior to use.[37] THF and Et_2O were freshly distilled over sodium metal under an atmosphere of N_2. Fluorobenzene and 1,4-dioxane were dried over 4Å molecular sieves, purged with N_2, and stored in bulbs with Teflon taps over activated 4Å molecular sieves. $CDCl_3$ (dried over anhydrous $CaCl_2$), CD_2Cl_2 (dried over CaH_2), and C_6D_6 (dried over sodium metal) were vacuum distilled, freeze-pump-thaw degassed three times, and stored in bulbs with Teflon taps. NMR spectra were taken at 21 °C on a Varian Unity INOVA 500 MHz spectrometer, with chemical shifts (in ppm) referenced to residual protio solvent peaks (^1H and $^{13}C\{^1H\}$), external 85% H_3PO_4 ($^{31}P\{^1H\}$) and external $BF_3 \cdot OEt_2$ solution ($^{11}B\{^1H\}$). Elemental analyses were performed by the Lakehead University Instrumentation Laboratory. All column dimensions are reported as (length x width). 1-(4-bromobenzyl)-1H-benzimidazole,[38] [Li(THF)$_2$][**1a**],[36] PdCl$_2$(TMEDA),[39] [Pd(cinnamyl)Cl]$_2$,[20] and Pd$_2$(dba)$_3 \cdot$CHCl$_3$[40] were prepared according to established literature procedures.

X = Br, n = 0; R = t-Bu
X = BPh$_3$, n = -1; R = Ph or t-Bu

Figure 3.1. Numbering schemes for 1-(4-bromobenzyl)-2-(di-*tert*-butylphosphino)-1H-benzimidazole, [Li(THF)$_4$][**1b**], [PPh$_4$][**1b**], 1-methylbenzimidazole, **2**, **6**, **9**, **10,** and **13**.

3.2 Synthesis of 1-(4-bromobenzyl)-2-(di-*tert*-butylphosphino)-1H-benzimidazole

The following procedure was adapted from the literature.[36] Lithium diisopropylamide (LDA) was first prepared by dissolving diisopropylamine (0.732 mL, 5.22 mmol) in THF (5 mL) and cooling it to -78 °C, after which n-BuLi (3.3 mL of a 1.6 M solution in hexanes, 5.22 mmol) was added dropwise via syringe over ~1 min. The LDA was generated over 1 h at -78 °C. The LDA was then added via cannula over ~1 min to a flask containing 1-(4-bromobenzyl)benzimidazole (1.50 g, 5.22 mmol) in THF (30 mL) cooled to -90 °C, using additional THF (5 mL) to ensure quantitative transfer. The clear, red-orange solution was stirred for 1 h between -80 °C and -90 °C, after which time (t-Bu)$_2$PCl (0.992 mL, 5.22 mmol) was added dropwise via syringe over ~1 min, yielding a clear, dark orange solution. The solution was then allowed to warm up to room temperature in the bath overnight, lightening to a cloudy, orange mixture. The volatiles were removed under reduced pressure, yielding a yellow-orange solid. The product was extracted into CH$_2$Cl$_2$ (2 x 25 mL) and filtered through Celite. The clear, orange filtrate was stripped of its volatiles, yielding a tacky, orange oil. The oil was redissolved in CH$_2$Cl$_2$ (30 mL) and filtered through a 3.5 x 4 cm column of silica. The volatiles were removed from the clear, pale yellow filtrate, yielding a sticky, yellow oil. The oil was allowed to dry under reduced pressure for several days, affording a crystalline, yellow solid. Yield: 1.69 g (75%). ^{1}H NMR (500 MHz, CDCl$_3$): δ 7.85 (broad s, 1H, C^8*H*), 7.30 (d, 2H, $^3J_{HH}$ = 8.1 Hz, C$^{3'}$*H* and C$^{5'}$*H*), 7.19, 7.13 (both t, 1H, $^3J_{HH}$ = 7.4 Hz, C^6*H* and C^7*H*), 7.08 (d, 1H, $^3J_{HH}$ = 7.9 Hz, C^5*H*), 6.86 (d, 2H, $^3J_{HH}$ = 8.1 Hz, C$^{2'}$*H* and C$^{6'}$*H*), 5.67 (d, 2H, $^4J_{PH}$ = 3.8 Hz, –C*H*$_2$–), 1.18 (d, 18H, $^3J_{PH}$ = 12.8 Hz, –C(C*H*$_3$)$_3$) ppm. ^{13}C{^{1}H} NMR (125 MHz, CDCl$_3$): δ 153.7 (d, $^1J_{PC}$ = 25 Hz, *C*^{2}), 143.0 (s, *C*^{4}) 134.6 (s, *C*$^{1'}$), 133.7 (s, *C*^{9}), 130.7, 127.2 (both s, *C*$^{2'}$, *C*$^{3'}$, *C*$^{5'}$ and *C*$^{6'}$), 122.1, 121.3 (both s, *C*^{6} and *C*^{7}), 120.3 (s, *C*$^{4'}$), 119.4 (s, *C*^{5}), 109.5 (s, *C*^{8}), 46.7 (d, $^3J_{PC}$ = 19.6 Hz, –*C*H$_2$–), 32.5 (d, $^1J_{PC}$

= 16.2 Hz, $-C(CH_3)_3$), 29.1 (d, $^2J_{PC}$ = 14.1 Hz, $-C(CH_3)_3$) ppm. ^{31}P{^{1}H} NMR (202 MHz, CDCl$_3$):

δ 5.8 (s, $-P$(t-Bu)$_2$) ppm.

3.3 Synthesis of [Li(THF)₄][1b]

The following procedure was adapted from the literature.[35] 1-(4-bromobenzyl)-2-(di-*tert*-butylphosphino)benzimidazole (1.00 g, 2.32 mmol) was dissolved in THF (30 mL) and cooled to -80 ºC. t-BuLi (1.4 mL of a 1.7 M pentane solution, 2.32 mmol) was added dropwise via syringe to the cooled solution over 2-3 min., affording a clear, dark orange solution upon complete addition. The solution was allowed to stir for 1 h between -80 ºC and -90 ºC, after which time a solution of BPh$_3$ in THF (10.9 mL of a 0.213 M solution, 2.32 mmol) was added dropwise via syringe to the cooled solution over 30 min, causing a slight lightening in colour upon complete addition. The solution was stirred at -90 ºC for 2 h, then allowed to warm up to room temperature in the bath overnight. The next day, excess hexanes (~100 mL) was added to the stirring, light orange solution, precipitating an orange oil. Then, stirring was discontinued and the mixture was allowed to stand for ~3 h, after which time the clear, light yellow supernatant was decanted, and the oil was washed with hexanes (2 x 10 mL). Drying under reduced pressure, afforded a pale yellow solid. Yield: 1.17 g (57%). ^{1}H NMR (500 MHz, CDCl$_3$): δ 7.76 (d, 1H, $^3J_{HH}$ = 7.9 Hz, C^8H), 7.45 (broad s, 6H, *ortho*-H of $-$BPh$_3$), 7.33 (d, 2H, $^3J_{HH}$ = 7.7 Hz, C$^{3'}$$H$ and C$^{5'}$$H$), 7.21–7.14 (overlapping m, 3H, C^5H-C^7H), 7.08 (t, 6H, $^3J_{HH}$ = 7.4 Hz, *meta*-H of $-$BPh$_3$), 6.95-6.91 (overlapping m, 5H, *para*-H of $-$BPh$_3$, C$^{2'}$$H$ and C$^{6'}$$H$), 5.67 (d, 2H, $^4J_{PH}$ = 3.7 Hz, $-CH_2-$), 3.52 (m, 16H, THF), 1.79 (m, 16H, THF), 1.23 (d, 18H, $^3J_{PH}$ = 12.6 Hz, $-C(CH_3)_3$) ppm. ^{13}C{^{1}H} NMR (125 MHz, CD$_2$Cl$_2$): δ 163.7 (q, $^1J_{BC}$ = 49.0 Hz, *ipso*-C of $-$BPh$_3$), 154.8 (d, $^1J_{PC}$ = 32.8 Hz, C^2), 141.9 (s, C^4), 135.8 (s, $C^{1'}$), 135.7 (s, *ortho*-C of $-$BPh$_3$), 135.0 (s, C^9), 129.6, 127.3 (both s $C^{2'}$, $C^{3'}$, $C^{5'}$ and $C^{6'}$), 126.0 (s, *meta*-H of $-$BPh$_3$), 123.5, 122.9 (both s, C^6 and C^7), 122.1 (s, *para*-C

of $-B$Ph$_3$), 118.3 (s, C^5) 111.9 (s, C^8), 68.3 (s, THF), 49.5 (d, $^3J_{PC}$ = 18.3 Hz, $-CH_2-$), 33.6 (d, $^1J_{PC}$ = 18.1 Hz, $-C(CH_3)_3$), 30.0 (d, $^2J_{PC}$ = 14.3 Hz, $-C(CH_3)_3$), 25.4 (s, THF) ppm. Note that the expected quartet corresponding to $C^{4'}$ could not be observed, despite multiple attempted acquisitions. ^{31}P{^{1}H} NMR (202 MHz, CDCl$_3$): δ 6.2 (s, $-P$(t-Bu)$_2$) ppm. ^{11}B{^{1}H} NMR (160 MHz, CDCl$_3$): δ -6.7 (s, $-B$Ph$_3$) ppm.

3.4 Synthesis of [PPh$_4$][1b]

A slight excess of PPh$_4$Br (0.122 g, 0.291 mmol) was added all at once, as a solid, to a stirring, pale yellow suspension of [Li(THF)$_4$][**1b**] (0.235 g, 0.264 mmol) in CH$_2$Cl$_2$ (10 mL), causing the precipitation of a white solid (LiBr). The resulting cloudy, off-white mixture was then stirred for 4 h, after which time it was filtered through Celite. The volatiles of the clear, pale yellow filtrate were then removed under reduced pressure, affording an off-white solid. The solid was washed with MeOH (10 mL) and dried under vacuum. Yield: 0.210 g (85%). ^{1}H NMR (500 MHz, CDCl$_3$): δ 7.69 (d, 1H, $^3J_{HH}$ = 8.1 Hz, C^8H), 7.62-7.58 (m, 4H, *para*-H of Ph$_4$P$^+$), 7.43-7.39 (m, 8H, *meta*-H of Ph$_4$P$^+$), 7.26-7.22 (overlapping m, 10H, *ortho*-H of Ph$_4$P$^+$, C$^{3'}$$H$ and C$^{5'}$$H$), 7.20-7.17 (m, 6H, *ortho*-H of $-B$Ph$_3$), 7.13-7.10 (overlapping m, 3H, C^5H- C^7H), 6.78 (t, 6H, $^3J_{HH}$ = 7.4 Hz, *meta*-H of $-B$Ph$_3$), 6.73 (d, 2H, $^3J_{HH}$ = 7.9 Hz, C$^{2'}$$H$ and C$^{6'}$$H$), 6.65 (t, 3H, $^3J_{HH}$ = 7.1 Hz, *para*-H of $-B$Ph$_3$), 5.58 (d, 2H, $^4J_{PH}$ = 4.0 Hz, $-CH_2-$), 1.15 (d, 18H, $^3J_{PH}$ = 12.5 Hz, $-C(CH_3)_3$) ppm. ^{13}C{^{1}H} NMR (125 MHz, CD$_2$Cl$_2$): δ 163.0 (q, $^1J_{BC}$ = 49.1 Hz, *ipso*-C of $-B$Ph$_3$), 154.4 (d, $^2J_{PC}$ = 23.3 Hz, C^2), 143.5 (s, C^4), 135.1 (broad s, *ortho*-C of $-B$Ph$_3$ and $C^{1'}$), 134.9 (s, *para*-C of Ph$_4$P$^+$ and C^9), 133.5 (d, $^2J_{PC}$ = 10.4 Hz, *ortho*-C of Ph$_4$P$^+$), 129.8 (d, $^3J_{PC}$ = 12.9 Hz, *meta*-C of Ph$_4$P$^+$), 129.2, 126.9 (both s $C^{2'}$, $C^{3'}$, $C^{5'}$ and $C^{6'}$), 124.7 (broad s, *meta*-C of $-B$Ph$_3$), 121.5 (s, C^6 or C^7), 120.9 (s, *para*-C of $-B$Ph$_3$), 120.6 (s, C^6 or C^7), 116.6 (d, $^1J_{PC}$ = 89.6 Hz, *ipso*-C of Ph$_4$P$^+$), 118.7 (s, C^5), 110.6 (s, C^8), 48.2 (d, $^3J_{PC}$ = 18.2 Hz, $-CH_2-$), 32.6 (d, $^1J_{PC}$ = 17.3 Hz, $-C(CH_3)_3$),

29.2 (d, $^2J_{PC}$ = 14.3 Hz, –C(CH_3)$_3$) ppm. The expected quartet corresponding to C$^{4\prime}$ appears to be buried beneath the quartet corresponding to the *ipso*-carbons of the –BPh$_3$ group, making exact peak identification difficult. ^{31}P{^{1}H} NMR (202 MHz, CDCl$_3$): δ 23.0 (s, Ph$_4$$P^+$), 5.8 (s, $-P$(t-Bu)$_2$) ppm. ^{11}B{^{1}H} NMR (160 MHz, CDCl$_3$): δ -6.7 (s, –BPh$_3$) ppm.

3.5 Synthesis of 1-methylbenzimidazole

The following procedure was adapted from the literature.[38] KO(t-Bu) (1.04 g, 9.31 mmol) was added all at once, as a solid, to a stirring solution of benzimidazole (1.00 g, 8.46 mmol) in THF (50 mL), affording a white precipitate. The cloudy, white mixture was allowed to stir for 1 h, after which time MeI (1.05 mL, 16.93 mmol) was added dropwise via syringe, with no apparent change. After the addition, the mixture was allowed to stir for 1 h, after which time the volatiles were removed via rotary evaporation, yielding a white solid. The solid was extracted into CH$_2$Cl$_2$ (2 x 30 mL) and filtered through Celite. The volatiles were removed from the clear, light yellow filtrate, yielding a yellow liquid. Yield: 0.790 g (71%). 1H NMR (500 MHz, CDCl$_3$): δ 7.76-7.74 (m, 1H, C^8H), 7.71 (s, 1H, C^2H), 7.23-7.20 (m, 3H, C^5H–C^7H), 3.63 (s, 3H, –CH_3) ppm. ^{13}C{^{1}H} NMR (125 MHz, CDCl$_3$): δ 143.5 (s, C^2), 143.4 (s, C^4), 134.4 (s, C^9), 122.8, 121.9 (both s, C^6 and C^7), 119.8 (s, C^5), 109.4 (s, C^8), 30.8 (s, $-CH_3$) ppm.

3.6 Synthesis of 2-(di-*tert*-butylphosphino)-1-methylbenzimidazole, 2

The title compound was prepared in a similar manner to 1-(4-bromobenzyl)-2-(di-*tert*-butylphosphino)-1H-benzimidazole. Lithium diisopropylamide (LDA) was first prepared by dissolving diisopropylamine (536 µL, 3.82 mmol) in THF (3 mL) and cooling it to -78 ºC, after which n-BuLi (2.4 mL of a 1.6 M solution in hexanes, 3.82 mmol) was added dropwise via syringe over ~1-2 min. The LDA was generated over 1 h at -78 ºC. The LDA was then added via cannula over ~2 min. to a flask containing 1-methylbenzimidzole (0.505 g, 3.82 mmol) in THF (20 mL)

cooled to -85 ºC, using additional THF (5 mL) to ensure quantitative transfer. The cloudy, yellow

mixture was stirred for 1 h between -80 ºC and -85 ºC, after which time (t-Bu)$_2$PCl (726 μL, 3.82

mmol) was added dropwise via syringe over ~1-2 min, yielding a cloudy, dark orange-brown

mixture. The solution was then allowed to warm to room temperature in the bath overnight,

lightening to a cloudy, yellow-brown mixture. The volatiles were removed under reduced pressure,

yielding a yellow-brown oil. The product was extracted into CH$_2$Cl$_2$ (2 x 15 mL) and filtered

through a column of silica (4 x 2 cm). The clear, yellow filtrate was stripped of its volatiles,

yielding a yellow oil. The oil was redissolved in CH$_2$Cl$_2$ (10 mL) and filtered through silica (5 x 2

cm), eluting with additional CH$_2$Cl$_2$ (30 mL). The volatiles were removed from the clear, pale

yellow filtrate, yielding a pale yellow solid. Yield: 0.470 g (45%). ^{1}H NMR (500 MHz, CDCl$_3$): δ

7.80 (d, 1H, $^3J_{HH}$ = 7.4 Hz, C^8H), 7.30 (d, 1H, $^3J_{HH}$ = 7.3 Hz, C^5H), 7.24-7.20 (overlapping m, 2H,

C^6H and C^7H), 3.93 (s, 3H, –CH_3), 1.21 (d, 18H, $^3J_{PH}$ = 12.7 Hz, –C(CH_3)$_3$) ppm. ^{13}C{^{1}H} NMR

(125 MHz, CDCl$_3$): δ 153.6 (d, $^1J_{PC}$ = 22.1 Hz, C^2), 142.9 (s, C^4), 134.7 (s, C^9), 121.5, 120.8 (both

s, C^6 and C^7), 119.2 (s, C^5), 108.6 (s, C^8), 32.4 (d, $^1J_{PC}$ = 15.9 Hz, –C(CH$_3$)$_3$), 29.1 (d, $^2J_{PC}$ = 14.3

Hz, –C(CH_3)$_3$), 25.4 (s, –CH$_3$) ppm. ^{31}P{^{1}H} NMR (202 MHz, CDCl$_3$): δ 6.0 (s, –P(t-Bu)$_2$) ppm.

3.7 Synthesis of Phosphine Selenides 3-5

This procedure was adapted from the literature.[13b] Each phosphinobenzimidazole was

combined with a three-fold excess of selenium in an NMR tube and dissolved in CDCl$_3$ (0.5 mL).

The solution was then heated at 60 °C for 3 h. After cooling to room temperature, the ^{31}P{^{1}H}

NMR spectrum of each solution was taken, and conversion to the appropriate phosphine selenide

was confirmed. The chemical shifts and $^1J_{PSe}$ coupling constants for selenides **3-5** can be found in

Table 4.1.

3.8 Synthesis of [(κ²-1a)PdCl(κ¹-TMEDA)], 6

CH_2Cl_2 (20 mL) was added to a mixture of $PdCl_2$(TMEDA) (0.075 g, 0.256 mmol) and [Li(THF)$_2$][**1a**] (0.200 g, 0.256 mmol) yielding a cloudy orange mixture, which quickly changed to cloudy yellow after several minutes. The mixture was allowed to stir for 1 h. After this time, the now cloudy orange mixture was filtered through Celite, and the volatiles were removed from the clear orange filtrate under reduced pressure, yielding a powdery, orange solid. The solid was then washed with Et_2O (2 x 10 mL) and dried under vacuum. Yield: 0.162 g (71%). Anal. Calcd. for $C_{50}H_{51}BClN_4PPd$: C, 67.4; H, 5.77; N, 6.28. Found: C, 67.8; H, 5.71; N, 5.51. ^1H NMR (500 MHz, $CDCl_3$): δ 7.98-6.87 (overlapping m, 33H, Ph of $-PPh_2$ and $-BPh_3$, C^5H–C^8H, $C^{3'}H$ and $C^{5'}H$), 6.83 (d, 2H, $^3J_{HH}$ = 7.8 Hz, $C^{2'}H$ and $C^{6'}H$), 5.82 (s, 2H, $-CH_2-$), 2.39 (broad s, 6H, $-N(CH_3)_2$), 2.18 (broad s, 4H, $-CH_2CH_2-$), 1.35 (broad s, 6H, $-N(CH_3)_2$) ppm. $^{13}C\{^1H\}$ NMR (125 MHz, CD_2Cl_2): δ 163.4-162.1 (overlapping q, *ipso*-C of $-BPh_3$ and $C^{4'}$), 154.2 (d, $^1J_{PC}$ = 21.3 Hz, C^2), 142.2 (s, C^4), 135.8-121.2 (Ph, $C^{1'}$–$C^{3'}$, $C^{5'}$, $C^{6'}$, and C^9), 120.0 (s, C^6 and C^7), 114.5 (s, C^5), 111.3 (s, C^8), 67.0 (s, $-N(CH_3)_2$), 61.8 (s, $-N(CH_3)_2$), 43.3 (broad s, $-CH_2CH_2-$) ppm. $^{31}P\{^1H\}$ NMR (202 MHz, $CDCl_3$): δ 7.9 (s, $-PPh_2$) ppm. $^{11}B\{^1H\}$ NMR (160 MHz, $CDCl_3$): δ -6.6 (s, $-BPh_3$) ppm.

3.9 Reaction of [Pd(cinnamyl)Cl]₂ and [Li(THF)₄][1b] in CH₂Cl₂: Formation of Complex 7

CH_2Cl_2 (5 mL) was added to a mixture of [Li(THF)$_4$][**1b**] (37 mg, 0.042 mmol) and [Pd(cinnamyl)Cl]$_2$ (11 mg, 0.021 mmol), yielding a cloudy orange mixture. The mixture was stirred for 1 h, after which time a sample was analyzed by $^{31}P\{^1H\}$ NMR spectroscopy, revealing two singlets at 64.6 and 53.9 ppm in a ~4:1 ratio. The mixture was then filtered through Celite, and the volatiles were removed under reduced pressure, yielding an orange-brown solid. NMR spectroscopic analyses revealed a complex mixture of products in the $^{31}P\{^1H\}$ NMR spectrum.

3.10 Synthesis of Complex 8

3.10.1 Method A: Reaction of [Pd(cinnamyl)Cl]₂ and [Li(THF)₄][1b] in Benzene

Benzene (5 mL) was added to a mixture of [Li(THF)₄][**1b**] (50 mg, 0.056 mmol) and [Pd(cinnamyl)Cl]₂ (15 mg, 0.028 mmol), yielding a cloudy, orange mixture. The mixture was allowed to stir for 3.5 h, after which time a sample of the reaction mixture was taken and analyzed via $^{31}P\{^1H\}$ NMR spectroscopy, revealing a singlet at 34.2 ppm (**8**). The mixture was then filtered through Celite, washing with benzene (2 x 2 mL), and the volatiles were removed from the clear, orange filtrate, yielding an oily orange solid. $^{31}P\{^1H\}$ NMR (202 MHz, C₆D₆): δ 55.9 (s, **8′**) ppm. The peak intensities in the ^1H NMR spectrum were very weak, preventing accurate peak designation. No signal was apparent in the $^{11}B\{^1H\}$ NMR spectrum.

3.10.2 Method B: Reaction of [Pd(cinnamyl)Cl]₂ and [Li(THF)₄][1b] in Fluorobenzene

Fluorobenzene (5 mL) was added to a mixture of [Li(THF)₄][**1b**] (50 mg, 0.056 mmol) and [Pd(cinnamyl)Cl]₂ (15 mg, 0.028 mmol), yielding a cloudy, orange mixture. The mixture was placed in a pre-heated, oil bath and heated at 40 °C for 2 h, after which time a sample of the reaction mixture was taken and analyzed via $^{31}P\{^1H\}$ NMR spectroscopy, revealing singlets at 34.2 (**8**) and 31.0 ppm in a ~3:1 ratio. The mixture was removed from the bath and allowed to cool to room temperature. Then, the mixture was filtered through Celite, and the volatiles were removed from the clear, orange filtrate, yielding an orange-brown solid. Both the ^1H and $^{31}P\{^1H\}$ NMR spectra revealed that a mixture of products had formed upon work-up.

3.11 Reaction of [Pd(cinnamyl)Cl]₂ and [PPh₄][1b]: Synthesis of Complex 9

THF (10 mL) was added to a mixture of [PPh₄][**1b**] (0.180 mg, 0.19 mmol) and [Pd(cinnamyl)Cl]₂ (0.050 mg, 0.097 mmol), yielding a clear, dark yellow solution. The solution was allowed to stir for 4 h, after which the volatiles were removed under reduced pressured,

affording a yellow solid. Recrystallization of the solid using CH_2Cl_2/hexanes (5/20 mL) afforded an orange/yellow oil. The clear, pale yellow supernatant was removed via cannula, and the oil was dried under reduced pressure, yielding a yellow-orange solid. ^{1}H NMR (500 MHz, CDCl$_3$): δ 7.81 (broad s, 1H, C^8H), 7.77-7.75 (m, 6H, *para*-H of Ph$_4$P$^+$ and *ortho*-H of cinnamyl Ph), 7.59-7.56 (m, 8H, *meta*-H of Ph$_4$P$^+$), 7.43-7.39 (overlapping m, 13H, *ortho*-H of Ph$_4$P$^+$, C$^{3'}$$H$, C$^{5'}$$H$ and *meta*-H and *para*-H of cinnamyl Ph), 7.32 (broad s, 6H, *ortho*-H of −BPh$_3$), 7.06-7.00 (overlapping m, 3H, C^5H-C^7H), 6.86 (t, 6H, $^3J_{HH}$ = 6.9 Hz, *meta*-H of −BPh$_3$), 6.74 (t, 3H, $^3J_{HH}$ = 7.0 Hz, *para*-H of −BPh$_3$), 6.68-6.64 (m, 1H, allyl CH), 6.58-6.56 (m, 3H, C$^{2'}$$H$, C$^{6'}$$H$ and allyl CH), 5.31 (d, 2H $^4J_{PH}$ = 17.2 Hz, −CH$_2$−), 3.63-3.62 (m, 1H, allyl CH), 2.60-2.57 (m, 1H, allyl CH), 1.69 (d, 9H $^3J_{PH}$ = 15.0 Hz, −C(CH_3)$_3$), 1.45 (d, 9H, $^3J_{PH}$ = 14.6 Hz, −C(CH_3)$_3$) ppm. ^{31}P{^{1}H} NMR (202 MHz, CDCl$_3$): δ 45.9 (s, −P(t-Bu)$_2$), 23.1 (s, Ph$_4$$P^+$) ppm. ^{11}B{^{1}H} NMR (160 MHz, CDCl$_3$): δ -6.7 (s, −BPh$_3$) ppm. Several attempts were made to acquire a ^{13}C NMR spectrum of the title compound, however decomposition of the complex was observed to occur over time, preventing its accurate characterization via this method.

3.12 Synthesis of [PPh$_4$][PdCl$_2$(κ^2-1b)], 10

To a clear, yellow solution of PdCl$_2$(COD) (30.6 mg, 0.107 mmol) in CH$_2$Cl$_2$ (5 mL) was added [PPh$_4$][**1b**] (100. mg, 0.107 mmol) all at once as a solid, resulting in a clear, dark yellow solution. The solution was allowed to stir for 1 h, after which time the volatiles were removed under reduced pressure yielding a powdery, yellow solid. The solid was washed with hexanes (2 x 5 mL), followed by Et$_2$O (2 x 5 mL) and dried under vacuum. Yield: 96 mg (81%). Anal. Calcd. for C$_{64}$H$_{63}$BCl$_2$N$_2$P$_2$Pd•0.5CH$_2$Cl$_2$: C, 67.2; H, 5.60; N, 2.43. Found: C, 67.8; H, 5.77; N, 2.17. ^{1}H NMR (500 MHz, CDCl$_3$): δ 8.32 (d, 1H, $^3J_{HH}$ = 6.3 Hz, C^8H), 7.73 (t, 4H, $^3J_{HH}$ = 7.6 Hz, *para*-H of Ph$_4$P$^+$), 7.61-7.57 (m, 8H, *meta*-H of Ph$_4$P$^+$), 7.45-7.41 (overlapping m, 10H, *ortho*-H of Ph$_4$P$^+$,

$C^{3\prime}H$ and $C^{5\prime}H$), 7.29 (broad s, 3H, C^5H-C^7H), 7.25-7.19 (m, 6H, *ortho*-H of −BPh₃), 6.88 (t, 6H,

$^3J_{HH}$ = 7.3 Hz, *meta*-H of −BPh₃), 6.75 (t, 3H, $^3J_{HH}$ = 7.1 Hz, *para*-H of −BPh₃), 6.57 (d, 2H, $^3J_{HH}$

= 7.8 Hz, $C^{2\prime}H$ and $C^{6\prime}H$), 5.42 (s, 2H, −CH_2−), 1.49 (d, $^3J_{PH}$ = 17.5 Hz, −C(CH_3)₃) ppm. $^{13}C\{^1H\}$

NMR (125 MHz, CD₂Cl₂): δ 165.2 (q, $^1J_{BC}$ = 48 Hz, $C^{4\prime}$), 162.5 (q, $^1J_{BC}$ = 49 Hz, *ipso*-C of −BPh₃),

152.4 (d, $^2J_{PC}$ = 24.6 Hz, C^2), 139.1 (d, $^3J_{PC}$ = 8.9 Hz, C^4), 135.9 (s, $C^{1\prime}$), 135.0 (broad s, *ortho*-C

of −BPh₃), 134.9 (s, *para*-C of Ph₄P⁺), 133.6 (d, $^2J_{PC}$ = 10.3 Hz, *ortho*-C of Ph₄P⁺), 129.8 (d, $^3J_{PC}$

= 12.9 Hz, *meta*-C of Ph₄P⁺), 127.8, 125.9 (both s, $C^{2\prime}$, $C^{3\prime}$, $C^{5\prime}$ and $C^{6\prime}$), 125.1 (s, C⁶ or C⁷), 124.9

(broad s, *meta*-C of −BPh₃), 124.5 (s, C⁶ or C⁷), 121.2 (s, *para*-C of −BPh₃), 118.6 (s, C^5), 116.6

(d, $^1J_{PC}$ = 89.6 Hz, *ipso*-C of Ph₄P⁺), 112.0 (s, C^8), 50.5 (s, −CH_2−), 37.8 (d, $^1J_{PC}$ = 8.7 Hz,

−C(CH₃)₃), 28.9 (s, $^2J_{PC}$ = 3.9 Hz, −C(CH₃)₃) ppm. $^{31}P\{^1H\}$ NMR (202 MHz, CDCl₃): δ 37.9 (s,

−P(t-Bu)₂), 23.1 (s, Ph₄P⁺) ppm. $^{11}B\{^1H\}$ NMR (160 MHz, CDCl₃): δ -6.7 (s, −BPh₃) ppm.

3.13 Reaction of Pd₂(dba)₃•CHCl₃ and [PPh₄][1b]: Formation of Complexes 11 and 12

In an NMR tube, [PPh₄][1b] (10 mg, 0.011 mmol) and Pd₂(dba)₃•CHCl₃ (5.5 mg, 0.0053

mmol) were combined and dissolved in 0.5 mL CH₂Cl₂, yielding a clear, dark red solution. The

solution was monitored via $^{31}P\{^1H\}$ NMR spectroscopy over time, revealing the formation of

complex **11** after ~1 h (δ = 34.5 and 22.9 ppm, both singlets), as well as unreacted ligand. After

~24 h, complete conversion to complex **12** was observed (δ = 39.4 and 24.3 ppm, both doublets,

$^2J_{PP}$ = 345 Hz).

3.14 Synthesis of [PdCl₂(κ²-2)], 13

To a clear, yellow solution of PdCl₂(COD) (77 mg, 0.27 mmol) in CH₂Cl₂ (5 mL) was

added ligand **3** (75 mg, 0.27 mmol) all at once, as a solid, yielding a clear, yellow-orange solution.

The solution was allowed to stir for 24 h, after which time, the stirring was discontinued, and

hexanes (20 mL) was layered onto the yellow solution. The next day, the supernatant liquid was

decanted and the resulting orange crystalline solid was washed with Et_2O (2 x 10 mL) and dried

under reduced pressure. Yield: 92 mg (75%). Anal. Calcd. for $C_{16}H_{25}Cl_2N_2PPd$: C, 42.4; H, 5.55;

N, 6.17. Found: C, 42.4; H, 5.38; N, 6.15. ^1H NMR (500 MHz, $CDCl_3$): δ 8.37 (d, 1H, $^3J_{HH}$ = 8.3

Hz, C^8H), 7.68 (d, 1H, $^3J_{HH}$ = 8.3 Hz, C^5H), 7.51, 7.42 (both t, 1H, $^3J_{HH}$ = 7.8 Hz, C^6H and C^7H),

4.16 (s, 3H, $-CH_3$), 1.67 (d, 18H, $^3J_{PH}$ = 17.4 Hz, $-C(CH_3)_3$) ppm. $^{13}C\{^1H\}$ NMR (125 MHz,

$CDCl_3$): δ 152.7 (d, $^1J_{PC}$ = 25.6 Hz, C^2), 139.4 (d, $^3J_{PC}$ = 8.7 Hz, C^4), 133.3 (s, C^9), 125.6, 119.9

(both s, C^6 and C^7), 117.0 (s, C^5), 111.2 (s, C^8), 38.3 (d, $^1J_{PC}$ = 9.2 Hz, $-C(CH_3)_3$), 31.1 (s, $-CH_3$),

30.0 ($^2J_{PC}$ = 3.9 Hz, $-C(CH_3)_3$) ppm. $^{31}P\{^1H\}$ NMR (202 MHz, $CDCl_3$): δ 35.4 (s, $-P$(t-Bu)$_2$) ppm.

3.15 Buchwald-Hartwig Amination of Bromobenzene with Aniline: Catalyst Optimization

The palladium precursor (0.006 mmol, 1 mol%), [Li(THF)$_4$][**1b**] (10.7 mg, 0.012 mmol, 2

mol%), and base (0.9 mmol) were loaded into a Schlenk tube, followed by the consecutive addition

of bromobenzene (63 μL, 0.6 mmol), aniline (66 μL, 0.72 mmol), and the appropriate solvent (2

mL) via syringe. The mixture was stirred at room temperature for 1 min., then placed in a pre-

heated oil bath set to the desired temperature, or allowed to react under ambient conditions. After

the designated time, the mixture was removed from the bath and cooled to room temperature (if

necessary), diluted with EtOAc (5 mL), and filtered through silica (1 x 4 cm, ~10 mL), eluting

with EtOAc (20 mL) or until the filtrate ran clear. The volatiles were removed from the filtrate via

rotary evaporation, and analyzed for conversion to diphenylamine using ^1H NMR spectroscopy

($CDCl_3$).

3.16 General Procedure for the Buchwald-Hartwig Amination of Aryl Bromides with Amines Using a Pd/[Li(THF)₄][1b] Catalyst System (General Procedure A)

[Pd(cinnamyl)Cl]$_2$ (3.1 mg, 0.006 mmol), [Li(THF)$_4$][**1b**] (10.7 mg, 0.012 mmol), and

KO(t-Bu) (81 mg, 0.72 mmol) were loaded into a Schlenk tube. If a solid aryl bromide or amine

was used, it was also added at this time. To the mixture of solids, aryl bromide (0.6 mmol) and amine (0.72 mmol) were added via syringe (if liquid), followed by toluene (2 mL). The resulting mixture was stirred at room temperature for 1 min., then placed in a pre-heated, 80 °C oil bath and allowed to react for 12 h. After this time, the mixture was removed from the bath and cooled to room temperature, diluted with EtOAc (5 mL), and filtered through silica (1 x 4 cm column, ~10 mL), eluting with EtOAc (20 mL) or until the filtrate ran clear. The volatiles were removed from the filtrate via rotary evaporation and the resulting residue was subjected to flash chromatography on silica gel (8 x 2 cm column, ~25 mL silica). The characterization and yields of the coupled products can be found in Appendix A.

3.17 General Procedure for the Buchwald-Hartwig Amination of Aryl Bromides with Amines Using a Pd/2 Catalyst System (General Procedure B)

General Procedure A was followed with the exception of using **2** (3.3 mg, 0.012 mmol) as ligand. The characterization and yields of the coupled products can be found in Appendix A.

3.18 General Procedure for the Buchwald-Hartwig Amination of Aryl Bromides with Amines Using a Pd/[PPh4][1b] Catalyst System (General Procedure C)

General Procedure A was followed with the exception of using [PPh$_4$][**1b**] (11.2 mg, 0.012 mmol) as ligand. The characterization and yields of the coupled products can be found in Appendix A.

3.19 Reaction of NiCl$_2$(DME) and [Li(THF)$_4$][1b]: Formation of Complex 14

CH$_2$Cl$_2$ (5 mL) was added to a mixture of [Li(THF)$_4$][**1b**] (81 mg, 0.091 mmol) and NiCl$_2$(DME) (20 mg, 0.091 mmol), yielding a cloudy, yellow mixture. Over time, the NiCl$_2$(DME) slowly dissolved and a white precipitate was observed to form. The mixture was allowed to stir overnight, with no apparent change. Then, the mixture was filtered through Celite, and the volatiles

were removed from the resulting opaque, yellow filtrate under reduced pressure, yielding an off-white solid. ^{1}H NMR (500 MHz, CDCl$_3$): δ 7.77-6.66 (overlapping m, 23H, C^{5}H-C^{8}H, C$^{2\prime}$H, C$^{3\prime}$H, C$^{5\prime}$H, C$^{6\prime}$H and Ph of –BPh$_3$), 5.62 (s, 2H, –CH$_2$–), 3.68 (s, residual THF), 3.42 (s, DME), 3.25 (s, DME), 1.79 (s, residual THF), 1.05 (d, 18H, $^3J_{PH}$ = 13.3 Hz, –C(CH$_3$)$_3$) ppm. ^{31}P{^{1}H} NMR (202 MHz, CDCl$_3$): δ 10.1 (s, **14**) ppm. ^{11}B{^{1}H} NMR (160 MHz, CDCl$_3$): δ -6.6 (s, –BPh$_3$) ppm.

3.20 General Procedure for the Attempted Ni-Catalyzed C-N Bond Formation of Chlorobenzene and Aniline

NiCl$_2$(DME) (0.011 g, 0.05 mmol, 5 mol%), [Li(THF)$_4$][**1b**] (0.044 g, 0.05 mmol, 5 mol%), and KO(t-Bu) (1.5 mmol, 0.168 g) were loaded into a Schlenk tube. PhB(OH)$_2$ (0.049 g, 0.4 mmol) was also added at this time, as applicable. This was followed by the consecutive addition of chlorobenzene (101 µL, 1.0 mmol), aniline (137 µL, 1.5 mmol), MeCN (52 µL, 1 mmol; as applicable) and the appropriate solvent (3 mL) via syringe. The mixture was then placed in a pre-heated, oil bath set to the desired temperature. After 48 h, the mixture was removed from the bath and cooled to room temperature, diluted with EtOAc or Et$_2$O (5 mL), washed with DDW (2 x 5 mL), and separated. The aqueous layer was further washed with EtOAc or Et$_2$O (2 x 5 mL). The combined organic fractions were dried using Na$_2$SO$_4$, and the supernatant liquid was decanted into a round-bottom flask. The volatiles were removed from the solution via rotary evaporation, and analyzed for conversion to diphenylamine using ^{1}H NMR spectroscopy (CDCl$_3$).

4. Results and Discussion

4.1 Synthesis of Ligands [Li(THF)₂][1a], [Li(THF)₄][1b], [PPh₄][1b], and 2

4.1.1 Synthesis of Ligands [Li(THF)₂][1a] and [Li(THF)₄][1b]

Ligands [Li(THF)$_2$][**1a**] and [Li(THF)$_4$][**1b**] share a common synthetic pathway (**Scheme 4.1**). The first step involves the coupling of benzimidazole and 4-bromobenzyl bromide using KOH. Phosphorylation of the coupled product, 1-(4-bromobenzyl)benzimidazole, at the C2-position is then accomplished through deprotonation using LDA, followed by the addition of chlorodiphenylphosphine[36] or di-*tert*-butylchlorophosphine at low temperatures. The resulting 1-(4-bromobenzyl)-2-(diphenylphosphino)-1H-benzimidazole exhibits a singlet at -28.3 ppm in its ^{31}P{^{1}H} NMR spectrum,[36] while a singlet is observed further downfield at 5.8 ppm for the *tert*-butyl analogue.
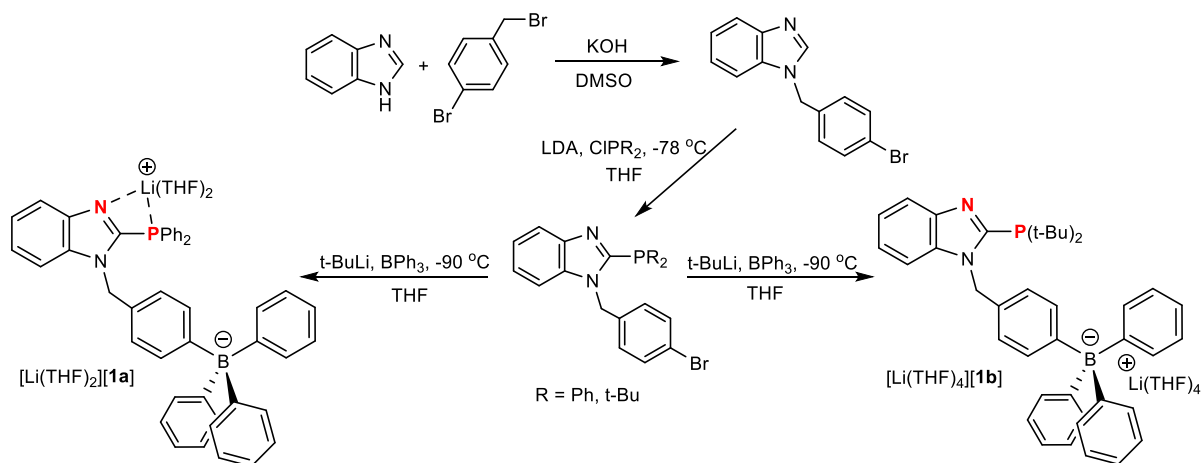
Scheme 4.1. Synthesis of ligands [Li(THF)$_2$][**1a**] and [Li(THF)$_4$][**1b**].

The final step in the synthesis involves a lithium-halogen exchange using t-BuLi, followed by the addition of BPh$_3$ at low temperatures, affording the desired [Li(THF)$_2$][**1a**] and [Li(THF)$_4$][**1b**]. The ^{11}B{^{1}H} NMR spectrum of each ligand displays a sharp singlet at -6.7 ppm, which is of similar magnitude to that observed for the anion in NaBPh$_4$ (δ = -6.2 ppm).[41] A singlet

at -24.1 ppm is observed in the $^{31}P\{^1H\}$ NMR spectrum of [Li(THF)$_2$][**1a**], a downfield shift of ~4 ppm compared to its neutral precursor.[36] Conversely, the singlet in the $^{31}P\{^1H\}$ NMR spectrum of [Li(THF)$_4$][**1b**] at 6.2 ppm is shifted only slightly downfield compared to its neutral precursor ($\Delta\delta$ = 0.4 ppm). This suggests that the chemical environment around the phosphorus atom in [Li(THF)$_2$][**1a**] has been more dramatically altered than that in [Li(THF)$_4$][**1b**], despite a similar chemical modification. Thus, it appears that the anion **1a** is in fact coordinating to the lithium centre,[35] whereas the anion **1b** forms a true ion pair with its counterion in solution. The number of THF molecules present in the solvated lithium counterion of each ligand (which is confirmed in their respective ^1H NMR spectra) is also suggestive of this – if the lithium is to be coordinatively saturated in [Li(THF)$_2$][**1a**] (as is the case in [Li(THF)$_4$][**1b**]), then chelation of **1a** to the lithium centre would see this accomplished. Indeed, $^7Li\{^1H\}$ NMR spectroscopic evidence further suggests that **1a** coordinates to the lithium centre.[36] Correspondingly, the bulkiness of the di(*tert*-butyl)phosphino group may preclude the coordination of **1b** to lithium, resulting in the observed [Li(THF)$_4$]$^+$ counterion for this ligand.

4.1.2 Synthesis of Ligand [PPh$_4$][1b]

While examining the coordination chemistry of [Li(THF)$_4$][**1b**] with palladium in order to generate a precatalyst containing **1b**, it was thought that an alternative 'source' of **1b** (*i.e.* a salt of **1b** with a different cation) might offer a more straightforward route to the desired complexes. A cation without halide-abstracting properties was considered ideal, as this would circumvent filtration and simplify work-up procedures. Also, a cation with alkyl or aryl substituents would enhance the solubility profile of the resulting **1b** salt in organic media, which might allow more facile reactions with palladium salts in solvents such as CH$_2$Cl$_2$ (in which [Li(THF)$_4$][**1b**] is only sparingly soluble). With these ideas in mind, the [PPh$_4$]$^+$ cation was considered a suitable substitute

for the [Li(THF)$_4$]$^+$ cation. Therefore, a salt metathesis was performed (**Scheme 4.2**). Two singlets at 23.0 ppm and 5.8 ppm appear in the ^{31}P{^{1}H} NMR spectrum of the new [PPh$_4$][**1b**] in ~1:1 ratio, corresponding to the tetraphenylphosphonium counterion and di(*tert*-butyl)phosphino group, respectively. The ^{1}H, ^{13}C{^{1}H} and ^{11}B{^{1}H} NMR spectroscopic features of [PPh$_4$][**1b**] are essentially identical to those of the lithium precursor, with new peaks appearing in the ^{1}H and ^{13}C{^{1}H} NMR spectra of [PPh$_4$][**1b**] corresponding to the [PPh$_4$]$^+$ cation.
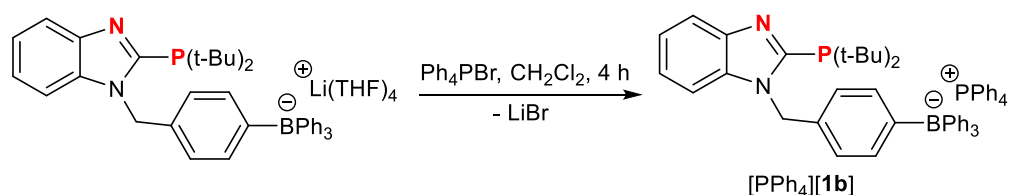
Scheme 4.2. Synthesis of ligand [PPh$_4$][**1b**].

The successful synthesis of [PPh$_4$][**1b**] prompted the preparation of [PPh$_4$][**1a**] from [Li(THF)$_2$][**1a**] through an analogous method to that presented in **Scheme 4.2**. The resulting [PPh$_4$][**1a**] exhibited two singlets in the ^{31}P{^{1}H} NMR spectrum at 23.0 and -28.2 ppm, corresponding to the tetraphenylphosphonium counterion and diphenylphosphino group respectively, in a ratio of ~3:1. Unfortunately, no appreciable change in the peak ratio was observed after multiple washings with MeOH (used to remove excess [PPh$_4$]$^+$). Given the large excess of [PPh$_4$]$^+$ present, [PPh$_4$][**1a**] was not reacted with palladium salts in an attempt to synthesize a precatalyst containing **1a**.

4.1.3 Synthesis of Ligand 2

In order to investigate the impact of using an anionic ligand in catalysis compared to an analogous neutral ligand, a neutral variant of [Li(THF)$_4$][**1b**], 2-(di-*tert*-butylphosphino)-1-methylbenzimidazole (**2**), was prepared (**Scheme 4.3**). The synthesis of **2** is similar to the two-step procedure for making 1-(4-bromobenzyl)-2-(di-*tert*-butylphosphino)-1H-benzimidazole. Firstly,

benzimidazole is methylated at the N1-position using KO(t-Bu) and methyl iodide in a procedure adapted from the literature.[38] Then, phosphorylation of 1-methylbenzimidazole at the C2-position using LDA and di-*tert*-butylchlorophosphine at low temperatures affords **2**. The essential difference between [Li(THF)$_4$][**1b**] and **2** is the replacement of the appended, anionic tetraphenylborate group in **1b** by a proton. Despite the vastly different steric and electronic properties of a proton and a tetraphenylborate group, the ^{31}P{^{1}H} NMR chemical shift of **2** does not differ greatly from that of [Li(THF)$_4$][**1b**] (δ = 6.0 ppm for **2** vs. δ = 6.2 ppm for [Li(THF)$_4$][**1b**]), which implies that the chemical environment around the phosphorus atoms in each ligand is essentially identical. This further suggests that **2** is effectively an isosteric, neutral variant of [Li(THF)$_4$][**1b**]. Thus, any differences in activity when employing **2** or [Li(THF)$_4$][**1b**] in catalysis should stem solely from the different electronic properties (*i.e.* charge) of these ligands.
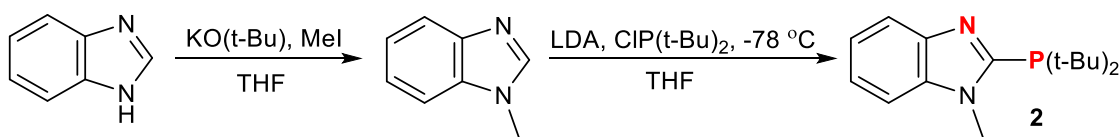
Scheme 4.3. Synthesis of ligand **2**.

4.1.4 Analyzing the Phosphine Donor Power of [Li(THF)$_4$][1b], [PPh$_4$][1b], and 2

It has been reported previously that, in some instances, anionic phosphines exhibit enhanced electron-donating abilities compared to their neutral counterparts.[13] Consequently, it was of interest to compare the electron-releasing properties of [Li(THF)$_4$][**1b**] and **2**, primarily because a more powerful electron-donating ligand will impart greater electron density to the metal to which it is coordinated, facilitating key catalytic steps such as oxidative addition.[14] Determining the electron-releasing ability of [PPh$_4$][**1b**] would also identify any counterion effects on this parameter.

The $^1J_{PSe}$ coupling constant was used to assess the electron-donating ability of the ligands. This method, which measures the apparent *s*-character of the phosphorus lone pair, has been used extensively in the literature,[42] with a larger $^1J_{PSe}$ value corresponding to a less basic phosphine. Therefore, phosphine selenides of [Li(THF)$_4$][**1b**], [PPh$_4$][**1b**], and **2** were prepared (**Scheme 4.4**) and subjected to ^{31}P{^{1}H} NMR spectroscopy. The chemical shift and $^1J_{PSe}$ coupling constant of selenides **3-5** appear in **Table 4.1**. Selenides **3-5** exhibit similar chemical shifts to related selenides of di(*tert*-butylphosphino)imidazoles ($\delta \approx$ 62-63 ppm).[31] Furthermore, the coupling constant of **3** is of similar magnitude to strongly-donating trialkylphosphines such as PMe$_3$ ($^1J_{PSe}$ = 684 Hz) or P(n-Bu)$_3$ ($^1J_{PSe}$ = 689 Hz).[42c] However, there appears to be a significant counterion effect, with the $^1J_{PSe}$ values of **3** and **4** differing by ~15 Hz.
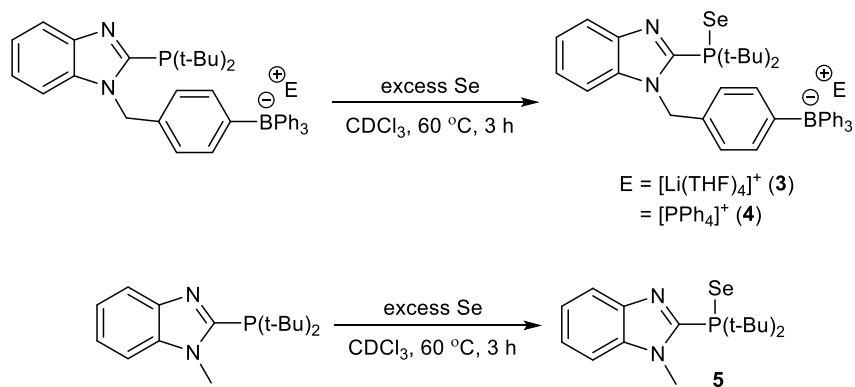
Scheme 4.4. Synthesis of phosphine selenides **3-5**.

Table 4.1. ^{31}P{^{1}H} NMR chemical shift and $^1J_{PSe}$ coupling constant data for selenides **3-5**.

Selenide	^{31}P (ppm)	$^1J_{PSe}$ (Hz)
3	63.9	688
4	64.2	704
5	64.4	705

Interestingly, the $^1J_{PSe}$ coupling constants of **4** and **5** are almost identical (704 vs. 705 Hz, respectively). This is perhaps not surprising, given the proximity of the tethered tetraphenylborate group to the phosphorus atom. Indeed, while investigating the effect of tetraphenylborate group

proximity on phosphine donor power in a series of monodentate anionic phosphines, we similarly found that the anionic group had little impact on the donating ability of the phosphine if the two moieties were separated by a large intramolecular distance (such as an aryl linker).[13b] Thus, it is likely that the anion **1b** and **2** have similar electron-donating abilities. Furthermore, the $[Li(THF)_4]^+$ counterion likely interacts with the generated phosphine selenide **3**, lowering its measured $^1J_{PSe}$ value. This might be explained by the ability of the $[Li(THF)_4]^+$ counterion to preferentially favour the $P^+–Se^-$ vs. the $P=Se$ form of the phosphine selenide, altering the polarity of the $P–Se$ bond and thus influencing the measured $^1J_{PSe}$ coupling constant . A previous example of this type of stabilization was seen for 2-hydroxyphenyl diphenylphosphine, which has a $^1J_{PSe}$ coupling constant of 683 Hz (vs. 732 Hz for PPh_3).[42c] This large discrepancy in $^1J_{PSe}$ values was attributed to the ability of the hydroxyl group to hydrogen bond to the selenium atom, favouring the $P^+–Se^-$ form of the phosphine selenide.[42c]

4.2 Synthesis of a Palladium Precatalyst Containing 1a

4.2.1 Reactions of [Li(THF)₂][1a] with PdCl₂(TMEDA): Synthesis of Complex 6

The development and use of distinct precatalyst complexes offers clear advantages over the more conventional method of combining a separate ligand and metal precursor to promote a catalytic transformation. Firstly, the use of a precatalyst is more cost-effective, consuming less ligand and metal on a per-mole basis than a conventional precursor/ligand catalyst system. More importantly, the successful promotion of a catalytic reaction by a distinct precatalyst allows insight into its mechanism, permitting rational fine-tuning of the ligand, and corresponding precatalyst, to further enhance their catalytic utility. Conversely, a precursor/ligand system is not amenable to mechanistic studies, as it is difficult to accurately predict the active, catalytic species in solution based solely on the initial conditions of the reaction. Thus, it was a goal of this investigation to

prepare a distinct precatalyst containing **1a** or **1b** that could be screened for activity in the Buchwald-Hartwig amination reaction.

[Li(THF)$_2$][**1a**] was reacted with a variety of palladium precursors in order to generate a distinct precatalyst containing **1a**. When examining the coordination chemistry of this ligand with ruthenium, it was found that the [Li(THF)$_2$]$^+$ counterion acted as a halide-abstracting agent, facilitating the coordination of **1a** to the metal centre.[36] It was anticipated that a similar reactivity pattern would occur with palladium, and, consequently, the reaction of [Li(THF)$_2$][**1a**] with halide-containing palladium precursors was initially examined. In this regard, PdCl$_2$(TMEDA)[39] was considered an ideal starting material, especially because the TMEDA ligand could potentially be displaced by the benzimidazole nitrogen to facilitate chelation of **1a** after its initial coordination through halide abstraction. Gratifyingly, combining equimolar amounts of [Li(THF)$_2$][**1a**] and PdCl$_2$(TMEDA) in CH$_2$Cl$_2$ resulted in the formation of a white precipitate (LiCl) suspended in an orange solution. Filtration, followed by removal of the volatiles under vacuum, yielded an orange powder, complex **6** (**Scheme 4.5**).
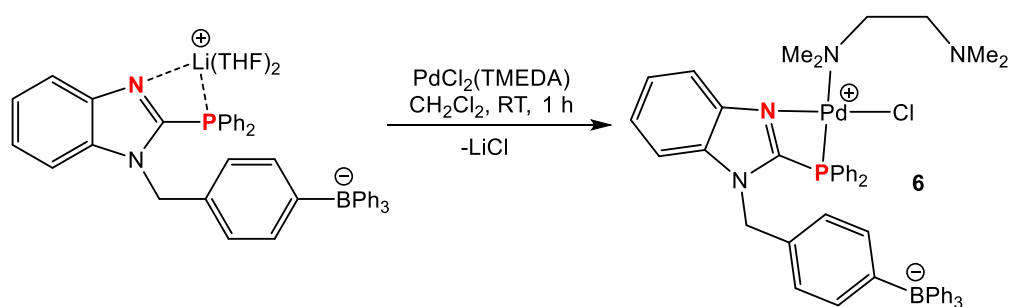
Scheme 4.5. Synthesis of complex **6**.

Complex **6** was characterized by NMR spectroscopy in order to determine its structure. This species exhibits a singlet at 7.9 ppm in the ^{31}P{^{1}H} NMR spectrum. This shift is noticeably downfield compared to that of free ligand (δ = -24.1 ppm), suggesting that **1a** has coordinated to the palladium centre. A sharp singlet appears at -6.6 ppm in the ^{11}B{^{1}H} NMR spectrum of

complex **6**, corresponding to the pendant tetraphenylborate group. ^{1}H and ^{13}C{^{1}H} NMR evidence provides further insight into the exact identity of this species. Three peaks appear at 2.39, 2.18 and 1.35 ppm of the ^{1}H NMR spectrum of complex **6**, in a ratio of ~3:2:3 respectively. The signals at 2.39 and 2.18 ppm are similar in magnitude to that of free TMEDA, where peaks corresponding to the dimethylamino and ethylene groups appear at 2.11 and 2.25 ppm respectively. Thus, the peaks at 2.39 and 2.18 ppm likely correspond to the uncoordinated dimethylamino group and the ethylene bridge respectively. This suggests that the peak at 1.35 ppm likely corresponds to the coordinated dimethylamino group. In the ^{13}C{^{1}H} NMR spectrum, complex **6** exhibits three peaks at 67.0, 61.8, and 43.3 ppm. Since free TMEDA exhibits two peaks at 57.0 ppm and 45.2 ppm, corresponding to the dimethylamino and ethylene groups respectively, the peaks at 67.0 and 61.8 ppm likely correspond to both dimethylamino groups, while the peak at 43.3 ppm corresponds to the ethylene linker.

Based on the above NMR spectroscopic data, complex **6** is tentatively identified as [(κ^2-**1a**)PdCl(κ^1-TMEDA)] (**Scheme 4.5**). This structural assignment is supported by the fact that two distinct signals appear for the dimethylamino groups in both the ^{1}H NMR and ^{13}C{^{1}H} NMR spectrum of complex **6**. Indeed, the ~1 ppm difference observed for the two dimethylamino signals in the ^{1}H NMR spectrum, as well as the ~5 ppm difference observed for the same signals in the ^{13}C{^{1}H} NMR spectrum, suggests a distinct chemical environment around each dimethylamino group, which is accounted for if the TMEDA is coordinated in a monodentate fashion. Furthermore, palladium complexes bearing a chelated TMEDA ligand, as well as two distinct, additional ligands, have been known to exhibit four signals corresponding to each individual methyl group of the dimethylamino moieties.[43] An examination of the literature did not uncover another example of a palladium complex bearing a κ^1-TMEDA ligand for comparative purposes.

However, a symmetric, dinuclear palladium complex containing a bridging κ^1-TMEDA ligand (**Figure 4.1**) exhibited one signal for both dimethylamino groups.[44] This implies that only one signal corresponding to the coordinated dimethylamino group of a κ^1-TMEDA ligand should be observed, as is the case for complex **6**.
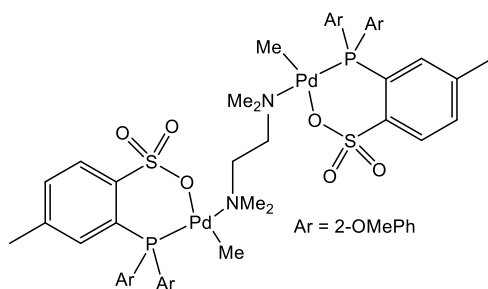
Figure 4.1. Structure of a dinuclear palladium complex containing a bridging TMEDA ligand.

To confirm the assigned structure of complex **6** in the solid state, efforts were made to obtain a sample of this compound suitable for crystallographic analysis. However, despite numerous attempts using various solvent combinations, recrystallization of complex **6** afforded only powders. In subsequent attempts, *p*-toluenesulfonic acid was used as a co-crystallizing agent, with the intent of protonating the uncoordinated dimethylamino group, to no avail. Given that complex **6** is formally neutral, and that such species are often difficult to recrystallize, a cationic derivative of complex **6** with the general formula $[(\kappa^2\text{-}\mathbf{1a})Pd(\kappa^2\text{-TMEDA})][X]$ (X = anion) was sought so as to be more amenable to recrystallization. Unfortunately, reactions of complex **6** with various halide-abstracting agents, including $NaBAr^F_4$, AgOTf, and $AgPF_6$, yielded a mixture of products, as determined through $^{31}P\{^1H\}$ NMR spectroscopy, hindering efforts to prepare a cationic derivative of complex **6**, and thus verify its structural assignment in the solid state.

4.2.2 Reactions of [Li(THF)₂][1a] with Other Palladium Precursors

In addition to $PdCl_2$(TMEDA), $[Li(THF)_2][\mathbf{1a}]$ was combined with other palladium precursors in an effort to generate a precatalyst containing **1a**. Unfortunately, reactions of the

ligand with $PdCl_2(NCPh)_2$[45] or $Pd(OAc)_2$ in THF at ambient temperatures, with $[Pd(cinnamyl)Cl]_2$, and $Pd_2(dba)_3 \cdot CHCl_3$ in CH_2Cl_2 at ambient temperatures, or with K_2PdCl_4 in THF at either ambient or reflux temperatures, resulted in a complex mixture of products based on $^{31}P\{^1H\}$ NMR spectroscopic analysis.

4.3 Synthesis of a Palladium Precatalyst Containing 1b

4.3.1 Reactions of [Li(THF)₄][1b] with [Pd(cinnamyl)Cl]₂

The coordination chemistry of **1b** with palladium precursors was then explored. Indeed, developing a distinct palladium precatalyst containing **1b** was of particular interest due to the fact that **1b** is a bulky, electron-rich ligand, which have generally proven to be ideal ancillary ligands for the successful promotion of the Buchwald-Hartwig amination reaction in the past. This is because electron-donating ligands facilitate oxidative addition of the aryl halide to the palladium centre, while sterically-encumbered ligands promote reductive elimination of the coupled product.[17]

As with $[Li(THF)_2][1a]$, the halide-abstracting properties of the $[Li(THF)_4]^+$ counterion in $[Li(THF)_4][1b]$ were expected to assist in coordination of **1b** to the palladium centre when halide-containing precursors were used. Therefore, $[Pd(cinnamyl)Cl]_2$ was selected as a suitable precursor, especially due to the observed activity of a $[Pd(cinnamyl)Cl]_2/[Li(THF)_4][1b]$ catalyst system in promoting the Buchwald-Hartwig amination reaction (*vide infra*). Preliminary reactions of $[Li(THF)_4][1b]$ with $[Pd(cinnamyl)Cl]_2$ in THF and MeCN, monitored by $^{31}P\{^1H\}$ NMR spectroscopy, resulted in a mixture of products. However, the reaction of $[Li(THF)_4][1b]$ and $[Pd(cinnamyl)Cl]_2$ in CH_2Cl_2 resulted in the formation of cloudy, orange solution after 1 h, signifying the presence of LiCl. Analysis of the reaction mixture revealed a major peak (~80%) at 64.6 ppm in the $^{31}P\{^1H\}$ NMR spectrum, signifying the formation of a new complex **7**.

Unfortunately, after filtration and evaporation of the filtrate under vacuum, the formation of new, additional peaks in the $^{31}P\{^1H\}$ NMR spectrum was evident. Modifying the reaction conditions or workup procedure, including slow addition of a solution of [Li(THF)₄][**1b**] to a solution of [Pd(cinnamyl)Cl]₂, or controlled evaporation of the filtrate, did not alleviate this problem. Additionally, solutions of complex **7** deposited Pd black over time, making its characterization difficult.

Despite these setbacks, the core structure of complex **7** can be tentatively assigned on the basis of literature precedent. Specifically, in the presence of CH_2Cl_2, a palladium complex containing di(isopropylphospino)imidazole ligands was found to react with the solvent and form a new palladium complex (**Scheme 4.6**), which was characterized crystallographically.[35b] Notably, the product of this reaction exhibits a singlet at 65.3 ppm in its $^1P\{^1H\}$ NMR spectrum,[35b] which is of similar magnitude to that observed for complex **7** ($\delta = 64.6$ ppm). Thus, a possible structure of this compound can be seen in **Figure 4.2**. In this representation, the benzimidazole nitrogen of **1b** has reacted with the methylene fragment of CH_2Cl_2 to generate a five-membered, κ^2-*P,C* chelate. The other ligands in complex **7** are purposefully left ambiguous, as the exact mechanism of its formation, which would dictate the identity of the other coordinated ligands, is currently unknown.
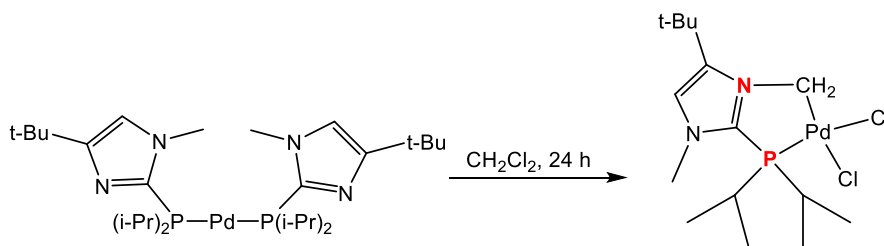
Scheme 4.6. Activation of CH_2Cl_2 by a palladium complex containing phosphinoimidazole ligands.
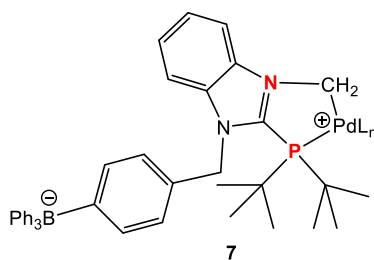
Figure 4.2. Proposed structure of complex **7**.

To avoid complications arising from undesired reactions of [Li(THF)$_4$][**1b**] with the solvent, inert solvents were utilized in subsequent reactions of this ligand with [Pd(cinnamyl)Cl]$_2$. Since the use of aromatic solvents in generating palladium complexes containing bulky phosphinoimidazoles was previously successful,[35b] reactions of [Li(THF)$_4$][**1b**] and [Pd(cinnamyl)Cl]$_2$ were subsequently conducted in benzene. As in previous reactions, a cloudy, orange mixture was generated, indicating the formation of LiCl. However, unlike reactions in CH$_2$Cl$_2$, the complete consumption of the ligand, along with the presence of a singlet at 34.2 ppm, was observed via ^{31}P{^{1}H} NMR spectroscopy after 3.5 h. This chemical shift is downfield from that of free [Li(THF)$_4$][**1b**], suggesting coordination of **1b** to palladium has occurred, generating a new species **8**. However, after filtration and removal of the volatiles, analysis of the resulting orange solid revealed a different singlet at 55.9 ppm in the ^{31}P{^{1}H} NMR spectrum, indicating that an entirely different palladium complex containing **1b** (complex **8′**) had formed. In another iteration of the experiment, a sample of the filtrate was analyzed using ^{31}P{^{1}H} NMR spectroscopy, revealing a singlet at 34.2 ppm. This then suggests that the removal of the volatiles is linked to the formation of complex **8′**. Further NMR spectroscopic analysis of this complex revealed a complicated ^{1}H NMR spectrum and no apparent tetraphenylborate signal, negating efforts to confirm its identity.

Though the transience of complex **8** prevented its isolation and complete characterization, supplementary experiments indicate that this species likely contains κ^2-**1b** and η^3-cinnamyl ligands, as depicted in **Figure 4.3**. Firstly, to ensure that halide-abstraction was indeed occurring, an equimolar amount of NaOTf was added to a mixture of [Li(THF)$_4$][**1b**] and [Pd(cinnamyl)Cl]$_2$ in THF. Here, THF (as opposed to benzene) was utilized so as to better solubilize the NaOTf. After 5 h, the clean formation of a singlet at 34.2 ppm was observed in the ^{31}P{^{1}H} NMR spectrum. The presence of both NaOTf and the [Li(THF)$_4$]$^+$ counterion ensured that all chloride ligands were essentially 'trapped', preventing their coordination to the palladium centre. This then suggests that a chloride is not present in complex **8** In a different reaction, [Li(THF)$_4$][**1b**] and [(cinnamyl)Pd(COD)]BF$_4$[46] were combined in THF. After only 1.5 h, ^{31}P{^{1}H} NMR spectroscopic analysis of the reaction mixture revealed a singlet at 34.3 ppm. In this instance, there are no chloride ligands that are able to coordinate to the metal, and the lability of the COD effectively makes this palladium precursor a potential source of '[Pd(cinnamyl)]$^+$'. Furthermore, the [Li(THF)$_4$]$^+$ counterion of the ligand is removed in the form of LiBF$_4$. Taken together, these reactions corroborate the proposed structure of complex **8**. Numerous examples of (cationic) palladium complexes bearing a chelated [P,N]-hybrid ligand, as well as an η^3-coordinated allyl ligand, exist in the literature,[47] providing additional support for the proposed structure. Despite the successful formation of complex **8** in these reactions, significant Pd black formation was also observed to occur, making isolation and characterization of this compound untenable via these methods.
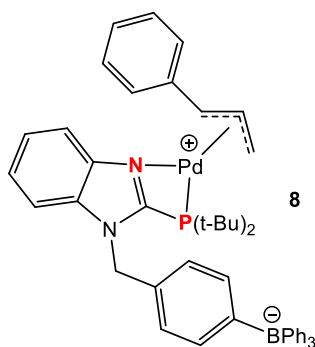
Figure 4.3. Proposed structure of complex **8**.

The search for additional solvents in which to conduct reactions of [Li(THF)$_4$][**1b**] and [Pd(cinnamyl)Cl]$_2$ led to the use of fluorobenzene. This solvent was considered ideal for these reactions, combining the inert nature of aromatic solvents with the polarity of halogenated solvents. Indeed, preliminary NMR-scale reactions of [Li(THF)$_4$][**1b**] and [Pd(cinnamyl)Cl]$_2$ led to the formation of complex **8** after 24 h, evidenced by the presence of a singlet at 34.2 ppm in the ^{31}P{^{1}H} NMR spectrum. However, when conducting similar reactions on a larger scale, ^{31}P{^{1}H} NMR spectroscopic analysis of the reaction mixture after 12 h indicated the formation of a secondary peak at 31.1 ppm in appreciable amounts (~40%), in addition to complex **8**. This unwanted side product could be minimized by shortening the reaction time to 2 h and heating the reaction mixture at 40 °C. However, a mixture of products was observed to form upon work-up (filtration and removal of the volatiles), preventing the isolation, and thus complete characterization, of complex **8**.

4.3.2 Reactions of [Li(THF)$_4$][1b] with Other Palladium Precursors

Given the apparent difficulties associated with reactions involving [Pd(cinnamyl)Cl]$_2$, other palladium precursors were also combined with [Li(THF)$_4$][**1b**] in an effort to synthesize a distinct precatalyst containing **1b**. Unfortunately, reactions involving the ligand and PdCl$_2$(COD) or Pd(acac)$_2$ in THF at room temperature were unsuccessful, affording a mixture of products and

no discernable product formation respectively after 24 h, as determined through ^{31}P{^{1}H} NMR spectroscopy. Changing the solvent to CH$_2$Cl$_2$ in the reaction with PdCl$_2$(COD) yielded similar results to that conducted in THF. Unlike [Li(THF$_2$)][1a], reactions of [Li(THF)$_4$][1b] and PdCl$_2$(TMEDA) in CH$_2$Cl$_2$ resulted in the formation of multiple peaks in the ^{31}P{^{1}H} NMR spectrum, while similar reactions in THF did not yield any new peaks at either ambient or reflux temperatures. Reactions of the ligand and [Pd(allyl)Cl]$_2$[20] at room temperature, in either CHCl$_3$ or fluorobenzene, were similarly unsuccessful.

However, preliminary, NMR-scale reactions of Pd$_2$(dba)$_3$•CHCl$_3$ with [Li(THF)$_4$][1b] in benzene yielded more fruitful results. Monitoring this reaction over time showed the initial formation of peaks at 45.4 and 34.2 ppm in a ratio of ~80:20 after 1.5 h in the ^{31}P{^{1}H} NMR spectrum. Over time, a concomitant decrease in the peak at 45.4 ppm and increase in the peak at 34.2 ppm culminated in the complete conversion to the peak at 34.2 ppm after 24 h. Unfortunately, upon replicating this reaction on a larger scale, spectroscopic analysis revealed that multiple peaks, all with chemicals shifts of ~34 ppm were in fact present after 24 h. The presence of multiple signals corresponding to the *tert*-butyl groups on the phosphine moiety of 1b in the ^{1}H NMR spectrum also confirmed the presence of several ligated complexes. The similarities in chemical shift of these compounds suggest that their steric and electronic properties are comparable, preventing them from being separated and characterized effectively.

Despite the formation of several peaks in the ^{31}P{^{1}H} NMR spectrum in this reaction, it is reasonable to speculate that these species adopt a similar structure to that of complex 8, given that the magnitude of these signals is similar to that observed for complex 8 (δ = 34.2 ppm). Specifically, these complexes likely contain a chelate of 1b, in addition to coordinated dba (**Figure 4.4**). Given that dba is a multidentate ligand, its various, potential coordination modes could give

rise to several distinct complexes with related characteristics, which may account for the multitude of peaks with similar chemical shift values observed in the $^{31}P\{^{1}H\}$ NMR spectrum. In this scenario, a $[Li(THF)_x]^+$ counterion is likely acting as a counterion to the anionic palladium complexes being generated. Furthermore, the transient peak at 45.4 ppm could in fact be a κ^1-**1b**-ligated intermediate, given that the monodentate chemical shift of a ligand is generally further downfield than its corresponding chelate shift.[48] This might account for the simultaneous decrease of this peak as the peak at ~34 ppm grows.
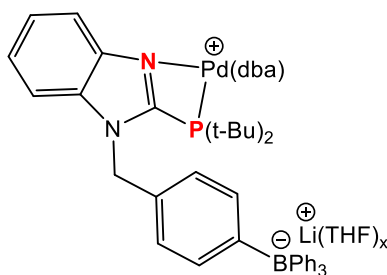
Figure 4.4. Proposed general structure of the products formed in the reaction of $[Li(THF)_4][$**1b**$]$ and $Pd_2(dba)_3 \cdot CHCl_3$ in benzene.

4.3.3 Reactions of [PPh₄][1b] with [Pd(cinnamyl)Cl]₂: Synthesis of Complex 9

The complications arising from the use of $[Li(THF)_4][$**1b**$]$ to generate a distinct palladium precatalyst containing **1b** necessitated an alternative route by which this could be accomplished. Therefore, a different salt of the ligand, namely $[PPh_4][$**1b**$]$, was utilized in subsequent reactions with palladium precursors. The $[PPh_4]^+$ counterion does not exhibit halide-abstracting properties, as evidenced with reactions of $[PPh_4][$**1a**$]$ and halide-containing ruthenium precursors.[36] Despite this, both palladium precursors with or without halide ligands were combined with $[PPh_4][$**1b**$]$ to see if a new complex containing **1b** could be formed.

Since reactivity between $[Li(THF)_4][$**1b**$]$ and $[Pd(cinnamyl)Cl]_2$ had been established, corresponding reactions between $[PPh_4][$**1b**$]$ and $[Pd(cinnamyl)Cl]_2$ were initially attempted in

order to generate a precatalyst containing **1b**. Halogenated solvents (especially CH_2Cl_2) as reaction media were avoided so as to prevent any unwanted reactions between the ligand and the solvent. Therefore, [PPh$_4$][**1b**] and [Pd(cinnamyl)Cl]$_2$ were combined in THF and monitored over time using $^{31}P\{^1H\}$ NMR spectroscopy. After 1 h, the formation of a new species, complex **9**, exhibiting singlets at 45.9 ppm and 23 ppm in a ~40:60 ratio, respectively, was apparent. These peaks likely correspond to a palladium species containing **1b** and the tetraphenylphosphonium counterion respectively. Further analysis at 2 h, 4 h, and 24 h showed that the species was stable in solution. In subsequent experiments, an optimized synthesis of complex **9** was developed. Equimolar amounts of [PPh$_4$][**1b**] and [Pd(cinnamyl)Cl]$_2$ were combined in THF, and reacted for 4 h. Removal of the volatiles, yielded complex **9** as a yellow solid, which could then be recrystallized from CH_2Cl_2/hexanes. Indeed, this species demonstrated moderate stability in halogenated solvents over periods of ~12 h.

The structural elucidation of complex **9** was aided by NMR spectroscopic analysis. This compound exhibits a signal at -6.7 ppm in the $^{11}B\{^1H\}$ NMR spectrum, corresponding to the anionic tetraphenylborate group. The signal at 45.9 ppm in the $^{31}P\{^1H\}$ NMR spectrum is distinct from that of complex **8** ($\delta \approx 34$ ppm), suggesting that **1b** is likely not chelated to the palladium centre. This makes sense, as there are no halide-abstracting agents present to remove the chloride ligands that appear in the starting material, and the benzimidazole nitrogen may not be basic enough to cause chloride dissociation. Indeed, the chemical shift of complex **9** is more similar to the transient, presumably mondentate species observed in the reaction of [Li(THF)$_4$][**1b**] and Pd$_2$(dba)$_3$•CHCl$_3$ ($\delta = 45.4$ ppm). Additionally, a monodentate palladium complex of **1b** would be anionic and therefore retain the [PPh$_4$]$^+$ counterion. Notably, the characteristic signal of this counterion at ~23 ppm in the $^{31}P\{^1H\}$ NMR spectrum is present in a ~1:1 ratio with that of the

coordinated phosphine signal. Finally, though both η^1 and η^3 coordination modes are possible for

the cinnamyl ligand,[47d] the signal pattern corresponding to the latter hapticity appears to be present

in the ^{1}H NMR spectrum of complex **9**. Based on this spectroscopic evidence, a tentative structure

of complex **9** can be assigned (**Figure 4.5**). Though this species proved to be moderately stable in

halogenated solvents over extended periods of time, efforts to obtain a sample suitable for

crystallographic analysis were unsuccessful, preventing the structural elucidation of complex **9** in

the solid state.
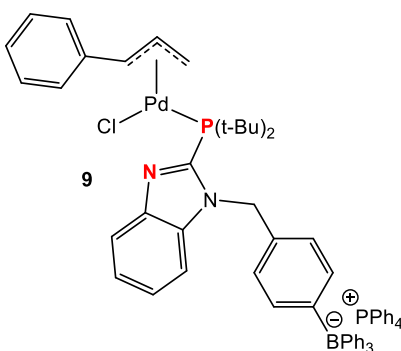
Figure 4.5. Proposed structure of complex **9**.

4.3.4 Reactions of [PPh₄][1b] with PdCl₂(COD): Synthesis of Complex 10

Encouraged by the preceding results, [PPh₄][**1b**] was reacted with other palladium

precursors in order to generate a distinct precatalyst. Though reactions of [Li(THF)₄][**1b**] with

PdCl₂(COD) yielded a mixture of products, subsequent reactions of this ligand with

[(cinnamyl)Pd(COD)]BF₄ showed that **1b** was able to displace COD and coordinate to the metal

centre. Therefore, reactions of [PPh₄][**1b**] with PdCl₂(COD) were examined with the hope that,

without the presence of the halide-abstracting [Li(THF)₄]⁺ counterion, **1b** would simply displace

COD and generate the desired complex. Gratifyingly, this was found to be the case – when

equimolar amounts of [PPh₄][**1b**] with PdCl₂(COD) were combined in CH₂Cl₂, a new species,

complex **10**, exhibiting peaks at 37.9 ppm and 23.1 ppm in a 1:1 ratio in the ^{31}P{^{1}H} NMR

spectrum was observed after 1 h (**Scheme 4.7**). The proposed structure of complex **10** is

[PPh$_4$][PdCl$_2$(κ^2-**1b**)], as seen in **Scheme 4.7**. This species displays a signal at -6.7 ppm in the

^{11}B{^{1}H} NMR spectrum, indicative of the pendant tetraphenylborate group. Coordination of **1b** to

the metal is confirmed by the large downfield shift of the coordinated di(*tert*-butyl)phosphino

group of the ligand ($\Delta\delta \approx 30$ ppm). Additionally, the resonance of this moiety is similar to that of

complex **8** ($\delta = 34.2$ ppm), which is also proposed to contain a κ^2-*P,N* chelate of **1b**. Furthermore,

complex **10** is anionic, requiring the retention of an equimolar amount of the [PPh$_4$]$^+$ counterion,

which is confirmed in the ^{31}P{^{1}H} NMR spectrum. Finally, a neutral dichloropalladium complex

containing a chelated di(*tert*-butylphosphino)imidazole ligand exhibits a signal at $\delta = 41.1$ ppm,[49]

which is of similar magnitude to that of complex **10**. Unfortunately, attempts to confirm the

structural designation of this species via crystallographic analysis were hampered by the almost

immediate formation of Pd black upon recrystallization.
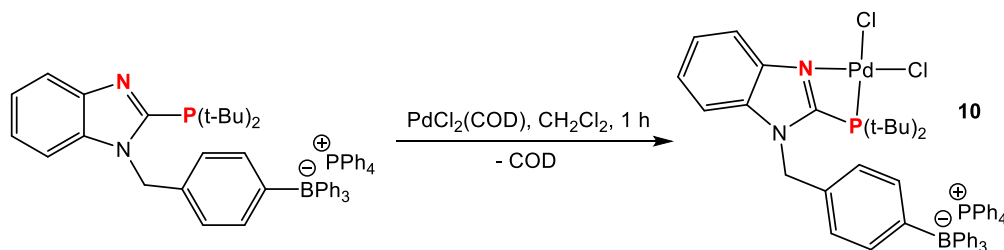
Scheme 4.7. Synthesis of complex **10**.

4.3.5 Reactions of [PPh$_4$][1b] with Pd$_2$(dba)$_3$•CHCl$_3$

In addition to halide-containing precursors, [PPh$_4$][**1b**] was also reacted with

Pd$_2$(dba)$_3$•CHCl$_3$ to investigate if a distinct precatalyst containing **1b** could be generated.

Preliminary reactions involved the combination of equimolar amounts of [PPh$_4$][**1b**] and

Pd$_2$(dba)$_3$•CHCl$_3$ in CH$_2$Cl$_2$, and monitoring the progress of the reaction over time using ^{31}P{^{1}H}

NMR spectroscopy. After 1 h, a new peak at 34.5 ppm was observed, with peaks at 23.0 and 5.4

ppm, corresponding to the [PPh$_4$]$^+$ counterion and ligand respectively, also present. After 10 h, the

ligand was completely consumed, and the formation of two distinct species in solution was evident. One species (**11**) exhibits peaks at 34.5 and 22.9 ppm in a ~1:1 ratio. This peak pattern is very similar to that of complex **8**, suggesting that **11** is a palladium complex containing a chelate of **1b** in addition to coordinated dba, and is charge-balanced by the [PPh₄]⁺ counterion (**Figure 4.6**). The specified hapticity of dba in the structure of complex **11** is based on literature precedent.[8] Surprisingly, the second species (**12**) exhibits two sets of doublets at 39.4 and 24.3 ppm, each with a coupling constant value of 345 Hz. Interestingly, complex **12** is the major species present in solution after 24h, along with residual amounts (~15%) of [PPh₄]⁺ counterion.
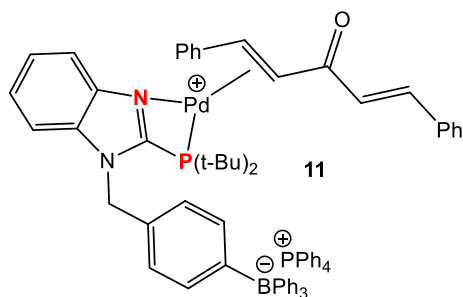
Figure 4.6. Proposed structure of complex **11**.

The splitting pattern exhibited by complex **12** in the ³¹P{¹H} NMR spectrum implies that two distinct phosphorus-containing species are coordinated to the palladium centre. Two equivalents of **1b** could not have chelated to the metal centre, as the resulting complex would be symmetric in both a *cis* or *trans* arrangement (with respect to the phosphorus atoms), giving rise to only one signal in the ³¹P{¹H} NMR spectrum. Alternatively, a complex containing chelated **1b**, in addition to another equivalent of **1b** coordinated in a monodentate fashion, would give rise to the observed set of doublets. One equivalent of dba, coordinated in a monodentate fashion, might also be present in the complex to keep the Pd(0) centre coordinatively saturated. However, this arrangement of ligands would render complex **12** anionic, and its ³¹P{¹H} NMR spectrum clearly indicates that the [PPh₄]⁺ counterion is not present in equimolar amounts. Since it appears

that a second equivalent of **1b** is not present in complex **12**, the $[PPh_4]^+$ counterion is the only remaining source of phosphorus in solution. Thus, it is tentatively proposed that the *activation* of a P–Ph bond in the $[PPh_4]^+$ counterion by the palladium centre is responsible for the formation of complex **12**. Indeed, previous reports have showcased the activation of tetraarylphosphonium species, either stoichiometrically or through *in situ* generation, by other palladium complexes.[50]

A proposed structure of complex **12** is shown in **Figure 4.7**. The large $^2J_{PP}$ coupling constant value observed for this complex suggests that the two phosphorus-containing species are arranged in a *trans* configuration.[48] Additionally, the doublet at 39.4 ppm in the $^{31}P\{^1H\}$ NMR spectrum of complex **12** is similar in magnitude to the chemical shifts of complexes **8** (δ = 34.2 ppm) and **10** (δ = 37.9 ppm) respectively, both proposed to contain a chelate of **1b**. Furthermore, the $^{31}P\{^1H\}$ NMR chemical shift of *trans*-$[PdCl_2(PPh_3)_2]$ (δ = 23.4 ppm)[51] and the other doublet observed for complex **12** (δ = 24.3 ppm) are similar in magnitude. The generation of complex **12** might occur via the following pathway. Complex **11** is formed initially and bears chelated **1b** and coordinated dba. Then, over the course of the reaction, the $[PPh_4]^+$ is oxidatively added to the metal centre, generating a coordinatively saturated, Pd(II) complex with two chemically distinct phosphorus species that is formally neutral. Since the above discussion is solely based on $^{31}P\{^1H\}$ NMR evidence, exploring the mechanism by which the counterion activation occurs, as well as confirming the proposed structure of complex **12** in the solid state, will be a focus of future work.
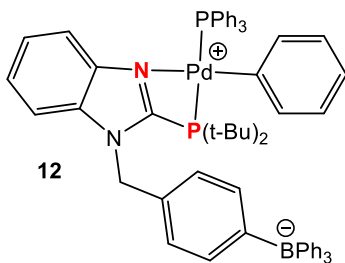
Figure 4.7. Proposed structure of complex **12**.

Reactions of [PPh$_4$][**1b**] and Pd$_2$(dba)$_3$•CHCl$_3$ in THF were also explored. Not surprisingly, similar results to reactions conducted in CH$_2$Cl$_2$ were obtained, with complex **12** being formed over extended periods of time. Despite this, an attempt was made to stop the reaction of [PPh$_4$][**1b**] and Pd$_2$(dba)$_3$•CHCl$_3$ in THF after 1 h in order to try and isolate complex **11**. However, after removal of the volatiles, the formation of a new peak at 55.6 ppm was observed in the ^{31}P{^{1}H} NMR spectrum. Additionally, a variety of boron signals resonating around -6.7 ppm were seen in the ^{11}B{^{1}H} NMR spectrum of this new species. Thus, future endeavours will focus on the isolation of complex **12**, as it appears to be a reaction 'sink' and thus more amenable to isolation and characterization.

4.4 Examining 1b as an Ancillary Ligand in the Buchwald-Hartwig Amination Reaction

4.4.1 The Pd-Catalyzed Amination of Bromobenzene with Aniline: Catalyst Optimization

One of the primary objectives of this investigation was to examine if [Li(THF)$_2$][**1a**] or [Li(THF)$_4$][**1b**] could act as an effective ancillary ligand in the promotion of the Buchwald-Hartwig amination reaction, as the properties of these ligands make them ideal for use in catalysis. Firstly, the combination of the 'soft' phosphorus and 'hard' nitrogen donor atoms, which is inherent in the phosphinobenzimidazole scaffold, offers many catalytic benefits, namely the potential stabilization of low-coordinate intermediates via hemilability. In this regard, comparisons can be drawn to the highly successful biarylphosphine class of ancillary ligands, where the *ipso*-carbon of the lower aryl ring has been shown to coordinate fleetingly to the palladium centre to stabilize unsaturated intermediates (**Figure 4.8**).[52] The propensity of [Li(THF)$_2$][**1a**] or [Li(THF)$_4$][**1b**] to engage in hemilabile behaviour is also encouraged by the strained, four-membered chelate that would form upon chelation to a metal centre. Secondly, the tethered, tetraphenylborate group in [Li(THF)$_2$][**1a**] and [Li(THF)$_4$][**1b**], which is strategically integrated

into the phosphinobenzimdiazole scaffold to minimize any adverse interactions with the metal centre, renders both ligands anionic, further increasing their catalytic utility. In particular, these negatively-charged ligands may exhibit more pronounced electron-donating characteristics than corresponding neutral ligands, which might assist in facilitating certain steps in the catalytic cycle (*e.g.* oxidative addition).[13b,14]
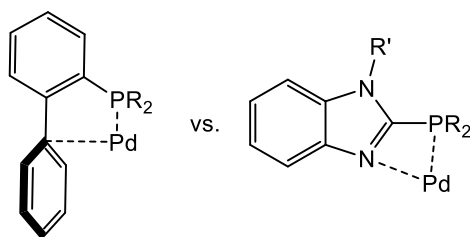
Figure 4.8. Comparing the Pd-ligand interactions of biarylphosphines and phosphinobenzimidazoles.

Since both the development of distinct palladium complexes containing **1a** or **1b** and the following catalytic studies were examined concurrently, the more conventional method of utilizing a separate palladium precursor and ligand as the catalyst system was implemented, as there was no guarantee that a distinct precatalyst would be successfully synthesized. Additionally, of the two ligands of interest, [Li(THF)$_4$][**1b**] was considered the better candidate for catalytic screening due to the bulky, electron-donating properties imparted by the −P(t-Bu)$_2$ group. An electron-rich ligand will impart greater electron density to the palladium centre, facilitating oxidative addition, while sterically-encumbered ligands will promote reductive elimination.[17]

Initial catalytic studies focused on the development of optimized catalytic conditions using a Pd/[Li(THF)$_4$][**1b**] catalyst system. The cross-coupling of bromobenzene and aniline was chosen for this optimization process. Numerous parameters, including time, temperature, base, solvent, and palladium precursor, were varied in order to investigate the effect each had on the outcome of the reaction (**Table 4.2**). [Pd(cinnamyl)Cl]$_2$ was selected as the initial palladium source based on

its successful implementation in other catalyst systems for C-N bond formation.[21,53] Additionally, KO(t-Bu) was selected as the initial base for its documented role in the activation of precatalysts containing allyl-type ligands.[17c] Firstly, the effect of temperature was examined (**Table 4.2**, **entries 1-4**). It was found that the reaction proceeded well at high temperatures, but poor conversions were observed for more moderate temperatures, including ambient temperature. The time parameter was then varied to observe its effect on the outcome of the reaction (**Table 4.2, entries 5-8**). Gratifyingly, the reaction was essentially complete after as little as nine hours. However, twelve-hour reaction times were deemed optimal for convenient set-up and work-up. Next, the effect of the identity of the palladium precursor was examined. It was found that the reaction did not proceed well when the common Pd(II) salt, Pd(OAc)$_2$, was used (**Table 4.2, entry 10**), while Pd$_2$(dba)$_3$•CHCl$_3$ was found to be a very suitable precursor (**Table 4.2, entry 11**). Despite this fact, the non-innocence of the dba ligand in catalysis is well-documented,[54] and so [Pd(cinnamyl)Cl]$_2$ was considered the more ideal palladium salt. The use of a weaker, carbonate base yielded a lower conversion than that observed for KO(t-Bu) (**Table 4.2, entries 12-13**). Also, the outcome of the reaction was impartial to solvent, as similar conversions were observed when either toluene or 1,4-dioxane was used (**Table 4.2, entries 14-15**). Finally, the use of only 1.2 equivalents of base was not detrimental to the outcome of the reaction (**Table 4.2, entry 16**). Control reactions in which ligand (**Table 4.2, entry 17**) or both ligand and precursor (**Table 4.2, entry 18**) were omitted revealed no conversion to diphenylamine, confirming that the optimized catalyst system is indeed responsible for the promotion of the reaction.
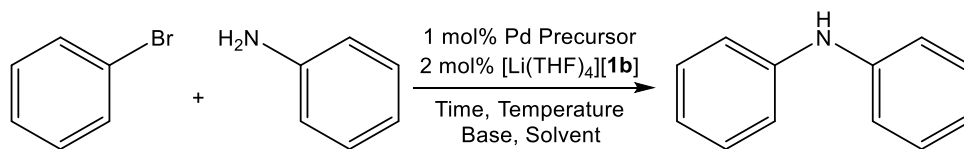
Table 4.2. Optimization of the Buchwald-Hartwig amination reaction of bromobenzene and aniline using [Li(THF)$_4$][**1b**] as ancillary ligand.[a]

Entry	Precursor	Time (h)	Temperature (°C)	Base	Solvent	Conversion (%)[b]
1	[Pd(cinnamyl)Cl]$_2$	24	110	KO(t-Bu)	toluene	92
2			80			92
3			50			64
4			RT			7
5	[Pd(cinnamyl)Cl]$_2$	24	80	KO(t-Bu)	toluene	92
6		12				91
7		9				96
8		6				87
9	[Pd(cinnamyl)Cl]$_2$	12	80	KO(t-Bu)	toluene	91
10	Pd(OAc)$_2$					35[c]
11	Pd$_2$(dba)$_3$•CHCl$_3$					97
12	[Pd(cinnamyl)Cl]$_2$	12	80	KO(t-Bu)	toluene	91
13				K$_2$CO$_3$		60
14	[Pd(cinnamyl)Cl]$_2$	12	80	KO(t-Bu)	toluene	91
15					1,4-dioxane	91
16	[Pd(cinnamyl)Cl]$_2$	12	80	KO(t-Bu)	toluene	90[d]
17	[Pd(cinnamyl)Cl]$_2$	12	80	KO(t-Bu)	toluene	0[d][e]
18	None	12	80	KO(t-Bu)	toluene	0[d][e]

[a] Reaction conditions: 0.6 mmol bromobenzene, 0.72 mmol aniline, 1 mol% Pd precursor, 2 mol% [Li(THF)$_4$][**1b**], 0.9 mmol base, 2 mL solvent. [b] Determined using ^{1}H NMR spectroscopy (CDCl$_3$) based on the consumption of bromobenzene. [c] 2 mol% Pd(OAc)$_2$ was used. [d] 0.72 mmol KO(t-Bu) was used. [e] No ligand was used.

4.4.2 Examining the Scope of the Pd/[Li(THF)$_4$][1b] Catalyst System in the BHA Reaction

With a set of optimized conditions in hand, the scope of the reaction, with regard to both the aryl bromide and amine coupling partner, were examined (**Table 4.3** and **Table 4.4**, respectively). Not surprisingly, the reaction of bromobenzene proceeded well using the optimized conditions (**Table 4.3, entry 1**). The reactions of aryl bromides bearing weakly electron-donating

groups also proceeded efficiently (**Table 4.3, entries 2-3**). Furthermore, the more sterically-demanding 2-bromotoluene could be utilized without loss of activity. However, the presence of the strongly electron-donating methoxy group led to only a moderate isolated yield (**Table 4.3, entry 4**). Fortunately, this could be remedied by increasing the catalyst loading. Aryl bromides bearing electron-withdrawing substituents, including the base-sensitive ketone group, were well-tolerated, affording the coupled products in excellent yields (**Table 4.3, entries 5-6**). The notable exception was 4-bromo-1-nitrobenzene, which did not react readily with aniline (**Table 4.3, entry 7**). Reduction of the nitro group *in situ*, affording 4-bromoaniline, might explain this observed discrepancy, as the resulting aryl bromide bears an electron-rich amino group, making it less amenable to oxidative addition. This is perhaps not surprising, given that the reduction of nitro-substituted aryl halides has been accomplished by catalyst systems designed to facilitate cross-coupling chemistry in the past.[55] Finally, the reaction of 2-bromopyridine with aniline did not occur readily (**Table 4.3, entry 8**), likely due to the coordination of the substrate, or the resulting, coupled product, to the palladium centre, effectively deactivating the catalyst system. Notably, in all instances, only the monoarylation product was observed, highlighting the selectivity of this catalyst system.

The scope of the amine coupling partner was examined next (**Table 4.4**). The catalyst system tolerated sterically demanding anilines well (**Table 4.4, entries 1-2**). The primary aliphatic amine cyclohexylamine could also be used, affording the desired product in moderate yield (**Table 4.4, entry 3**). However, secondary amines were not suitable coupling partners for this catalyst system. Morpholine (**Table 4.4, entry 4**) did not react under these conditions, while the use of piperidine (**Table 4.4, entry 5**) afforded a poor yield of the corresponding coupled product. This
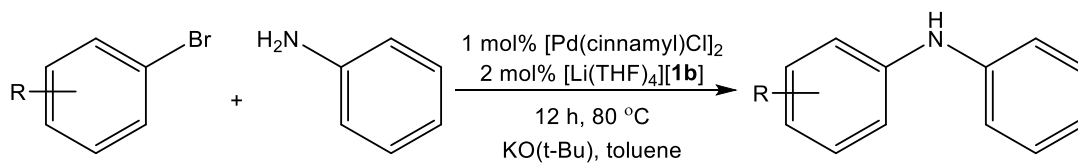
Table 4.3. Examination of the aryl bromide scope using the Pd/[Li(THF)₄][**1b**] catalyst system in the Buchwald-Hartwig amination reaction.[a]

Entry	Aryl Bromide	Product	Yield (%)[b]
1			92
2			96
3			97
4			57 (71)[c]
5			91
6			86
7			0
8			36

[a] Reaction conditions: 0.6 mmol aryl bromide, 0.72 mmol aniline, 1 mol% [Pd(cinnamyl)Cl]₂, 2 mol% [Li(THF)₄][**1b**], 0.72 mmol KO(t-Bu), 2 mL toluene. [b] Isolated yield (average of two runs). [c] 1.5 mol% [Pd(cinnamyl)Cl]₂ and 3 mol% [Li(THF)₄][**1b**] were used.

1 mol% [Pd(cinnamyl)Cl]₂ → $1\ \text{mol\%}\ [Pd(cinnamyl)Cl]_2$

Reaction scheme:

Br (on benzene) + HNR¹R² → (with conditions: $1\ \text{mol\%}\ [Pd(cinnamyl)Cl]_2$, $2\ \text{mol\%}\ [Li(THF)_4][\mathbf{1b}]$, 12 h, 80 °C, KO(t-Bu), toluene) → Ph-NR¹R²
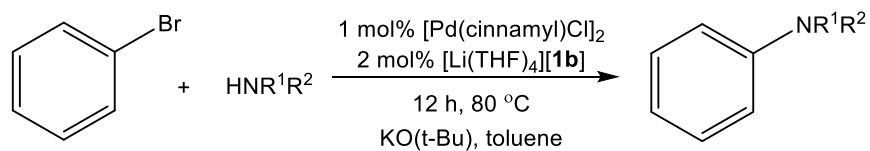
Table 4.4. Examination of the amine scope using the Pd/[Li(THF)₄][**1b**] catalyst system in the Buchwald-Hartwig amination reaction.[a]

Entry	Amine	Product	Yield (%)[b]
1	2,4,6-trimethylaniline	N-phenyl-2,4,6-trimethylaniline	73
2	2,6-diisopropylaniline	N-phenyl-2,6-diisopropylaniline	76
3	cyclohexylamine	N-phenylcyclohexylamine	72
4	morpholine	4-phenylmorpholine	0
5	piperidine	1-phenylpiperidine	31
6	diphenylamine	triphenylamine (NPh₂)	0

[a] Reaction conditions: 0.6 mmol bromobenzene, 0.72 mmol amine, 1 mol% [Pd(cinnamyl)Cl]₂, 2 mol% [Li(THF)₄][**1b**], 0.72 mmol KO(t-Bu), 2 mL toluene. [b] Isolated yield (average of two runs).

discrepancy might be explained by the ability of morpholine to chelate to the palladium centre,[47d] generating a catalytically inactive species. The reaction of bromobenzene and diphenylamine also did not occur readily.

Clearly, the [Pd(cinnamyl)Cl]$_2$/[Li(THF)$_4$][**1b**] catalyst system displays a preference for coupling primary amines over secondary amines. The source of this selectivity likely stems from the proposed nature of the active catalyst (**Scheme 4.8**). If the typical activation pathway for other allyl-based precatalysts is followed by this catalyst system,[17c,56] the catalytically active species is anionic. Thus, all subsequent catalytic intermediates are anionic. This would further suggest that these intermediates are more electron-rich than corresponding intermediates generated from a complex containing an analogous neutral ligand. Since an electron-rich palladium centre exhibits slower rates of reductive elimination,[57] it is possible that the palladium-amido complex that is formed when a secondary amine is used is too electron-rich, and reductive elimination to furnish the coupled product is disfavoured. This is in contradiction to the fact that an electron-rich amido ligand (such as those formed from a secondary, cyclic, alkyl amine) typically exhibit faster rates of reductive elimination.[57] The decreased tendency for diarylamido ligands to undergo reductive elimination is also well-documented, which might explain why diphenylamine was a poor coupling partner in these reactions.[57] Ultimately, mechanistic studies would offer greater insight into the observed selectivity exhibited by the of the [Pd(cinnamyl)Cl]$_2$/[Li(THF)$_4$][**1b**] catalyst system. This avenue of investigation might also shed light onto the purported hemilability of the anion **1b** and its potential role in the selectivity, and activity, of the catalyst system.
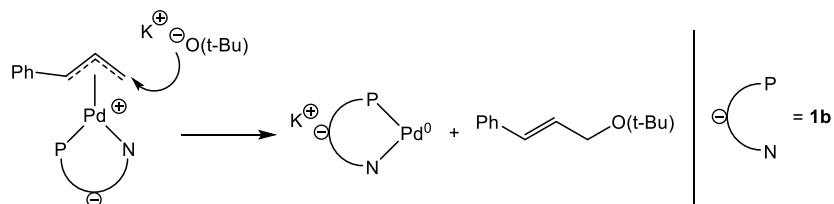
Scheme 4.8. Possible activation pathway for the [Pd(cinnamyl)Cl]$_2$/[Li(THF)$_4$][**1b**] catalyst system.

4.4.3 Anionic vs. Neutral Ligands in the Buchwald-Hartwig Amination Reaction

Given the successful application of the [Pd(cinnamyl)Cl]$_2$/[Li(THF)$_4$][**1b**] catalyst system for the Buchwald-Hartwig amination reaction, it was of significant interest to compare the efficacy of a corresponding catalyst system utilizing an analogous neutral ligand and observe any differences in activity. Therefore, neutral ligand **2** was employed, in conjunction with [Pd(cinnamyl)Cl]$_2$, to promote C-N bond formation between various aryl bromides and amines (**Table 4.5**). A [Pd(cinnamyl)Cl]$_2$/[PPh$_4$][**1b**] catalyst system was also screened for activity in some of these reactions to investigate if the choice of cation has an impact on catalytic efficiency.

Gratifyingly, in almost all cases, the catalyst system employing [Li(THF)$_4$][**1b**] out-performed the catalyst system utilizing **2**, often by a significant margin. This includes when electron-donating or electron-withdrawing substituents were present on the aryl bromide (**Table 4.5, entries 1-4**), and when bulky anilines were employed (**Table 4.5, entries 5-6**). It was also clear that the neutral catalyst system did not tolerate the use of cyclohexylamine as well as the anionic catalyst system (**Table 4.5, entry 7**). Surprisingly, the coupling of bromobenzene and piperidine proceeded with poor yields when both the anionic and neutral catalyst systems were employed (**Table 4.5, entry 8**). At this time, it is unclear why both catalyst systems performed similarly when this substrate was employed. It is also worth noting that the identity of the cation does not appear to have a significant impact on catalysis, as the reactions employing the [Pd(cinnamyl)Cl]$_2$/[PPh$_4$][**1b**] catalyst system gave comparable yields to those that utilized the [Pd(cinnamyl)Cl]$_2$/[Li(THF)$_4$][**1b**] catalyst system. This might further suggest that the choice of cation does not play a substantial role in promoting the desired transformation.

One explanation as to why the anionic catalyst system out-performed the neutral catalyst
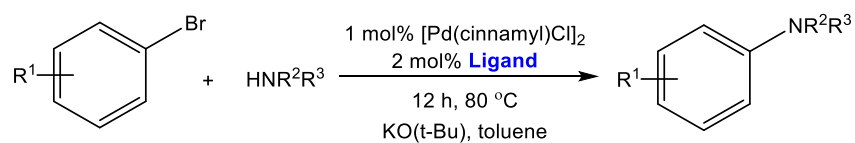
Table 4.5. Comparing the effects of utilizing [Li(THF)$_4$][**1b**], **2**, and [PPh$_4$][**1b**] as ancillary ligands in the Buchwald-Hartwig amination reaction.[a]

Entry	Product	Yield Using [Li(THF)$_4$][1b] (%)[b]	Yield Using 2 (%)[b]	Yield Using [PPh$_4$][1b] (%)[b]
1		96	70	95
2		97	40	-
3		57	11	62
4		86	46	-
5		73	55	-
6		76	30	72
7		72	33	70
8		31	35	-

[a] Reaction conditions: 0.6 mmol aryl bromide, 0.72 mmol amine, 1 mol% [Pd(cinnamyl)Cl]$_2$, 2 mol% ligand, 0.72 mmol KO(t-Bu), 2 mL toluene. [b] Isolated yield (average of two runs).

system in this reaction involves the anionic intermediates generated using the [Pd(cinnamyl)Cl]$_2$/[Li(THF)$_4$][**1b**] catalyst system. The more electron-rich, anionic Pd(0) intermediate would undergo oxidative addition much faster than the corresponding neutral species. Indeed, it has been shown that anionic bisphopshine complexes such as [PdX(PPh$_3$)$_2$]$^-$, [Pd(μ-X)(PPh$_3$)$_2$]$_2^{2-}$ and [PdX$_2$(PPh$_3$)$_2$]$^{2-}$, initiate oxidative addition of aryl halides at an increased rate, compared to analogous neutral complexes.[58] Thus, this phenomenon is the likely source of the observed discrepancies between the catalyst systems employing anionic [Li(THF)$_4$][**1b**] and neutral **2**.

Altogether, this result has major implications for ligand design, as it would be of great interest to develop anionic versions of those ligand that have established reactivity for a particular catalytic reaction. As seen in the above example, this simple modification might correspond to a profound increase in catalytic activity. For example, the ease with which dialkylbiarylphosphines can be tailored, as well as their status as privileged ancillary ligands in the Buchwald-Hartwig amination reaction, makes them excellent candidates for the installation of a negatively-charged, tetraphenylborate group. Indeed, future work will involve modifying such ligand scaffolds and screening their utility as ancillary ligands in C-N bond-forming reactions, as well as other cross-coupling reactions.

4.4.4 Anionic vs. Neutral Precatalysts in the Buchwald-Hartwig Amination Reaction

The increased activity of the [Pd(cinnamyl)Cl]$_2$/[Li(THF)$_4$][**1b**] catalyst system over the corresponding system employing neutral **2** prompted further study of the discrepancies that might arise when utilizing anionic ligands vs. neutral ligands in catalysis. Specifically, it was of interest to develop two palladium precatalysts, containing **1b** and **2**, and screen them for activity in the Buchwald-Hartwig amination reaction. Since the identity of complex **10** was known (see **Scheme**

4.7), an analogous dichloropalladium complex containing **2** was prepared. The synthesis of this new compound was modelled after the preparation of complex **10** – equimolar amounts of PdCl$_2$(COD) and **2** were combined and allowed to react in CH$_2$Cl$_2$, with the progress of the reaction being monitored via ^{31}P{^{1}H} NMR spectroscopy (**Scheme 4.9**). After 24 h, the formation of a new singlet at 35.4 ppm was observed, indicating coordination of **2** to the palladium centre. Removal of the volatiles yielded a yellow solid, complex **13**, [PdCl$_2$(κ^2-**2**)], which could be recrystallized from CH$_2$Cl$_2$/hexanes, affording an orange crystalline solid. The ^{31}P{^{1}H} NMR chemical shift of complex **13** is similar to that of complex **10** (δ = 37.9 ppm for the coordinated di(*tert*-butyl)phosphino group), suggesting that these two complexes are structurally similar.
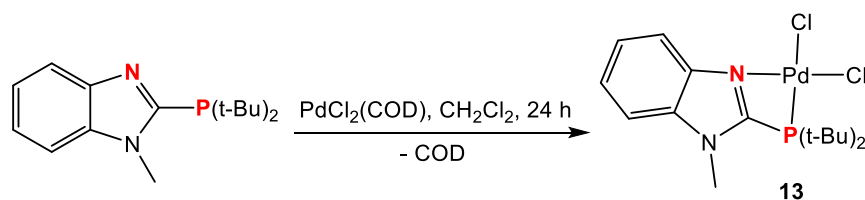
Scheme 4.9. Synthesis of complex **13**.

With both anionic **10** and neutral **13** in hand, the efficacy with which each precatalyst could effect the cross-coupling of bromobenzene and aniline was examined (**Scheme 4.10**). Conversion to diphenylamine was assessed using ^{1}H NMR spectroscopy (CDCl$_3$), based on the consumption of bromobenzene. To our delight, the anionic precatalyst **10** displayed superior activity in promoting the desired reaction compared to neutral **13**, where the conversion to diphenylamine using the former complex was 30% greater than when the latter was used. Since the cation was not observed to significantly impact the outcome of the reaction in previous trials involving both [Li(THF)$_4$][**1b**] and [PPh$_4$][**1b**] as ancillary ligands, and the core steric and electronic properties of each ligand are essentially identical, it is highly likely that the origin of the enhanced activity of complex **10** stems from the anionic nature of the catalyst. In this instance, the anionic precatalyst

might initiate oxidative addition of the aryl bromide at a faster rate due to the more electron-rich palladium center, as was observed for the [Pd(cinnamyl)Cl]$_2$/[Li(THF)$_4$][**1b**] catalyst system. Though the use of complex **10** yielded only a moderate conversion value (~50%), this might be attributed to the fact that a dihalopalladium complex is not a common intermediate in the catalytic cycle of the Buchwald-Hartwig amination reaction,[17a,d] and thus may have difficulty entering the catalytic cycle to furnish the desired products. Despite this, it remains clear that the anionic precatalyst **10** displayed greater activity in promoting the desired reaction than the neutral precatalyst **13**.

Precatalyst = **10**: 48%
= **13**: 18%
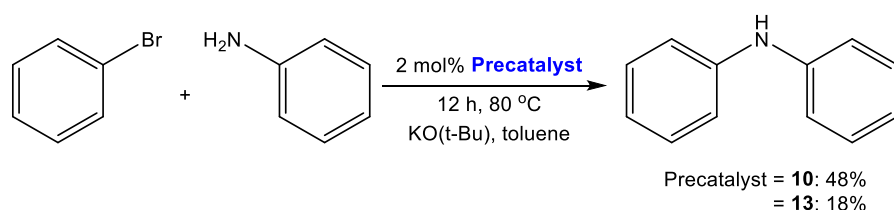
Scheme 4.10. The cross-coupling of bromobenzene and aniline using precatalysts **10** and **13**.

4.5 Synthesis of a Nickel Precatalyst Containing 1b

4.5.1 Reactions of [Li(THF)$_4$][1b] and [PPh$_4$][1b] with NiCl$_2$(DME)

The success of [Li(THF)$_4$][**1b**] as an ancillary ligand in the promotion of the Buchwald-Hartwig amination reaction prompted its preliminary screening for activity in related Ni-catalyzed C-N bond-forming chemistry. As with the corresponding studies using palladium, the coordination chemistry of [Li(THF)$_4$][**1b**] with nickel was first examined in order to develop a nickel precatalyst containing **1b** that might be used to promote the desired transformation. Given that the [Li(THF)$_4$][**1b**]$^+$ counterion demonstrated halide-abstracting properties in reactions with halide-containing palladium precursors, halide-containing nickel precursors were reacted with [Li(THF)$_4$][**1b**] in the hope that similar chemistry would be observed.

NiCl$_2$(DME) is among the most common, halide-containing nickel precursors due to its moderate air stability and the lability of the DME ligand,[59] making it an obvious candidate for reactions with [Li(THF)$_4$][**1b**]. Unfortunately, initial reactions of NiCl$_2$(DME) and [Li(THF)$_4$][**1b**] in THF at ambient or elevated (50 °C) temperatures did not afford a new species, as determined by ^{31}P{^{1}H} NMR spectroscopy. However, when CH$_2$Cl$_2$ was used as the solvent, a new peak at 9.5 ppm in the ^{31}P{^{1}H} NMR spectrum was observed to form after 18 h at room temperature, with ~20% of the ligand remaining unreacted. Encouraged by this result, the reaction was repeated on a preparatory scale, where a cloudy, yellow solution formed after 24 h, suggesting the formation of LiCl. The mixture was filtered and stripped of its volatiles to yield the new species, **14**, as an off-white solid.

In addition to the singlet corresponding to **14** in the ^{31}P{^{1}H} NMR spectrum, a singlet at -6.6 ppm is observed in the ^{11}B{^{1}H} NMR spectrum, indicative of the appended tetraphenylborate group. The ^{1}H NMR spectrum of this species exhibits peaks corresponding to free DME, suggesting that **1b** has coordinated to the metal center. However, the difference in the ^{31}P{^{1}H} NMR chemical shift of the free ligand and **14** ($\Delta\delta \approx 4$ ppm) is rather small, considering the typically large downfield shift exhibited by other phosphines coordinated to a nickel centre.[60] This may call into question whether **14** is actually a new complex, or simply a product of some decomposition pathway initiated by the NiCl$_2$(DME). Additionally, the easy accessibility of Ni(I) and Ni(III) oxidation states does not rule out the possibility of radical chemistry occurring in this reaction,[26] especially in the presence of a halogenated alkane such as CH$_2$Cl$_2$. Regardless of this fact, the similar solubility profiles of both **14** and free [Li(THF)$_4$][**1b**] impeded attempts at separation, and thus complete characterization, of the new species.

The difficulties associated with the use of [Li(THF)$_4$][**1b**] in reactions with NiCl$_2$(DME) led to the use of [PPh$_4$][**1b**] as an alternative source of the **1b** anion. Unfortunately, no reaction was observed to occur after 24 h at ambient or elevated (50 °C) temperatures when NiCl$_2$(DME) and [PPh$_4$][**1b**] were combined in THF, as determined through ^{31}P{^{1}H} NMR spectroscopy. Additionally, an attempt was made to prepare a Ni(0) complex containing **1b** through the *in situ* reduction of NiCl$_2$(DME) using Zn in the presence of [PPh$_4$][**1b**], modelled after a procedure by Hartwig *et al.*[27a] Once again, no new species was observed to form in the ^{31}P{^{1}H} NMR spectrum. This apparent lack of coordination may be attributed to the strained chelate that would form upon coordination of **1b** to nickel, or the mismatch of the soft di(*tert*-butyl)phosphino group and the harder nickel centre. In the latter instance especially, the lack of a proper 'anchoring' donor group to the metal centre might prevent coordination from occurring.

4.5.2 Reactions of [Li(THF)$_4$][1b] with Other Nickel Precursors

Given the lack of success in developing a nickel precatalyst containing **1b** using NiCl$_2$(DME), other halide-containing nickel precursors were also reacted with [Li(THF)$_4$][**1b**]. Unfortunately, neither NiCl$_2$(PPh$_3$)$_3$[26a] nor NiCl$_2$•2H$_2$O[61] was seen to react with the ligand of interest, as determined through ^{31}P{^{1}H} NMR spectroscopy. A modified literature procedure[26a] that involved combining NiCl$_2$•6H$_2$O and [Li(THF)$_4$][**1b**] in refluxing EtOH was also attempted, but coordination of **1b** to nickel was not observed in the ^{31}P{^{1}H} NMR spectrum. In future work, the use of more established precursors, such as Ni(COD)$_2$ or [(TMEDA)Ni(*o*-tolyl)Cl)],[59] may increase the chances of developing a nickel precatalyst containing **1b**.

4.6 Examining 1b as an Ancillary Ligand in Ni-Catalyzed C-N Bond Formation

Though a distinct precatalyst containing **1b** could not be prepared, a more conventional Ni/[Li(THF)$_4$][**1b**] catalyst system was assessed for activity in the Ni-catalyzed C-N cross-

coupling reaction (**Table 4.6**). NiCl$_2$(DME) was selected as the nickel source, as it has an established role as a precursor for the reaction of interest.[27c,28b] The catalyst loading is typical of similar, nickel-catalyzed procedures in the literature.[27,28] Chlorobenzene was used as substrate due to the many reports indicating the facile oxidative addition of aryl chlorides vs. aryl bromides to the nickel centre.[26] Thus, it was anticipated that only moderately high temperatures (80 °C) would be required to promote the desired amination of chlorobenzene using aniline. The initial reaction conditions did not reveal any conversion to diphenylamine after 48 h (**Table 4.6, entry 1**). To ameliorate this issue, an additive was used in subsequent trials in an attempt to stabilize, or better generate, the Ni(0) species forming in solution. In previous reports, both nitrile[27a,b] and alkyl borate[27c,28b] additives have been used with great success in Ni-catalyzed C-N bond formation, however the use of MeCN (**Table 4.6, entry 2**) or phenylboronic acid (**Table 4.6, entry 3**) did not afford any of the desired coupled product. Increasing the temperature to 110 °C (and switching to the higher-boiling, ethereal solvent 1,4-dioxane) also did not result in conversion to diphenylamine (**Table 4.6, entry 4**). Additionally, changing the solvent to toluene did not have an impact on the success of the reaction (**Table 4.6, entry 5**). It should be noted that only phenylboronic acid was used as the additive at higher temperatures, as the boiling point of MeCN is ~80 °C.
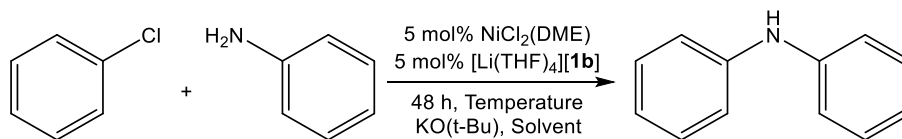
Table 4.6. Optimization of Ni-catalyzed C-N cross-coupling of chlorobenzene and aniline using [Li(THF)$_4$][**1b**] as ancillary ligand.[a]

Entry	Additive	Temperature (°C)	Solvent	Conversion (%)[b]
1	None	80	THF	0
2	MeCN	80	THF	0
3	PhB(OH)$_2$	80	THF	0
4	PhB(OH)$_2$	110	1,4-dioxane	0
5	PhB(OH)$_2$	110	toluene	0

[a] Reaction conditions: 1 mmol bromobenzene, 1.2 mmol aniline, 5 mol% NiCl$_2$(DME), 5 mol% [Li(THF)$_4$][**1b**], 1.2 mmol KO(t-Bu), 2 mL solvent. [b] Determined using ^{1}H NMR spectroscopy (CDCl$_3$) based on the consumption of chlorobenzene.

The lack of conversion to diphenylamine in the preliminary trials outlined in **Table 4.6** is, perhaps, not surprising, given that the **1b** anion was reluctant to coordinate to the nickel centre in the stoichiometric reactions described above. Without the generation of an active catalyst, comprising of both ligand and metal *in situ*, the desired C-N cross-coupling reaction would likely cease to proceed. In the future, modifications such as increasing the catalyst loading, modifying the nickel precursor-to-ligand ratio from 1:1 to 1:2, or using a different alkylborate (*e.g.* PhBPin) to facilitate the generation of a Ni(0) species *in situ*, might allow for a reaction to occur.

5. Conclusions

In summary, the ability of anionic, phosphinobenzimidazoles [Li(THF)$_2$][**1a**] and [Li(THF)$_4$][**1b**] to act as ancillary ligands in the Buchwald-Hartwig amination reaction was explored, given the inherent catalytic benefits associated with both anionic and hybrid ligands. Two methods of inquiry were used to investigate the catalytic utility of these ligands: (1) the attempted synthesis of a distinct palladium precatalyst incorporating **1a** or **1b**, which could then be screened for catalytic activity; and (2) the screening of a Pd/[Li(THF)$_4$][**1b**] catalyst system for activity in the reaction of interest, which was conducted concurrently with the preceding studies.

Examining the coordination chemistry of [Li(THF)$_2$][**1a**] with PdCl$_2$(TMEDA) led to the preparation of complex **6**, [(κ^2-**1a**)PdCl(κ^1-TMEDA)], which was characterized by multinuclear NMR spectroscopy. Additionally, reactions of either [Li(THF)$_4$][**1b**] or [PPh$_4$][**1b**] with common palladium precursors, including [Pd(cinnamyl)Cl]$_2$ and Pd$_2$(dba)$_3$•CHCl$_3$, led to the formation of complexes **8**, **9**, **10** ([PPh$_4$][PdCl$_2$(κ^2-**1b**)]), and **11**. It was also postulated that complex **11** could activate its [PPh$_4$]$^+$ counterion over time, generating complex **12**, which is presumed to contain PPh$_3$ and η^1-Ph ligands. Though NMR spectroscopy was used to assign a potential structure for all of these complexes, future efforts will focus on the isolation and characterization of these species in the solid state in order to elucidate their structures definitively.

An optimized [Pd(cinnamyl)Cl]$_2$/[Li(THF)$_4$][**1b**] catalyst system for the Buchwald-Hartwig amination was also developed in this study. A variety of aryl bromide substrates were well-tolerated by this catalyst system, but a preference for primary amine over secondary amine coupling partners was evident. The tendency for this catalyst system to react preferentially with primary vs. secondary amines was likely linked to the more electron-rich, palladium amido

complex that formed when secondary amines were employed, slowing the rate of reductive elimination, and correspondingly, the rate of reaction.

A major focus of this work was to identify if a catalyst system incorporating an anionic ligand would demonstrate greater catalytic activity than a corresponding system utilizing an equivalent neutral ligand. Therefore, a [Pd(cinnamyl)Cl]$_2$ catalyst system incorporating the neutral analogue of [Li(THF)$_4$][**1b**], **2**, was screened for activity in the Buchwald-Hartwig amination reaction. Upon comparing efficacies of the [Pd(cinnamyl)Cl]$_2$/[Li(THF)$_4$][**1b**] and [Pd(cinnamyl)Cl]$_2$/**2** catalyst systems, it was found that the system incorporating anionic [Li(THF)$_4$][**1b**] displayed superior activity compared to the system utilizing neutral **2** in almost all trials. The significant differences observed between the anionic and neutral systems was attributed to the comparatively electron-rich active palladium catalyst generated when anionic [Li(THF)$_4$][**1b**] was used, which would facilitate more efficient oxidative addition of the aryl bromide, and thus increase catalytic turnover. The simultaneous screening of a [Pd(cinnamyl)Cl]$_2$/[PPh$_4$][**1b**] catalyst system led to the conclusion that the success of the anionic catalyst system appears to be cation independent, since similar results were obtained for this catalyst system and the [Pd(cinnamyl)Cl]$_2$/[Li(THF)$_4$][**1b**] system. The superiority of anionic vs. neutral catalyst systems was further showcased when the anionic precatalyst [PPh$_4$][PdCl$_2$(κ^2-**1b**)] (**10**) displayed higher catalytic activity in the cross-coupling of bromobenzene and aniline than neutral [PdCl$_2$(κ^2-**2**)] (**13**). With this precedent set, developing new anionic ancillary ligands for applications in other catalytic reactions will be a focus of future work.

Finally, the success of **1b** as an ancillary ligand in the Buchwald-Hartwig amination reaction spurred preliminary investigations into its subsequent use in related Ni-catalyzed C-N bond forming reactions. The coordination chemistry of **1b** with nickel was first examined, leading

to the synthesis of complex **14**. The identity of this species was not strictly defined due to inconclusive NMR spectroscopic data. Though only Ni(II) precursors were utilized in this line of investigation, the reaction of Ni(0) precursors (*e.g.* Ni(COD)$_2$) with either [Li(THF)$_4$][**1b**] or [PPh$_4$][**1b**] might yield more fruitful results in the future. Unfortunately, the preliminary screening of a NiCl$_2$(DME)/[Li(THF)$_4$][**1b**] catalyst system did not demonstrate activity for Ni-catalyzed C-N bond formation, despite the use of additives, high temperatures, and extended reaction times. Incorporating different additives, or selecting a more active nickel precursor (*e.g.* Ni(COD)$_2$ or [(TMEDA)Ni(*o*-tolyl)Cl)]) might allow for improved results in subsequent assessments.

6. <u>References</u>

1. See, for example: (a) Barbaro, P.; Bianchini, C.; Giambastiani, G.; Parisel, S.L. *Coord. Chem. Rev*. **2004**, *248*, 2131-2150. (b) Grabulosa, A.; Granell, J.; Muller, G. *Coord. Chem. Rev*. **2007**, *251*, 25-90. (c) Gillespie, J.A.; Dodds, D.L.; Kamer, P.C.J. *Dalton Trans*. **2010**, *39*, 2751-2764. (d) Seechurn, C.C.C.J.; Kitching, M.O.; Colacot, T.J.; Snieckus, V. *Angew. Chem. Int. Ed*. **2012**, *51*, 5062-5085.

2. Fleckenstein, C.A.; Plenio, H. *Chem. Soc. Rev*. **2010**, *39*, 694-711.

3. Zapf, A.; Ehrentraut, A.; Beller, M. *Angew. Chem. Int. Ed*. **2000**, *39*, 4153-4155.

4. (a) Hayashi, T.; Konishi, M.; Kumada, M. *Tetrahedron Lett*. **1979**, *20*, 1871-1874. (b) Hayashi, T.; Konishi, M.; Kobori, Y.; Kumada, M.; Higuchi, T.; Kortsu, K. *J. Am. Chem. Soc*. **1984**, *106*, 158-163.

5. Zhang, W.-H.; Chien, S.W.; Hor, T.S.A. *Coord. Chem. Rev*. **2011**, *255*, 1991-2024.

6. See, for example: (a) Bader, A.; Lindner, E. *Coord. Chem. Rev*. **1991**, *108*, 27-110. (b) Espinet, P.; Soulantica, K. *Coord. Chem. Rev*. **1999**, *193-195*, 499-556. (c) Kwong, F.L.; Chan, A.S.C. *Synlett* **2008**, *10*, 1440-1448. (d) Kostas, I.D. *Curr. Org. Synth*. **2008**, *5*, 227-249.

7. (a) Braunstein, P.; Naud, F. *Angew. Chem. Int. Ed*. **2001**, *40*, 680-699. (b) Bassetti, M. *Eur. J. Inorg. Chem*. **2006**, 4473-4482.

8. Weng, Z.; Teo, S.; Hor, T.S.A. *Acc. Chem. Res*. **2007**, *40*, 676-684.

9. Weng, Z.; Teo, S.; Koh, L.L.; Hor, T.S.A. *Organometallics* **2004**, *23*, 4342-4345.

10. Nakamura, A.; Anselment, T.M.J.; Claverie, J.; Goodall, B.; Jordan, R.F.; Mecking, S.; Rieger, B.; Sen, A.; Van Leeuwen, P.W.N.M.; Nozaki, K. *Acc. Chem. Res*. **2013**, *46*, 1438-1449.

11. (a) Gott., A.L.; Piers, W.E.; Dutton, D.L.; McDonald, R.; Parvez, M. *Organometallics* **2011**, *30*, 4236-4249. (b) Kim, Y.; Jordan, R.F. *Organometallics* **2011**, *30*, 4250-4256.

12. Stradiotto, M.; Cipot, J.; McDonald, R. *J. Am. Chem. Soc*. **2003**, *125*, 5618-5619.

13. (a) Thomas, J.C.; Peters, J.C. *Inorg. Chem*. **2003**, *42*, 5055-5073. (b) Tassone, J.P.; Mawhinney, R.C.; Spivak, G.J. *J. Organomet. Chem*. **2015**, *776*, 153-156.

14. Labinger, J.A. *Organometallics* **2015**, *34*, 4784-4795.

15. Stradiotto, M.; Hesp, K.D.; Lundgren, R.J. *Angew. Chem. Int. Ed*. **2010**, *49*, 494-512.

16. Lundgren, R.J.; Rankin, M.A.; McDonald, R.; Schatte, G.; Stradiotto, M. *Angew. Chem. Int. Ed*. **2007**, *46*, 4732-4735.

17. (a) Surry, D.S.; Buchwald, S.L. *Angew. Chem. Int. Ed*. **2008**, *47*, 6338-6361. (b) Hartwig, J.F. *Acc. Chem. Res*. **2008**, *41*, 1534-1544. (c) Marion, N.; Nolan, S.P. *Acc. Chem. Res*. **2008**, *41*, 1440-1449. (d) Valente, C.; Pompeo, M.; Sayah, M.; Organ, M.G. *Org. Process Res. Dev*. **2014**, *18*, 180-190.

18. (a) Schlummer, B.; Scholz, U. *Adv. Synth. Catal*. **2004**, *346*, 1599-1626. (b) Tasler, S.; Mies, J.; Lang, M. *Adv. Synth. Catal*. **2007**, *349*, 2286-2300. (c) Torborg, C.; Beller, M. *Adv. Synth. Catal*. **2009**, *351*, 3027-3043.

19. Maiti, D.; Fors, B.P.; Henderson, J.L.; Nakamura, Y.; Buchwald, S.L. *Chem. Sci*. **2011**, *2*, 57-68.

20. Marion, N.; Navarro, O.; Mei, J.; Stevens, E.D.; Scott, N.M.; Nolan, S.P. *J. Am. Chem. Soc*. **2006**, *128*, 4101-4111.

21. Lundgren, R.J.; Sappong-Kumankumah, A.; Stradiotto, M. *Chem. Eur. J*. **2010**, *16*, 1983-1991.

22. Lundgren, R.J.; Stradiotto, M. *Aldrichimica Acta* **2012**, *45*, 59.

23. Chen, G.; Lam, W.H.; Fok, W.S.; Lee, H.W.; Kwong, F.Y. *Chem. Asian J*. **2007**, *2*, 306-313.

24. (a) Butts, C.P.; Crosby, J.; Lloyd-Jones, G.C.; Stephen, S.C. *Chem. Commun*. **1999**, 1707-1708. (b) Fujita, K.; Yamashita, M.; Puschmann, F.; Alvarez-Falcon, M.M.; Incarvito, C.D.; Hartwig, J.F. *J. Am. Chem. Soc*. **2006**, *128*, 9044-9045.

25. Chen, L.; Yu, G.-A.; Li, F.; Zhu, X.; Zhang, B.; Guo, R.; Li, X.; Yang, Q.; Jin, S.; Liu, C.; Liu, S.-H. *J. Organomet. Chem*. **2010**, *695*, 1768-1775.

26. (a) Standley, E.A.; Smith, S.J.; Müller, P.; Jamison, T.F. *Organometallics* **2014**, *33*, 2012-2018. (b) Tasker, S.Z.; Standley, E.A.; Jamison, T.F. *Nature* **2014**, *509*, 299-309. (c) Ananikov, V.P. *ACS Catal*. **2015**, *5*, 1964-1971.

27. For example, see: (a) Ge, S.; Green, R.A.; Hartwig, J.F. *J. Am. Chem. Soc*. **2014**, *136*, 1617-1627. (b) Park, N.A.; Teverovskiy, G.; Buchwald, S.L. *Org. Lett*. **2014**, *16*, 220-223. (c) Nathel, N.F.F.; Kim, J.; Hie, L.; Jiang, X.; Garg, N.K. *ACS Catal*. **2014**, *4*, 3289-3293. (d) Martin, A.R.; Nelson, D.J.; Meiries, S.; Slawin, A.M.Z.; Nolan, S.P. *Eur. J. Org. Chem*. **2014**, 3127-3131.

28. For additional examples, see: (a) Green, R.A.; Hartwig, J.F. *Angew. Chem. Int. Ed*. **2015**, *54*, 3768-3772. (b) Borzenko, A.; Rotta-Loria, N.L.; MacQueen, P.M.; Lavoie, C.M.; McDonald, R.; Stradiotto, M. *Angew. Chem. Int. Ed*. **2015**, *54*, 3773-3777. (c) Kampmann, S.S.; Skelton, B.W.; Wild, D.A.; Koutsantonis, G.A.; Stewart, S.G. *Eur. J. Org. Chem*. **2015**, 5995-6004.

29. Harkal, S; Rataboul, F.; Zapf, A.; Fuhrmann, C.; Riermeier, T.; Monsees, A.; Beller, M. *Adv. Synth. Catal*. **2004**, *346*, 1742-1748.

30. Schulz, T.; Torborg, C; Enthaler, S.; Schäffner, B.; Dumrath, A.; Spannenberg, A.; Neumann, H.; Börner, A.; Beller, M. *Chem. Eur. J*. **2009**, *15*, 4528-4533.

31. Schulz, T.; Torborg, C.; Schäffner, B.; Huang, J.; Zapf, A.; Kadyrov, R.; Börner, A.; Beller, M. *Angew. Chem. Int. Ed*. **2009**, *48*, 918-921.

32. Sergeev, A.G.; Schulz, T.; Torborg, C.; Spannenberg, A.; Neumann, H.; Beller, M. *Angew. Chem. Int. Ed*. **2009**, *48*, 7595-7599.

33. (a) Kamijo, S.; Yamamoto, Y. *Chem. Asian J*. **2007**, *2*, 568-578. (b) Jiang, B.; Rajale, T.; Wever, W.; Tu, S.-J.; Li, G. *Chem. Asian J*. **2010**, *5*, 2318-2335. (c) Bellina, F.; Rossi, R. *Adv. Synth. Catal*. **2010**, *352*, 1223-1276.

34. (a) Carvalho, L.C.R.; Fernandes, E.; Marques, M.M.B. *Chem. Eur. J*. **2011**, *17*, 12544-12555. (b) Shi, X.; Guo, J.; Liu, J.; Ye, M.; Xu, Q. *Chem. Eur. J*. **2015**, *21*, 9988-9993.

35. (a) Jalil, M.A.; Yamada, T.; Fujinami, S.; Honjo, T.; Nishikawa, H. *Polyhedron* **2001**, *20*, 627-633. (b) Grotjahn, D.B.; Gong, Y.; Zakharov, L.; Golen, J.A.; Rheingold, A.L. *J. Am. Chem. Soc*. **2006**, *128*, 438-453. (c) Milde, B.; Schaarschmidt, D.; Ruffer, T.; Lang, H. *Dalton Trans*. **2012**, *41*, 5377-5390.

36. Walker, J.M.; Tassone, J.P.; Jenkins, H.A.; Spivak, G.J. *J. Organomet. Chem*. **2014**, *761*, 56-63.

37. Pangborn, A.B.; Giardello, M.A.; Grubbs, R.H.; Rosen, R.K.; Timmers, F.J. *Organometallics* **1996**, *15*, 1518-1520.

38. Wan, Y.; Wallinder, C.; Plouffe, B.; Beaudry, H.; Mahalingam, A.K.; Wu, X.; Johansson, B.; Holm, M.; Botoros, M.; Karlén, A.; Pettersson, A.; Nyberg, F.; Fändriks, L.; Gallo-Payet, N.; Hallberg, A.; Alterman, M. *J. Med. Chem*. **2004**, *47*, 5995-6008.

39. de Graaf, W.; Boersma, J.; Smeets, W.J.J.; Spek, A.L.; van Koten, G. *Organometallics* **1989**, *8*, 2907-2917.

40. Zalesskiy, S.S.; Ananikov, V.P. *Organometallics* **2012**, *31*, 2302-2309.

41. Nöth, H; Vahrenkamp, H. *Chem. Ber*. **1966**, *99*, 1049-1067.

42. For example, see: (a) Andersen, N.G.; Keay, B.A. *Chem. Rev.* **2001**, *101*, 997-1030. (b) Adams, D.J.; Bennett, J.A.; Duncan, D.; Hope, E.G.; Hopewell, J.; Stuart, A.M.; West, A.J. *Polyhedron* **2007**, *26*, 1505-1513. (c) Beckmann, U.; Süslüyan, D.; Kunz, P.C. *Phosphorus, Sulfur Silicon Related Elem.* **2011**, *186*, 2061-2070.

43. For example, see: (a) Markies, B.A.; Kruis, D.; Rietweld, M.H.P.; Verkerk, K.A.N.; Boersma, J.; Kooijman, H.; Lakin, M.T.; Spek, A.L.; van Koten, G. *J. Am. Chem. Soc.* **1995**, *117*, 5263-5274. (b) Vicente, J.; Abad, J.-A.; Frankland, A.D.; López-Serrano, J.; de Arellano, M.C.R.; Jones, P.G. *Organometallics* **2002**, *21*, 272-282.

44. Skupov, M.K.; Marella, P.R.; Smiard, M.; Yap, G.P.A.; Allen, N.; Conner, D.; Goodall, B.L.; Claverie, J.P. *Macromol. Rapid Commun.* **2007**, *28*, 2033-2038.

45. Anderson, G.K. Lin, M. *Inorg. Synth.* **1990**, *28*, 60–63.

46. Murrall, N.W.; Welch, A.J. *J. Organomet. Chem.* **1986**, *301*, 109-130.

47. For example, see: (a) Braunstein, P.; Zhang, J.; Welter, R. *Dalton Trans.* **2003**, 507-509. (b) Zhang, J.; Braunstein, P.; Welter, R. *Inorg. Chem.* **2004**, *43*, 4172-4177. (c) Johansson, C.; Lloyd-Jones, G.C.; Norrby, P.-O. *Tetrahedron: Asymmetry* **2010**, *21*, 1585-1592. (d) Alsabeh, P.G.; Lundgren, R.J.; McDonald, R.; Seechurn, C.C.C.J.; Colacot, T.J.; Stradiotto, M. *Chem. Eur. J.* **2013**, *19*, 2131-2141.

48. Kühl, O. *Phosphorus-31 NMR Spectroscopy: A Concise Introduction for the Synthetic Organic and Organometallics Chemist*; Springer: Berlin, 2008.

49. Seacome, R.J.; Coles, M.P.; Glover, J.E.; Hitchcock, P.B.; Rowlands, G.J. *Dalton Trans.* **2010**, *39*, 3687-3694.

50. For example, see: (a) Kong, K.-C.; Cheng, C.-H. *J. Am. Chem. Soc.* **1991**, *113*, 6313-6315. (b) Segelstein, B.E.; Butler, T.W.; Chenard, B.L. *J. Org. Chem.* **1995**, *60*, 12-13. (c) Goodson,

F.E.; Wallow, T.I.; Novak, B.M. *J. Am. Chem. Soc*. **1997**, *119*, 12441-12453. (d) Grushin, V.V. *Organometallics* **2000**, *19*, 1888-1900. (e) Kwong, F.Y.; Lai, C.W.; Chan, K.S. *Tetrahedron Lett*. **2002**, *43*, 3537-3539. (f) Kwong, F.Y.; Lai, C.W.; Yu, M.; Chan, K.S. *Tetrahedron* **2004**, *60*, 5635-5645. (g) Hwang, L.K.; Na, Y.; Lee, J.; Do, Y.; Chang, S. *Angew. Chem. Int. Ed*. **2005**, *44*, 6166-6169.

51. Trzeciak, A.M.; Bartosz-Bechowski, H.; Ciunik, Z.; Niesyty, K.; Ziółkowski, J.J. *Can. J. Chem*. **2001**, *79*, 752-759.

52. Barder, T.E.; Buchwald, S.L. *J. Am. Chem. Soc*. **2007**, *129*, 12003-12010.

53. For an additional example, see: Crawford, S.M.; Lavery, C.B.; Stradiotto, M. *Chem. Eur. J*. **2013**, *19*, 16760-16771.

54. Jarvis, A.G.; Fairlamb, I.J.S. *Curr. Org. Chem*. **2011**, *15*, 3175-3196.

55. For example, see: (a) Wang, H.-S.; Wang, Y.-C.; Pan, Y.-M.; Zhao, S.-L. Chen, Z.-F. *Tetrahedron Lett*. **2008**, *49*, 2634-2637. (b) Rohilla, S.; Pant, P.; Jain, N. *RSC Adv*. **2015**, *5*, 31311-31317.

56. Melvin, P.R.; Balcells, D.; Hazari, N.; Nova, A. *ACS Catal*. **2015**, *5*, 5596-5606.

57. Hartwig, J.F. *Inorg. Chem*. **2007**, *46*, 1936-1947.

58. See: Mitchell, E.A.; Jessop, P.G.; Baird, M.C. *Organometallics* **2009**, *28*, 6732-6738, and the references therein.

59. See: (a) Shields, J.D.; Gray, E.E.; Doyle, A.G. *Org. Lett*. **2015**, *17*, 2166-2169. (b) Magano, J.; Monfette, S. *ACS Catal*. **2015**, *5*, 3120-3123, and the references therein.

60. Garrou, P.E. *Chem. Rev*. **1981**, *81*, 229-266.

61. Kayser, L.; Pattacini, R.; Rogez, G.; Braunstein, P. *Chem. Commun*. **2010**, *46*, 6461-6463.

Appendix A. <u>Supplementary Information for Catalytic Studies</u>

A.1 Characterization of Coupled Products

The characterization of the coupled products resulting from the catalytic trials is detailed below. Experimental details regarding substrates that did not yield any discernable product are omitted. The yields refer to the highest yield achieved during the two runs.
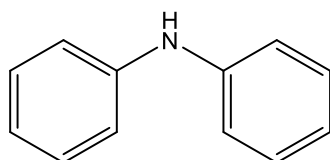
Diphenylamine.[A1] (**Table 4.3, entry 1**). General Procedure A was followed using bromobenzene (63 μL, 0.6 mmol) and aniline (66 μL, 0.72 mmol). After flash chromatography on silica gel (hexane/EtOAc, 95/5), the title compound was obtained as a white solid (93 mg, 92%). ^{1}H NMR (500 MHz, CDCl$_3$): δ 7.18-7.14 (m, 4H, ArH), 6.97-6.95 (m, 4H, ArH), 6.84-6.81 (m, 2H, ArH), 5.55 (br. s, 1H, –N*H*) ppm. ^{13}C{^{1}H} NMR (125 MHz, CDCl$_3$): δ 143.2, 129.5, 121.1, 117.9 ppm.
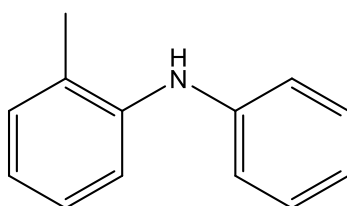
2-methyl-*N*-phenylaniline.[A2] (**Table 4.3, entry 2**). General Procedure A was followed using 2-bromotoluene (72 μL, 0.6 mmol) and aniline (66 μL, 0.72 mmol). After flash chromatography on silica gel (hexane/EtOAc, 20/1), the title compound was obtained as a pale yellow oil (107 mg, 97%). ^{1}H NMR (500 MHz, CDCl$_3$): δ 7.38–7.35 (m, 3H, ArH), 7.31 (d, 1H, J = 7.5 Hz, ArH), 7.25 (t, 1H, J = 7.6 Hz, ArH), 7.07–7.00 (m, 4H, ArH), 5.47 (br. s, 1H, –N*H*), 2.36 (s, 3H, –C*H$_3$*) ppm. ^{13}C{^{1}H} NMR (125 MHz, CDCl$_3$): δ 144.1, 141.4, 131.1, 129.5, 128.5, 126.9, 122.2,

120.6, 119.0, 117.6, 18.1 ppm. Similar workup procedures were followed using General Procedure B and General Procedure C, affording 80 mg (70%) and 107 mg (97%) of the title compound respectively.
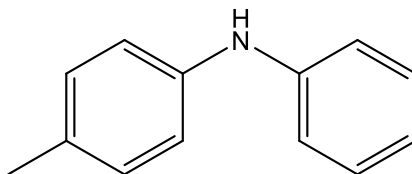
4-methyl-*N*-phenylaniline.[A2] (**Table 4.3, entry 3**). General Procedure A was followed using 4-bromotoluene (74 μL, 0.6 mmol) and aniline (66 μL, 0.72 mmol). After flash chromatography on silica gel (hexane/EtOAc, 97/3), the title compound was obtained as an off-white solid (107 mg, 97%). ^{1}H NMR (500 MHz, CDCl$_3$): δ 7.16 (t, 2H, $J = 7.7$ Hz ArH), 7.00 (d, 2H, $J = 8.0$ Hz, ArH), 6.94–6.91 (m, 4H, ArH), 6.80 (t, 1H, $J = 7.3$ Hz, ArH), 5.52 (br. s, 1H, –N*H*), 2.22 (s, 3H, –C*H*$_3$) ppm. ^{13}C{^{1}H} NMR (125 MHz, CDCl$_3$): δ 142.9, 139.2, 129.9, 128.8, 128.3, 119.2, 117.8, 115.8, 19.7 ppm. Similar workup procedures were followed using General Procedure B, yielding 46 mg (42%) of the title compound.
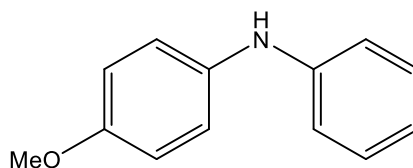
4-methoxy-*N*-phenylaniline.[A2] (**Table 4.3, entry 4**). General Procedure A was followed using 4-bromoanisole (75 μL, 0.6 mmol) and aniline (66 μL, 0.72 mmol). After flash chromatography on silica gel (hexane/Et$_2$O, 95/5), the title compound was obtained as a white solid (68 mg, 57%). ^{1}H NMR (500 MHz, CDCl$_3$): δ 7.12-7.08 (m, 2H, ArH), 6.96-6.93 (m, 2H, ArH), 6.80-6.71 (m, 5H, ArH), 5.37 (br. s, 1H, –N*H*), 3.67 (s, 3H, –OC*H*$_3$) ppm. ^{13}C{^{1}H} NMR (125 MHz, CDCl$_3$): δ 155.3, 145.3, 135.8, 129.4, 122.3, 119.6, 115.7, 114.8, 55.7 ppm. Similar workup procedures were

followed using General Procedure B and General Procedure C, affording 16 mg (13%) and 75 mg (63%) of the title compound respectively.
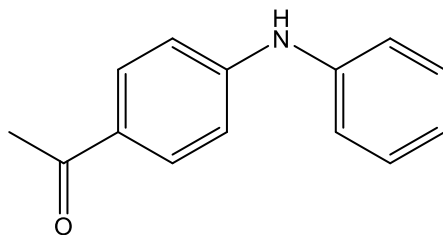
1-(4-(phenylamino)phenyl)ethanone.[A3] (**Table 4.3, entry 5**). General Procedure A was followed using 4′-bromoacetophenone (0.119 g, 0.6 mmol) and aniline (66 μL, 0.72 mmol). After flash chromatography on silica gel (hexane/EtOAc, 7/3), the title compound was obtained as a yellow solid (0.118 g, 93%). ^{1}H NMR (500 MHz, CDCl$_3$): δ 7.78 (d, 2H, J = 8.7 Hz, ArH), 7.26 (d, 2H, J = 7.7 Hz, ArH), 7.10 (d, 2H, J = 8.3 Hz, ArH), 7.01-6.98 (m, 1H, ArH), 6.91 (d, 2H, J = 8.7 Hz, ArH), 6.19 (br. s, 1H, –NH), 2.45 (s, 3H, –CH_3) ppm. ^{13}C{^{1}H} NMR (125 MHz, CDCl$_3$): δ 196.5, 148.4, 140.6, 130.7, 129.6, 129.0, 123.4, 120.7, 114.4, 26.2 ppm.
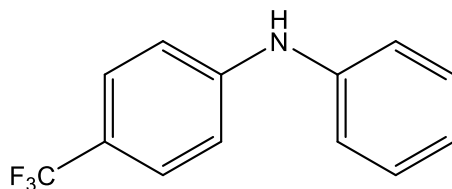
N-phenyl-4-(trifluoromethyl)aniline.[A2] (**Table 4.3, entry 6**). General Procedure A was followed using 4-bromobenzotrifluoride (84 μL, 0.6 mmol) and aniline (66 μL, 0.72 mmol). After flash chromatography on silica gel (DCM), the title compound was obtained as an off-white solid (125 mg, 88%). ^{1}H NMR (500 MHz, CDCl$_3$): δ 7.37 (d, 2H, J = 8.5 Hz, ArH), 7.25-7.22 (m, 2H, ArH), 7.06-7.04 (m, 2H, ArH), 6.98-6.93 (m, 3H, ArH), 5.81 (br. s, 1H, –NH) ppm. ^{13}C{^{1}H} NMR (125 MHz, CDCl$_3$): δ 145.7, 140.1, 131.0, 125.6 (q, J_{CF} = 3.8 Hz), 125.2 (q, J_{CF} = 230 Hz), 121.8, 120.5

(q, J_{CF} = 32.7 Hz), 118.9, 114.2 ppm. Similar workup procedures were followed using General Procedure B, affording 67 mg (47%) of the title compound.
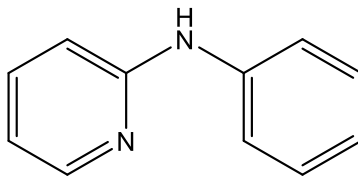
N-phenylpyridin-2-amine.[A2] (**Table 4.3, entry 8**). General Procedure A was followed using 2-bromopyridine (57 μL, 0.6 mmol) and aniline (66 μL, 0.72 mmol). After flash chromatography on silica gel (hexane/EtOAc, 4/1), the title compound was obtained as an orange solid (40 mg, 39%). ^{1}H NMR (500 MHz, CDCl$_3$): δ 8.13 (ddd, 1H, *J* = 5.0, 1.9, 0.8 Hz, ArH), 7.43-7.39 (m, 1H, ArH), 7.28-7.24 (m, 4H, ArH), 6.99-6.96 (m, 1H, ArH), 6.81 (d, 1H, *J* = 8.4, ArH), 6.77 (br. s, 1H, –N*H*), 6.67-6.34 (m, 1H, ArH) ppm. ^{13}C{^{1}H} NMR (125 MHz, CDCl$_3$): δ 155.0, 147.3, 139.4, 136.7, 128.2, 121.8, 119.3, 114.0, 107.1 ppm.
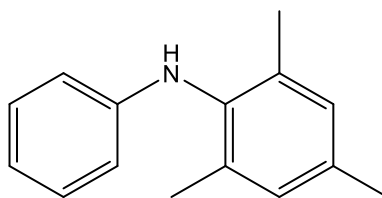
2,4,6-trimethyl-N-phenylaniline.[A4] (**Table 4.4, entry 1**). General Procedure A was followed using bromobenzene (63 μL, 0.6 mmol) and 2,4,6-trimethylaniline (101 μL, 0.72 mmol). After flash chromatography on silica gel (hexane/Et$_2$O, 9/1), the title compound was obtained as a pale orange oil (94 mg, 74%). ^{1}H NMR (500 MHz, CDCl$_3$): δ 7.06-7.02 (m, 2H, ArH), 6.84 (s, 2H, ArH), 6.64-6.61 (m, 1H, ArH), 6.39-6.37 (m, 2H, ArH), 4.96 (broad s, 1H, –N*H*), 2.21 (s, 3H, *para*-C*H$_3$*), 2.07 (s, 6H, ortho-CH$_3$) ppm. ^{13}C{^{1}H} NMR (125 MHz, CDCl$_3$): δ 145.5, 134.9, 134.4,

134.3, 128.1, 116.8, 112.1, 19.8, 17.2 ppm. Similar workup procedures were followed using General Procedure B, affording 71 mg (56%) of the title compound.
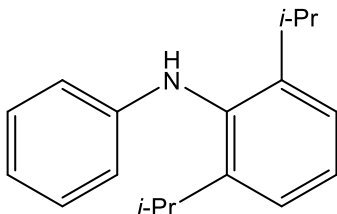
2,6-diisopropyl-N-phenylaniline.[A5] (**Table 4.4, entry 2**). General Procedure A was followed using bromobenzene (63 μL, 0.6 mmol) and 2,6-diisopropylaniline (136 μL, 0.72 mmol). After flash chromatography on silica gel (hexanes/DCM, 4/1), the title compound was obtained as a colourless oil (118 mg, 78%). ^{1}H NMR (500 MHz, CDCl$_3$): δ 7.19 (t, 1H, J = 7.5 Hz, ArH), 7.13 (d, 2H, J = 7.7 Hz, ArH), 7.03 (t, 2H, J = 7.4 Hz, ArH), 6.61 (t, 1H, J = 7.2 Hz, ArH), 6.38 (d, 2H, J = 7.8 Hz, ArH), 5.01 (broad s, 1H, –NH), 3.11 (septet, 1H, J = 6.8 Hz, –CH–), 1.05 (d, 12H, J = 6.8 Hz, –CH(CH_3)$_2$) ppm. ^{13}C{^{1}H} NMR (125 MHz, CDCl$_3$): δ 148.2, 147.7, 135.2, 129.3, 127.3, 123.9, 117.8, 113.0, 28.3, 24.0 ppm. Similar workup procedures were followed using General Procedure B and General Procedure C, affording 47 mg (31%) and 114 mg (75%) of the title compound respectively.
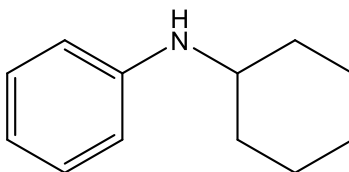
N-cyclohexylaniline.[A5] (**Table 4.4, entry 3**). General Procedure A was followed using bromobenzene (63 μL, 0.6 mmol) and cyclohexylamine (82 μL, 0.72 mmol). After flash chromatography on silica gel (hexane/EtOAc, 10/1), the title compound was obtained as a yellow oil (0.076 g, 72%). ^{1}H NMR (500 MHz, CDCl$_3$): δ 7.09-7.05 (m, 2H, ArH), 6.59-6.56 (m, 1H,

ArH), 6.51-6.49 (m, 2H, ArH), 3.42 (broad s, 1H, −NH), 3.17 (tt, 1H, J = 10.1, 3.7 Hz, −CH−),

1.99-1.96 (m, 2H, aliphatic H), 1.68 (dt, 2H, J = 13.5, 3.8 Hz, aliphatic H), 1.57 (dt, 1H, J = 12.8,

3.8 Hz, aliphatic H), 1.33-1.24 (m, 2H, aliphatic H) ppm. ^{13}C{^{1}H} NMR (125 MHz, CDCl$_3$): δ

146.4, 128.2, 115.8, 112.1, 50.6, 32.4, 24.9, 24.0 ppm. Similar workup procedures were followed

using General Procedure B and General Procedure C, affording 37 mg (35%) and 74 mg (70%) of

the title compound respectively.
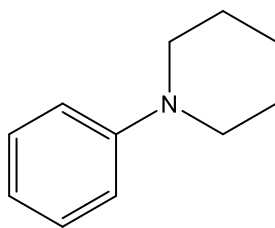
1-phenylpiperidine.[A3] (**Table 4.4, entry 5**). General Procedure A was followed using

bromobenzene (63 μL, 0.6 mmol) and piperidine (71 μL, 0.72 mmol). After flash chromatography

on silica gel (hexane/Et$_2$O, 95/5), the title compound was obtained as a colourless oil (0.032 g,

33%). ^{1}H NMR (500 MHz, CDCl$_3$): δ 7.19-7.15 (m, 2H, ArH), 6.87 (d, 2H, J = 8.7 Hz, ArH),

6.76-6.73 (m, 1H, ArH), 3.07 (t, 4H, J = 5.4 Hz, −CH_2−), 1.66-1.61 (m, 4H, −CH_2−), 1.52-1.48

(m, 2H, −CH_2−) ppm. ^{13}C{^{1}H} NMR (125 MHz, CDCl$_3$): δ 152.3, 129.0, 119.3, 116.6, 50.7, 25.9,

24.4 ppm. Similar workup procedures were followed using General Procedure B, yielding 37 mg

(38%) of the title compound.

A.2 NMR Spectra of Coupled Products

Diphenylamine (Table 4.3, entry 1)
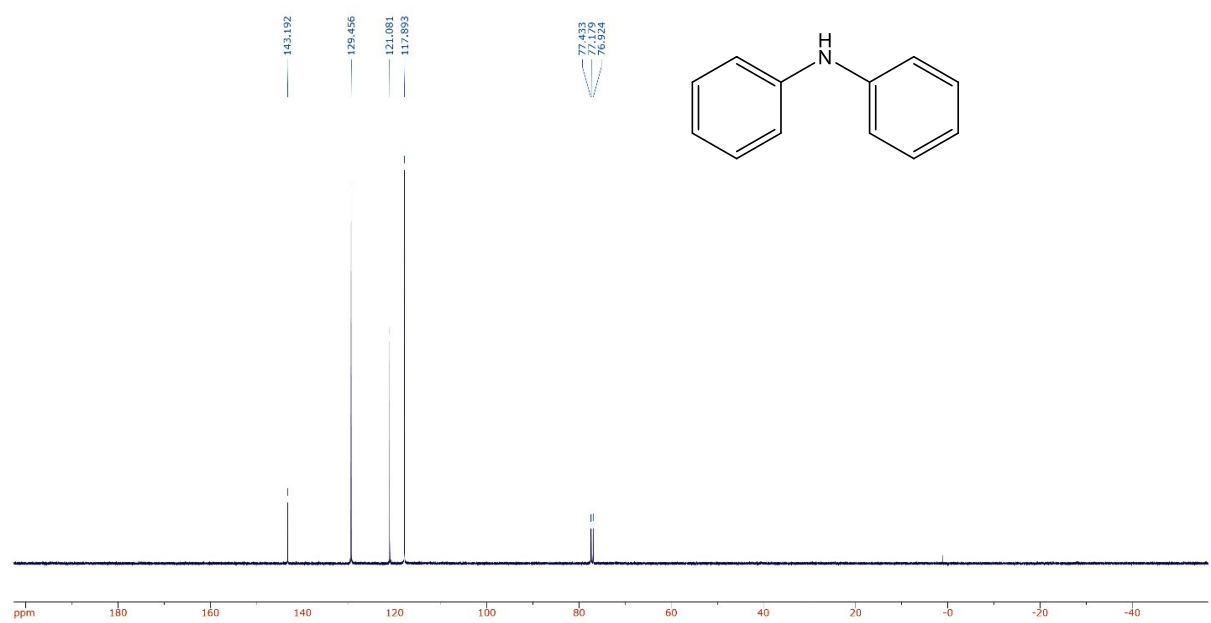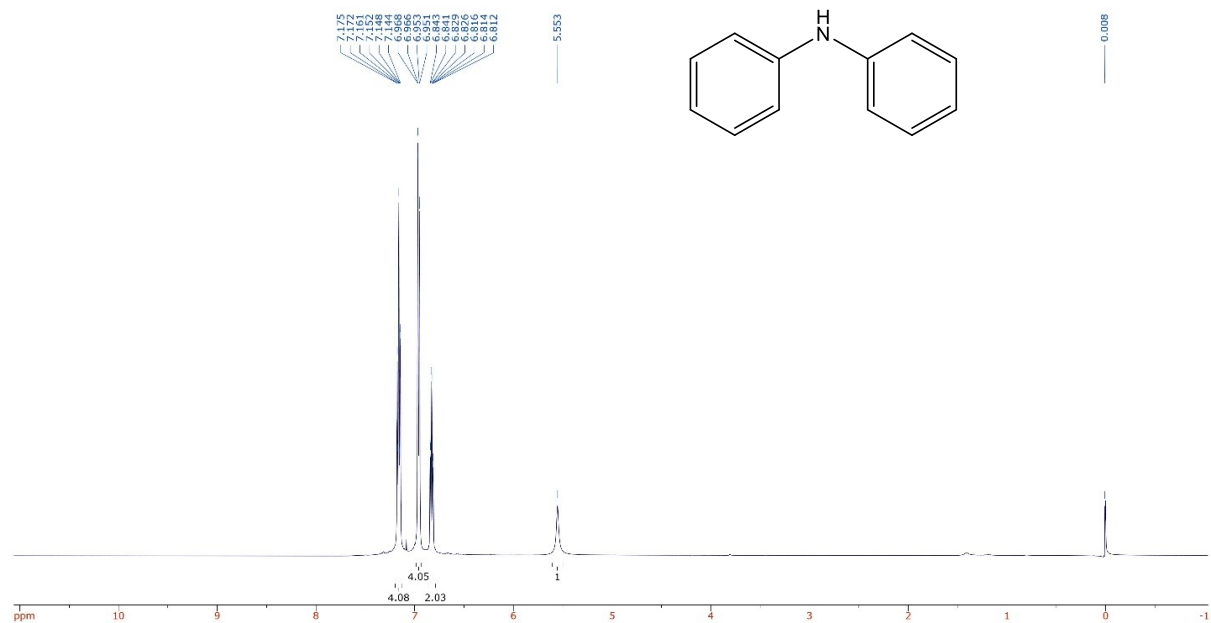
2-methyl-*N*-phenylaniline (Table 4.3, entry 2)

4-methyl-*N*-phenylaniline (Table 4.3, entry 3)
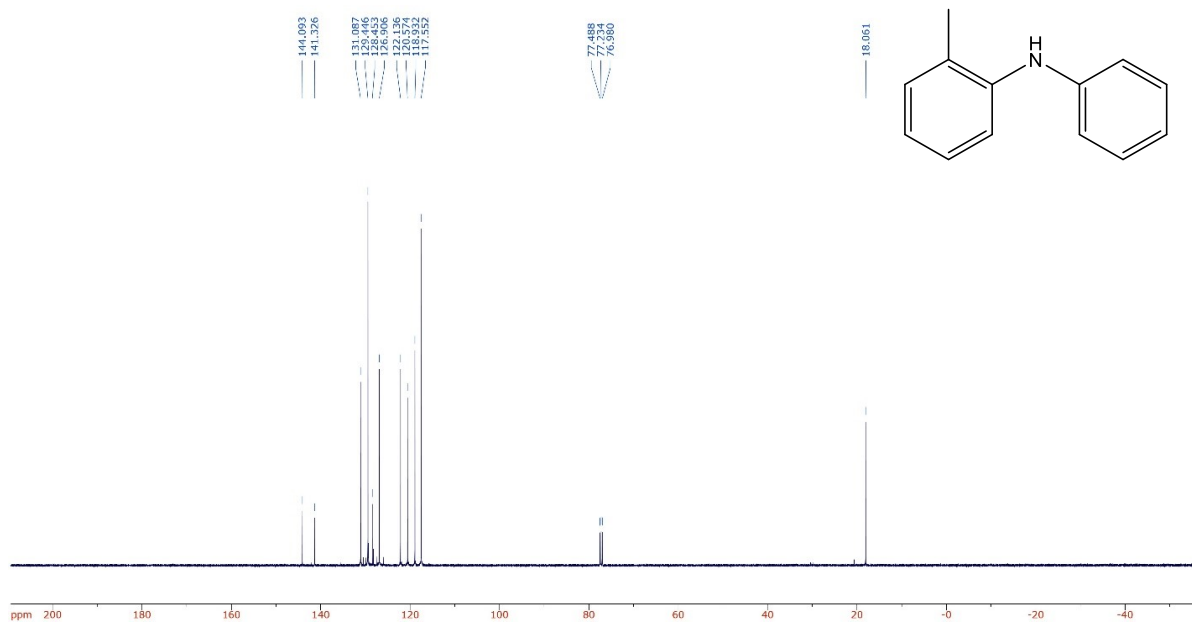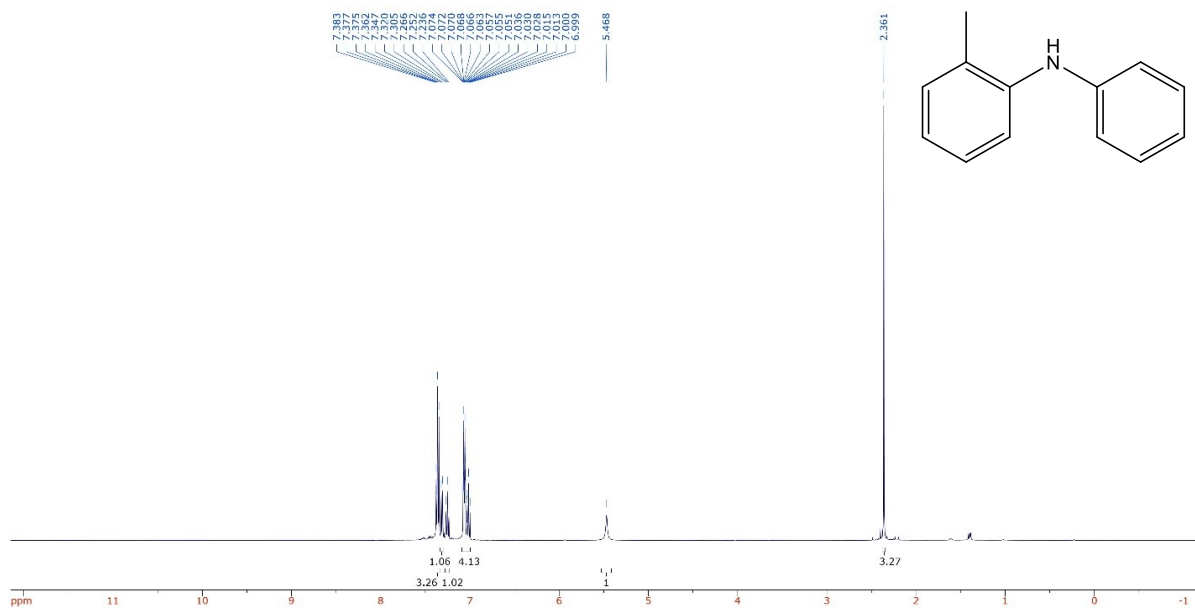
4-methoxy-N-phenylaniline (Table 4.3, entry 4)
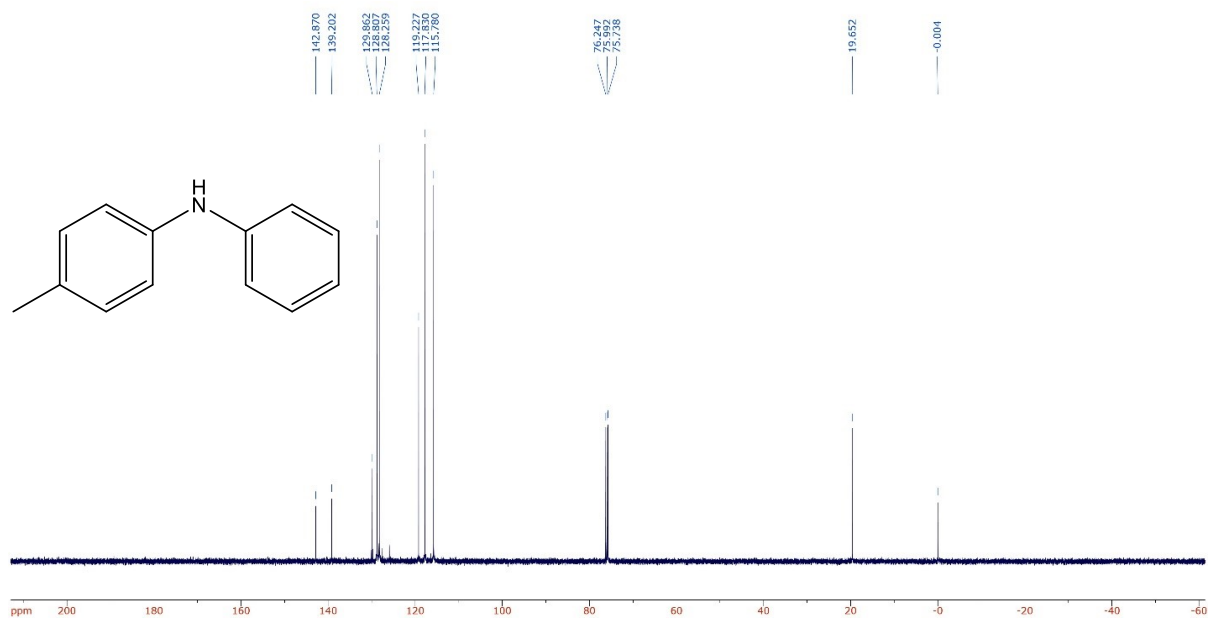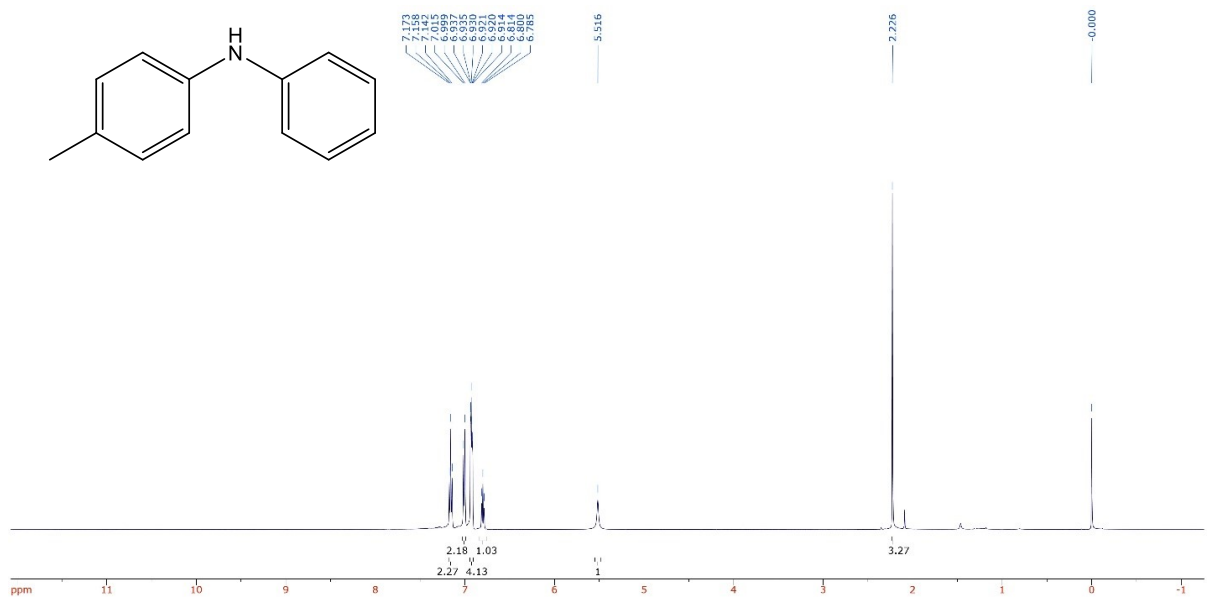
1-(4-(phenylamino)phenyl)ethanone (Table 4.3, entry 5)

***N*-phenyl-4-(trifluoromethyl)aniline (Table 4.3, entry 6)**

N-phenylpyridin-2-amine (Table 4.3, entry 8)
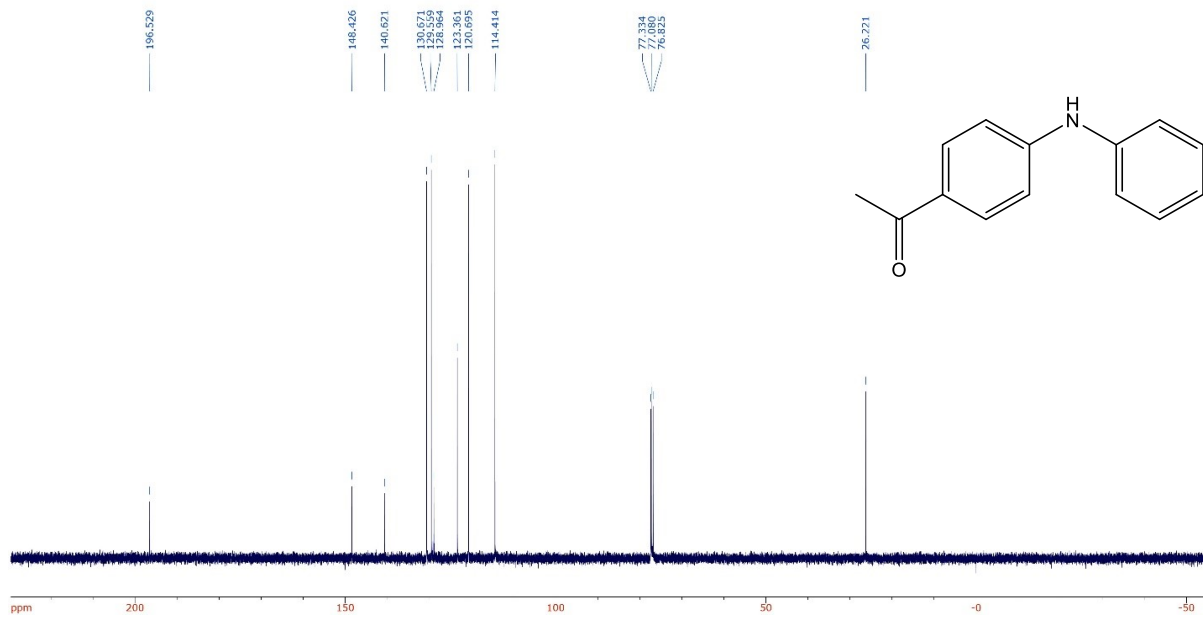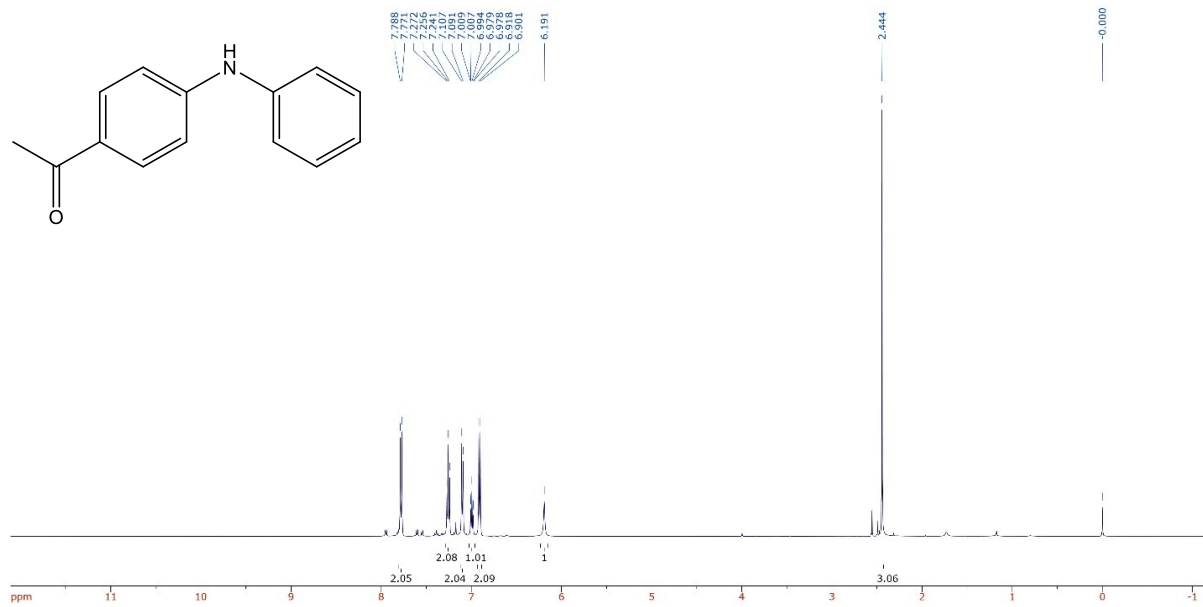
2,4,6-trimethyl-*N*-phenylaniline (Table 4.4, entry 1)
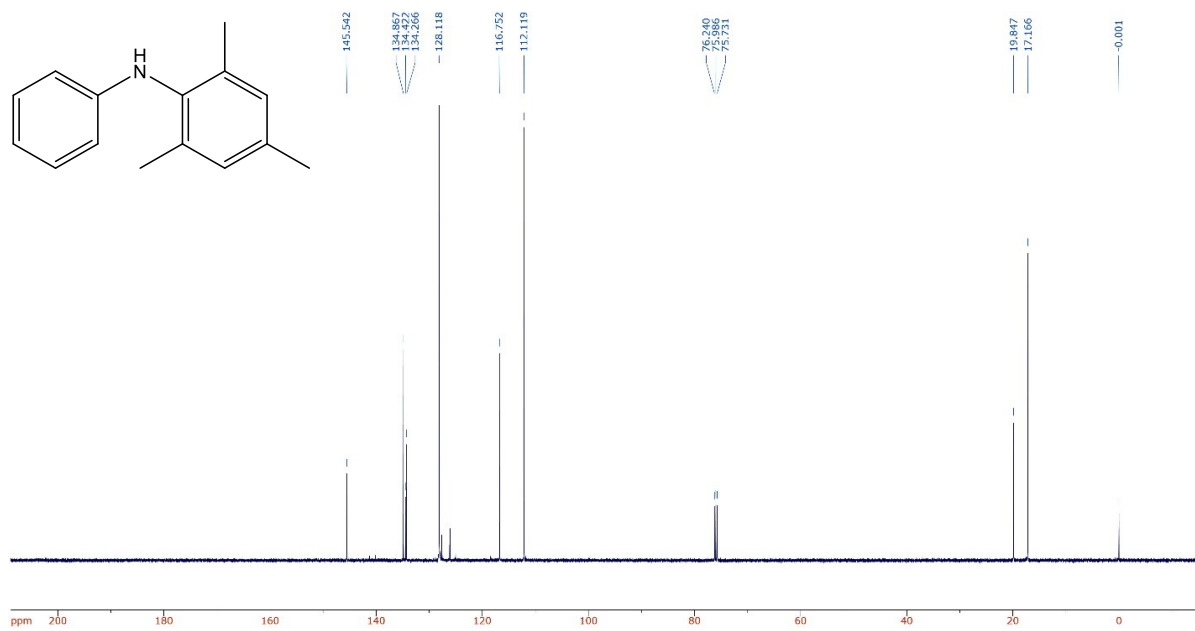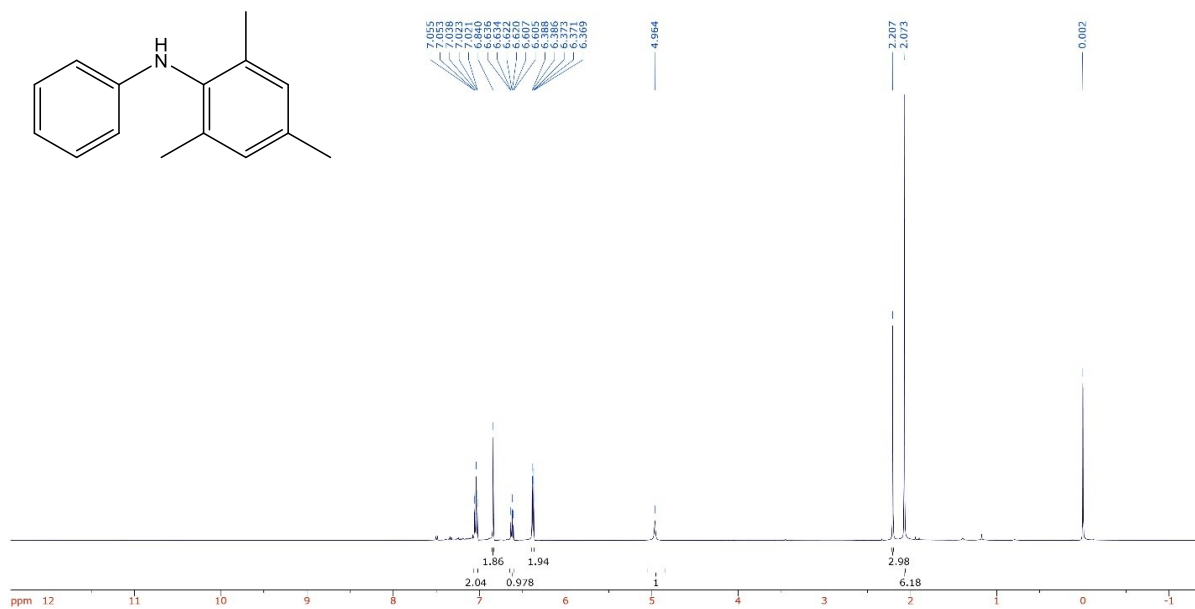
2,6-diisopropyl-*N*-phenylaniline (Table 4.4, entry 2)
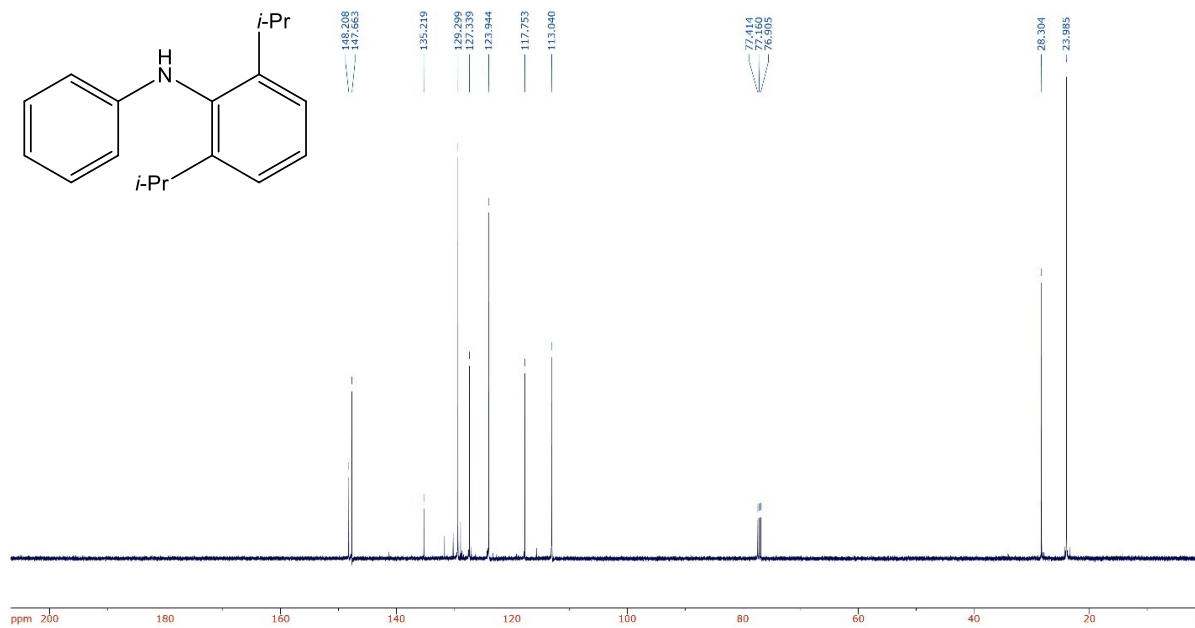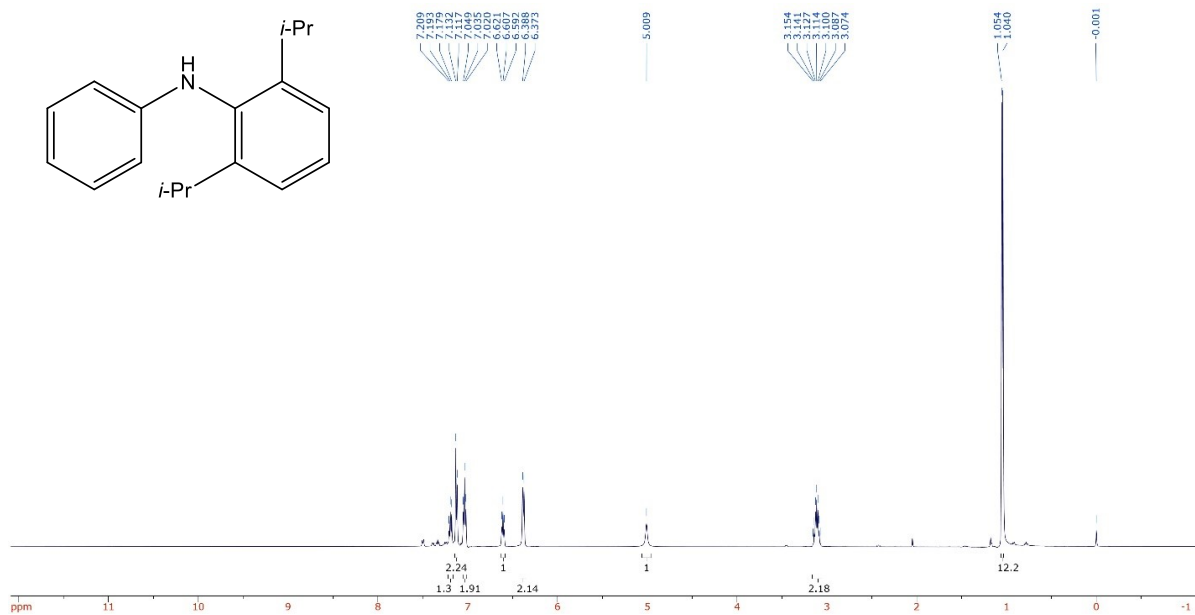
N-cyclohexylaniline (Table 4.4, entry 3)
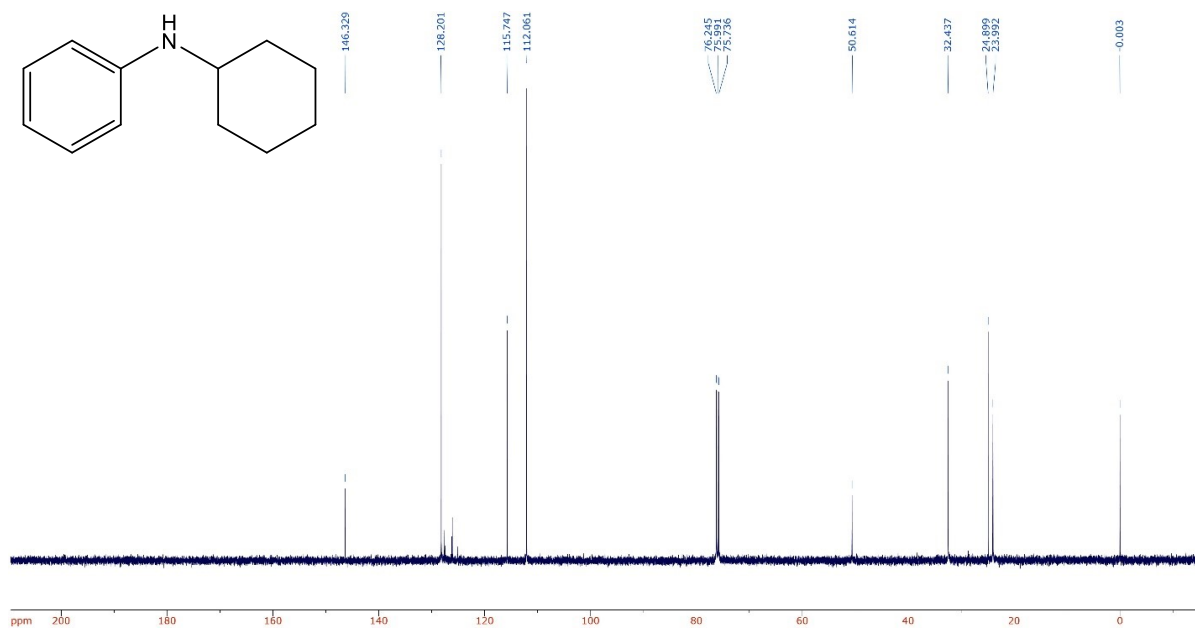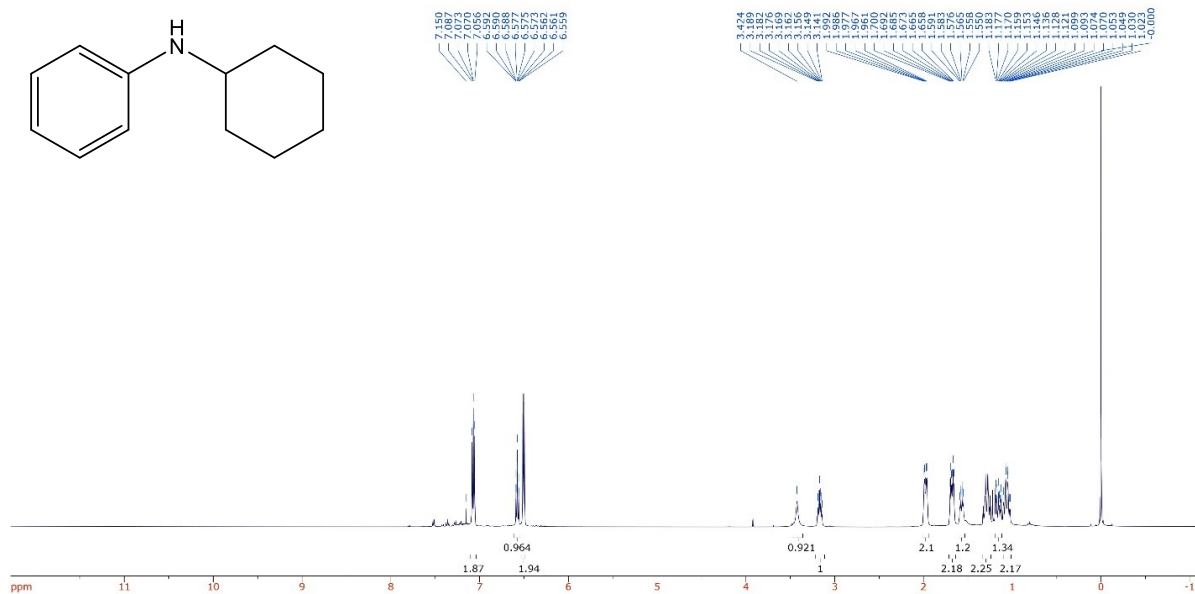
1-phenylpiperidine (Table 4.4, entry 5)
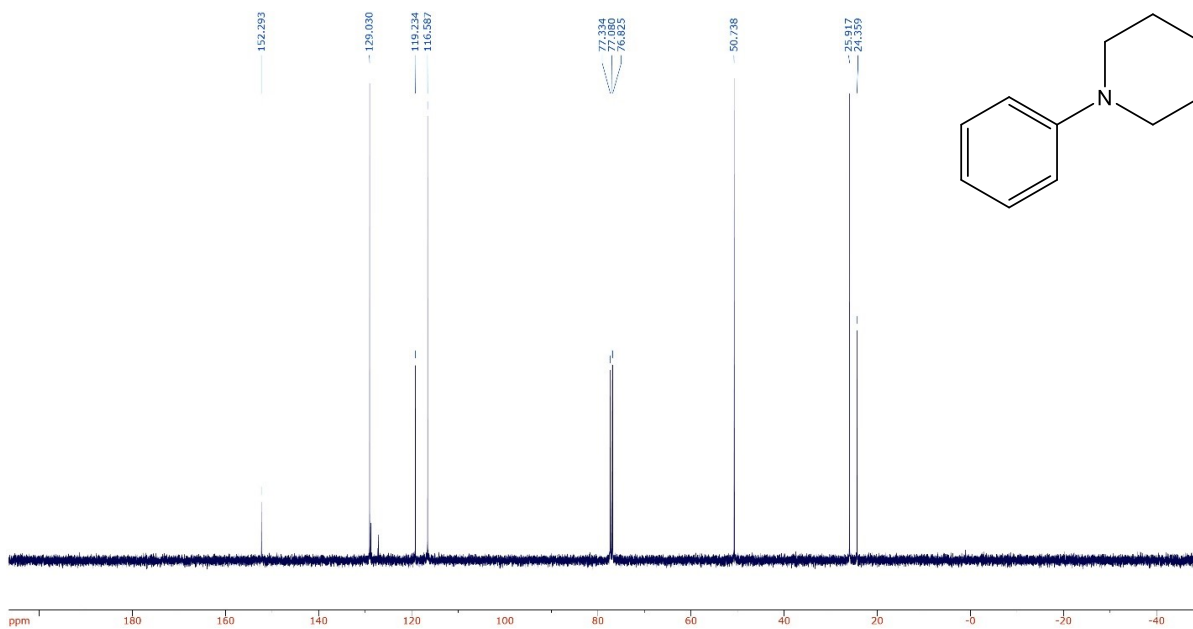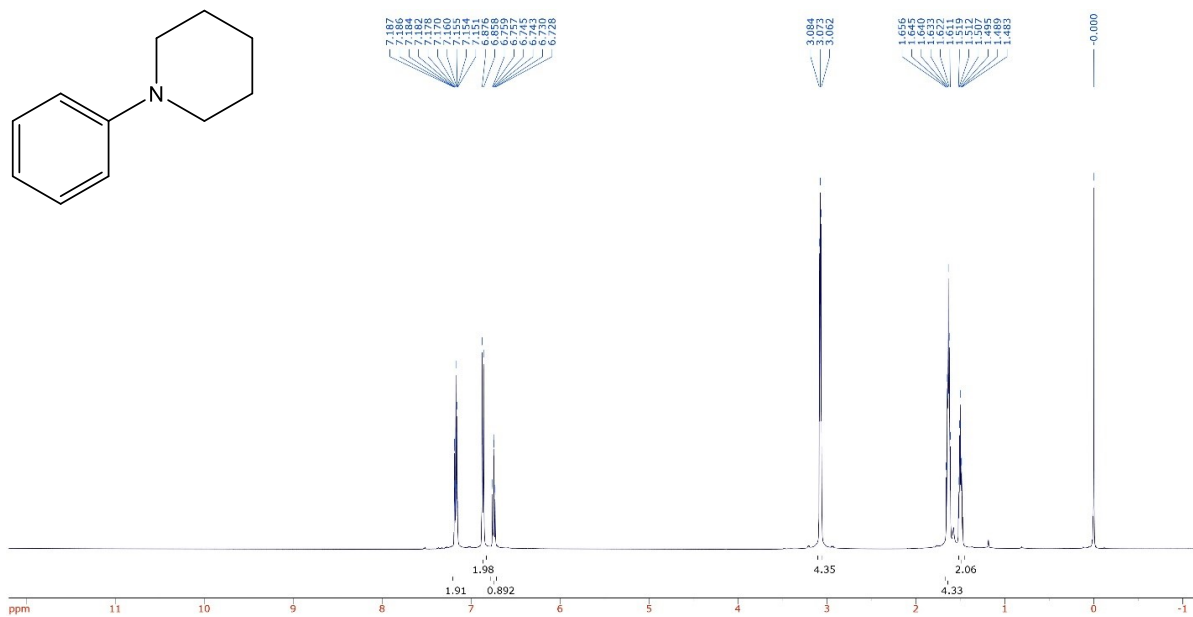
A.3 References

A1 Xie, X.; Ni, G.; Ma, F.; Ding, L.; Xu, S.; Zhang, Z. *Synlett* **2011**, *7*, 955-958.

A2 Tardiff, B.J.; Stradiotto, M. *Eur. J. Org. Chem*. **2012**, 3972-3977.

A3 Zhang, Y.; César, V.; Lavigne, G. *Eur. J. Org. Chem*. **2015**, 2042-2050.

A4 Desmarets, C.; Schneider, R.; Fort, Y. *J. Org. Chem*. **2002**, *67*, 3029-3036.

A5 Wheaton, C.A.; Bow, J.-P.J.; Stradiotto, M. *Organometallics* **2013**, *32*, 6148-6161.